2015-05-27

Characterization of a PDGF-AA Initiated Model of Glioblastoma with Predictable Onset

DePetro, Jessica

UNIVERSITY OF CALGARY

Characterization of a PDGF-AA Initiated Model of Glioblastoma with Predictable Onset

by

Jessica DePetro

A THESIS

SUBMITTED TO THE FACULTY OF GRADUATE STUDIES

IN PARTIAL FULFILMENT OF THE REQUIREMENTS FOR THE

DEGREE OF MASTER OF SCIENCE

GRADUATE PROGRAM IN MEDICAL SCIENCE

CALGARY, ALBERTA

MAY, 2015

Abstract

Glioblastoma multiforme is a fatal brain cancer which has eluded therapeutic advances. Although the genetic and epigenetic landscape of GBM is now well annotated, its pathogenesis remains elusive and difficult to study in the laboratory. By imitating two well documented alterations of GBM - p53 loss of function and activation of platelet derived growth factor receptor-alpha - we have created a new model of GBM and a tool to explore the kinetics of GBM initiation. In this model, cells from the subventricular zone of p53 null mice transform *in vitro* after approximately 100 days in PDGF-AA. Transformation is marked by abrupt, rapid proliferation, exogenous PDGF-AA independence, and the capacity to form invasive GBM-like tumors in p53 wild type, immunocompetent mice. This model offers the opportunity to study the nature and sequence of transformation-related events and potentially test novel therapeutics that target GBM in its earliest stages.

Acknowledgements

I have many individuals to thank for their support during the pursuit of my Masters. I would first like to thank Greg, for supporting me in my return to education and believing in my 'lab hands.' I feel fortunate to have had the opportunity to be mentored by Greg; his thoughtful guidance has helped me grow and become a true scientist. I would like to thank my committee members: John Kelly, for his positive and encouraging support; Steve Robbins for challenging me to think outside the box; and Sam Lawn, for his input, technical guidance and vital assistance with all things NanoString. I appreciate the mentorship from my committee as well as their enthusiasm for my project and science. I owe many thanks to Mike Blough and Alex Rogers for guidance and assistance in lab techniques as well as navigating graduate school. To those that have helped me with my cultures: Lori Maxwell, and summer students Alice Yuan and Matthaeus Ware. To Matthaeus, I owe a special thank you for his keen and positive attitude, and for asking me questions, which challenged me. Lori Maxwell did far more than just care for my cultures; she has been a friend, guidance counselor, and a voice of reason for me. Shahana Safdar, my fellow 'Fierce Girl,' helped me design thoughtful experiments and also played the role of friend and guidance counselor, often together with Lori at morning coffees, thank you both. To the Kelly lab, Martha Hughes and Candice Poon thank you for the chats, both science-related and not. To members of the Chan and Weiss labs, past and present: Jennifer Chan, Christian Perotti, Tanveer Sheihk, Rajiv Dixit, Colleen Anderson, Artee Luchman, Carlo Cusulin, Charles Chesnelong, and Rozina Hassam: thank you for technical assistance, troubleshooting and collaboration. Lastly, I need to thank Roman for supporting me in all ways possible during this sometimes crazy journey, and for understanding when I had to work, which was most of the time.

This thesis is dedicated to my parents, John and Pat DePetro for having always supported me in my decisions and telling me to do “what makes me happy.” Although neither of you could be here to see this, you would have been proud.

Table of Contents

List of Tables

List of Figures and Illustrations

List of Symbols, Abbreviations and Nomenclature

Symbol	Definition
AKT	protein kinase B
ALV-A	avian leukosis virus-A vector
ASCL1	Achaete-scute homolog 1
ASLV	Avian sarcoma leukosis virus
BTIC	brain tumor initiating cell
BTSC	brain tumor stem cell
CDK	cyclin-dependent kinase
CDKN2A	cyclin-dependent kinase inhibitor 2A
CDKN2B	cyclin-Dependent Kinase Inhibitor 2B
CHI3L1	chitinase-3-like protein 1
CNPase	2',3'-Cyclic-nucleotide 3'-phosphodiesterase
CpG	—C—phosphate—G—
Cre	tyrosine recombinase enzyme (causes recombination)
BSA	bovine serum albumin
DAB	3,3'-Diaminobenzidine
DAPI	4',6-diamidino-2-phenylindole
DDR	DNA damage repair markers
DLL3	delta-like protein 3
DNA	deoxyribonucleic acid
DTT	dithiothreitol

ECL	enhanced chemoluminescence
EGF	epidermal growth factor
EGFR	epidermal growth factor receptor
EGF/FGF	serum free media with EGF, FGF-2 and heparin
FACS	fluorescence-activated cell sorting
Fas	Fas cell surface death receptor
FGF	fibroblast growth factor 2
FGFR2	fibroblast growth factor receptor 2
FISH	fluorescence *in situ* hybridization
FITC	fluorescein isothiocyanate
GBM	glioblastoma multiforme
G-CIMP	Glioma CpG Island Methylator Phenotype
GF	growth factor
GFAP	glial fibrillary acidic protein
H&E	hematoxylin and eosin
IHC	immunohistochemistry
IDH1/2	isocitrate dehydrogenase 1/2
IRES	internal ribosome entry site
LOH	loss of heterozygosity
MADM	mosaic analysis with double markers
MAPK	mitogen-activated protein kinase
MET	hepatocyte growth factor receptor

MGMT	O-6-Methylguanine-DNA Methyltransferase
mTOR	mammalian target of rapamycin
NES	nestin
NF1	neurofibromin
NG2	neuron-glial antigen 2
NKX2-2	NK2 Homeobox 2
NSC	neural stem cell
OCT	optimal cutting temperature
OLIG2	oligodendrocyte transcription factor 2
OPC	oligodendrocyte progenitor cell
PBS	phosphate buffered saline
PDGF-AA -AB, -BB, -CC,-DD	platelet derived growth factor - dimerized ligand AA, AB, BB, CC or DD
PDGFR-α	platelet derived growth factor receptor alpha
PDK1	PDK1, 3-phosphoinositide-dependent protein kinase 1
PFA	paraformaldehyde
PI3K	phosphoinositide 3-kinase
PIK3CA	phosphatidylinositol-4,5-bisphosphate 3-kinase, catalytic subunit alpha
PIK3R1	phosphatidylinositol 3-kinase regulatory subunit alpha
PIP_2	phosphatidylinositol-4,5-bisphosphate
PIP_3	phosphatidylinositol-3,4,5-trisphosphate
PTEN	phosphatase and tensin homolog

RAD51	DNA repair protein RAD51 homolog 1
RAS	rat sarcoma protein
RB1	retinoblastoma protein
RCAS/TV-A	replication competent ASLV long terminal repeat with splice acceptor
rcf	relative centrifugal force
RIPA	radio-immunoprecipitation assay buffer
RNA	ribonucleic acid
RT-PCR	real-time polymerase chain reaction
RTK	receptor tyrosine kinase
SDS-PAGE	sodium dodecyl sulfate polyacrylamide gel electrophoresis
SFM	serum free medium
SLC12A5	solute carrier family 12 member 5
Sox 2	SRY (sex determining region Y)-box 2
SVZ	subventricular zone
SYT1	synaptotagmin-1
TBS	tris-buffered saline
TBST	tris-buffered saline with Tween 20
TCF4	transcription factor 4
TCGA	The Cancer Genome Atlas
TMZ	temozolomide
TP53	tumor protein 53
Tris	tris(hydroxymethyl)aminomethane

WHO	World Health Organization
WT	wild type
β3 Tubulin	tubulin beta-3 chain
γH2AX	gamma H2A histone family, member X

Chapter One: Introduction

1.1 Characterization of glioblastoma

1.1.1 Epidemiology and clinical features

Glioblastoma multiforme (GBM) is a fatal brain cancer, with a five-year survival rate of less than 5%. This disease most commonly occurs in older individuals, with a median age at diagnosis of 64 years. The survival rate generally decreases with older age at diagnosis: 75 to 84 year olds show the highest incidence (3.19 per 100,000) and lowest survival (1). The current standard treatment for GBM is maximal surgical resection followed by radiation therapy with concurrent and adjuvant temozolomide (2). Two subclasses of GBM have been recognized clinically and there is now evidence for genetic differences between the two. Histologically, *primary* and *secondary* glioblastomas appear similar, however they differ in their pathways of malignant progression. *Primary* is the more commonly observed type (90%), appearing to develop spontaneously, or *de novo*, without prior evidence of a less aggressive lower grade glioma (3). *Secondary* (10% of glioblastomas) is the stepwise development of glioblastoma which progresses from a low-grade diffuse astrocytoma or anaplastic astrocytoma. Over time, these lower grade gliomas acquire additional molecular alterations and develop into a high grade lethal GBM. *Secondary* GBM tends to manifest in younger patients (45 years old) and holds a better prognosis. The *primary* and *secondary* designations have molecular correlates and may be two distinct diseases from a therapeutic perspective although they look identical

down the microscope. The official classification system developed by The World Health Organization (WHO) uses degrees of cellularity, nuclear pleomorphism, mitotic activity, vascular proliferation and necrosis to grade gliomas and assigns a rating of I to IV with the most aggressive being grade IV (**Table 1**). The most aggressive, diffuse glioma of astrocytic lineage corresponds to GBM (4) (**Fig. 1**).

Table 1: WHO Grading system for gliomas

Grade	**Histological features**
Grade I (juvenile pilocytic astrocytoma)	Benign, slow growing lesions; often can be removed by resection and are least likely to recur
Grade II (astrocytoma)	Hypercellular, infiltrating lesions with low mitotic activity; can progress to higher grades of malignancy or recur
Grade III (anaplastic astrocytoma)	Hypercellular, mitotic with nuclear atypia and infiltrative capacity; usually treated with aggressive adjuvant therapy; high rate of recurrence
Grade IV (glioblastoma)	Hypercellular, mitotically active, vascularization and necrosis-prone lesions; usually treated with aggressive adjuvant therapy; rapid progression and fatal outcome

Adapted From Louis *et al*. Acta Neuropathologica. 2007 (5).

a **b**

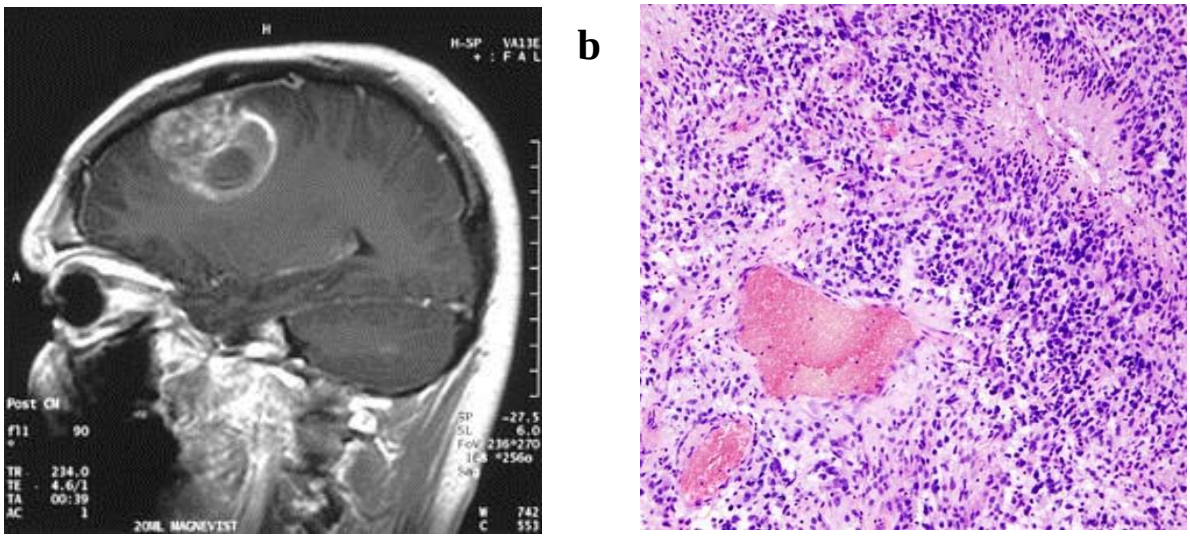

Figure 1: Histological characteristics of glioblastoma multiforme

Magnetic resonance image (MRI) of a sagittal view revealing a mass in the brain that was later shown to be glioblastoma (WHO grade IV astrocytoma) (**a**). Histopathological image of cerebral glioblastoma, hematoxylin & esoin (H&E) stain reveals a hypercellular tumor with areas of pseudopalisading necrosis (**b**) (6).

1.1.2 Molecular features of clinical subtypes

1.1.2.1 Primary GBM

The majority of GBM are *primary*. While *primary* GBMs may present without previous clinical, radiological, or histopathological evidence of a preceding low grade tumor, these are not simple molecular diseases at diagnosis. Instead, *primary* GBM at initial diagnosis is a complex and heterogeneous genetic disease but with certain recurring alterations. *Primary* GBM is characterized by loss of heterozygosity of 10q (70%), epidermal derived growth factor receptor (*EGFR*) amplification (36%), and loss of tumor suppressor function including p53, $p16^{INK4a}$, PTEN and RB1 (7). Changes in growth factor signaling from receptor tyrosine kinases (RTKs) are characteristic molecular alterations in GBM (**Fig. 2**). In *primary* GBM, aberrant RTK signaling is most commonly observed in EGFR. The *EGFR* gene (7p12) is frequently amplified and is also known to have a deletion (exons 2-7) in approximately 50 percent of *EGFR* amplified GBMs (8,9). This deletion leads to loss of a portion of the extracellular regulatory domain of the protein, which then promotes persistent receptor activation even in the absence of ligand. This mutant form of EGFR is referred to as EGFR variant III (EGFR-vIII) (9). While EGFR is the RTK most commonly associated with *primary* GBM, there is evidence that it may arise from a clinically silent lower grade lesion and may share common initiating pathways with *secondary* GBM (10). Primarily due to the shortened clinical course, little is known about the initiation and the sequence of genetic alterations in the early stages of *primary* GBM (11). Other RTKs such as platelet derived growth factor (PDGFR-α and PDGFR-β) and

MET have been shown to be co-activated in *primary* GBM (12) and may prove to play a vital role in the early and silent stage, warranting further investigation.

1.1.2.2 Secondary GBM

Secondary glioblastomas develop gradually, through progression from low-grade or anaplastic astrocytoma. The first alteration in the pathway to *secondary* GBM is thought to be a heterozygous mutation of isocitrate dehydrogenase 1 or 2 (*IDH1/2*) (13). *IDH1/2* mutations are observed far more frequently in *secondary* GBM (73%) than in *primary* (3.7%) (14). Accordingly, IDH1/2 mutational status is now used as a diagnostic marker to differentiate the *primary* versus *secondary* clinical subclass of GBM. Mutation and subsequent loss of function of the tumor suppressor protein p53, either directly or indirectly through the p53 pathway, is considered to be another defining feature of *secondary* GBM (4). *TP53* mutations are an early and common genetic alteration in *secondary* GBM, found to be present in 60% of precursor, WHO grade II astrocytomas (11). Similar to *primary* GBM, loss of tumor suppressors $p16^{INK4a}$, PTEN and RB1 are observed in *secondary* GBM as well (15). Followed closely behind the loss of p53 is aberrant signaling through PDGFR-α. Over-expression of the PDGF receptor (4q11-12) and ligand is a common alteration in *secondary* GBM (16,17). *PDGFRA* is the second most common amplified RTK gene, however *PDGFRA* genetic alterations are also observed in the form of intrachromosomal deletion and activating point mutation. In an unselected series of GBMs, most of which may have been *IDH* wild type (WT), Ozawa *et al*. found that 40% of GBMs with amplification of *PDGFRA* were also *PDGFRA*[4]*8,9*

mutant. An in-frame deletion of 243 bp in exons 8 and 9 of the extracellular portion of *PDGFRA* leads to the formation of *PDGFRA*$^{\Delta}$*8,9* (17). This raises the possibility that alterations of the PDGFR-α signaling pathway may be features of both *primary* and *secondary* GBM.

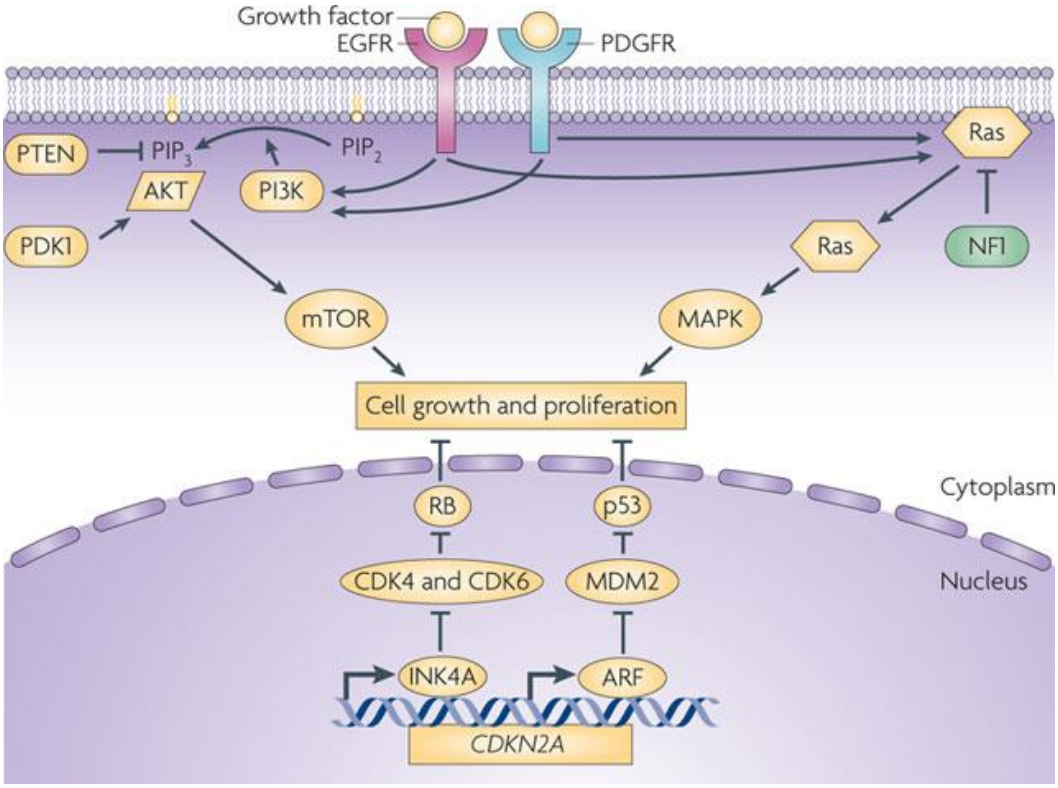

Figure 2: Schematic diagram of RTK oncogenic signaling pathways in GBM

The downstream pathways of EGFR and PDGFR overlap: they both activate the PI3K–AKT–mTOR and Ras–MAPK signaling networks. Activation of these RTKs results in phosphorylation of many downstream substrates including other kinases and transcription factors, which stimulate proliferation, survival and differentiation. (Adapted from Huse and Holland (18)).

1.1.3 Molecular subtypes based on genomic alteration

The molecular heterogeneity within both the *primary* and *secondary* clinical subtypes has prompted several groups to explore further classification of GBM. Based on gene expression, GBM can be divided into distinct subtypes, each harboring different genetic abnormalities; however unlike the *primary* and *secondary* clinical distinction, it is not clear that these subtypes have clinical relevance. Using unsupervised clustering, Phillips *et al*. classified GBM into three subtypes, defined by expression of genes related to survival: ***proliferative*** **-** amplification or mutation of *EGFR*; ***proneural*** **-** mutations in *TP53* and *PDGFRA*; and ***mesenchymal*** **-** mutations in *TP53, PTEN* and *NF1* (19). Using unbiased genomic analyses of a large cohort of clinical GBM specimens Verhaak *et al*. classified GBMs into four subtypes based on gene expression profiles: ***proneural***, ***neural***, ***classical***, and ***mesenchymal*** (10). In The Cancer Genome Atlas Network (TCGA) Phillips' proliferative group is divided into neural and classical subtypes.

In the Verhaak *et al.* scheme, the ***proneural*** subtype of GBM is associated with genetic alterations including *TP53* mutation (54%), *PDGFRA* amplification (35%) and mutation (11%), *IDH1* Mutation (30%), *PI3K* (*PIK3R1/PIK3CA*) mutation (27%), *CDKN2A/CDKN2B* deletion (56%), *EGFR* amplification (17%) and mutation (19%), and predominant expression of oligodendrocyte markers such as *PDGFRA*, *NKX2-2*, and *OLIG2*, and proneural development genes such as *SOX2*, *DLL3*, *ASCL1*, and *TCF4* (10). The ***neural*** subtype is characterized by *PTEN* deletion (96%) and mutation (21%), *EGFR* amplification (67%), and mutation (26%), *ERBB2* mutations (16%), *CDKN2A/CDKN2B*

deletion (71%), *PI3K* (*PIK3R1/PIK3CA*) (16%) and *IDH1* mutations (5%), and predominant expression of neuronal markers such as *SYT1*, and *SLC12A5* (10). The ***classical*** subtype is associated with signature genetic aberrations such as chromosome 7 amplification and chromosome 10 loss (100%), *EGFR* amplification (95%) and mutation (55%), *CDKN2A/CDKN2B* deletion (95%), *PTEN* deletion (100%), as well as predominant expression of neural stem cell markers such as *NES* (encoding Nestin) (10). The ***mesenchymal*** subtype is characterized by the presence of signature genetic alterations such as *NF1* deletion (38%) and mutation (37%), *PTEN* mutation (32%), and expression of mesenchymal markers such as *CHI3L1*, and *MET* (10) (**Fig. 3**).

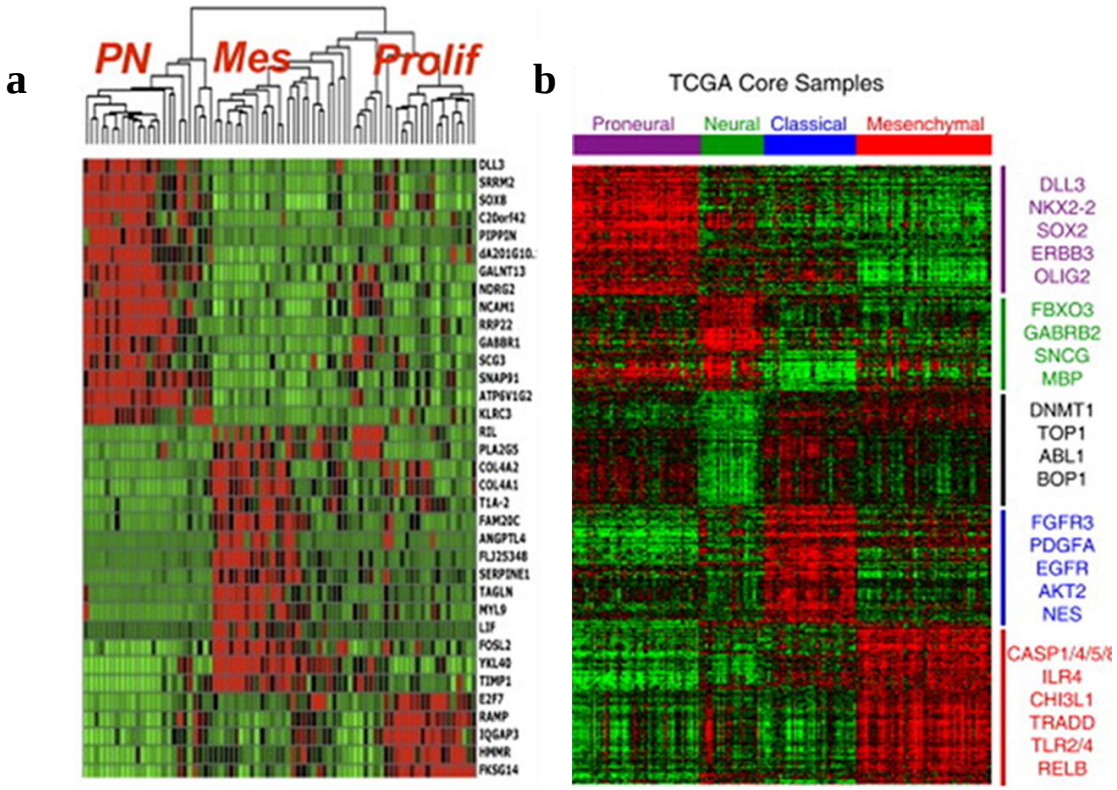

Figure 3: GBM subtypes based on gene expression profiles and genomic alterations
Phillips *et al.*'s subtyping (**a**) (19) and Verhaak *et al.*'s (**b**) (10)

1.1.4 Epigenetic alterations in GBM

Patterns of gene methylation have been the subject of intense study in glioma, including GBM. Documentation of methylation patterns in GBM has contributed to the characterization of subtypes and more importantly has helped improve our understanding of how a GBM will respond to treatment. GBMs with extensive DNA methylation in CpG islands, or stretches of DNA in which high GC (guanine and cytosine) content are found have been characterized by TCGA and termed G-CIMP (Glioma with CpG Island Methylator Phenotype) (20). Using methylation arrays TCGA found that methylation within CpG islands in gene promoters occurs mainly within *secondary* GBM that also harbor mutant *IDH1/2*. Thus far, no *IDH1/2* WT gliomas with the G-CIMP phenotype have been identified (21). Promoter methylation of *MGMT* is strongly correlated with *IDH* mutant *secondary* GBM, however *MGMT* methylation also occurs in the absence of *IDH* mutations (21). In addition, promoter methylation of the tumor suppressor *RB1* is approximately three times more common in *secondary* GBM than in *primary* (22).

1.1.5 Molecular diagnostics of glioma have not changed management of GBM

Although it is an incredibly heterogeneous disease, current standard therapy for GBM remains relatively uniform. Molecular diagnostics which have attempted to guide and form new treatment options have only been moderately successful in predicting response to treatment. Molecular prognostic tests have been developed such as testing for methylation of the *MGMT* promoter in GBM to predict response to temozolomide (TMZ)

chemotherapy (23), but at this point in time treatment remains the same regardless of the result and predicted response to treatment. Within the subtyping defined by Phillips *et al*., the proliferative and mesenchymal subtypes displayed the shortest overall survival, and proneural GBM a more favorable clinical outcome (19). The proneural subtype did not take into account *IDH* mutational status, as *IDH* mutations were not discovered until 2008 and thus the more favorable outcome may have been due to *IDH* mutations. Unfortunately, these prognostic gene signatures have yet to translate into effective treatments. Despite increased understanding and advancement in surgical procedures, the outcome for patients with GBM has not changed radically in the last few decades, indicating a need for better understanding of tumor initiation that can more effectively guide treatment.

1.2 Cancer Cell of Origin

1.2.1 Oligodendrocyte precursor cells, and glioma cell of origin

Many studies have investigated the glioma cell of origin, suggesting brain tumor stem cells (BTSCs) and brain tumor initiating cells (BTICs) as highlighted by Singh *et al*. (24,25). The work by Singh *et al.* suggests neural stem cells (NSCs) as the cell of origin; however, it is difficult to discern if the NSC phenotype of glioma-prone cells mirror that of the original cell type or if such characteristics were acquired during transformation (26). In addition, while promoter targeted systems are somewhat better than non-targeted retroviral systems that do not allow for identification of transduced cells, it remains

challenging within these systems to distinguish between the normal cells from which the tumor originates, and cells that are capable of de-differentiation (26). Despite the challenges associated with deriving the tumor cell of origin by analyzing end stage tumors, recent studies have implicated oligodendrocyte progenitor cells (OPCs) as a candidate cell of origin for gliomagenesis (27). Through a novel double labeling, lineage tracing technique called mosaic analysis with double markers (MADM), Liu *et al.* were able to induce a small number of LOH aberrations and track which cells acquired mutations (27). They found that while NSCs possessed the ability to acquire mutations; in fact, it was the OPC population that acquired mutations and expanded into gliomas (27).

While the cell of origin can be inferred through model systems, the molecular features of the glioma cell of origin remain to be defined. Studies that investigated the role of PDGFR-α in oligodendrocyte production have shown that mice null for PDGFR-α produced very few oligodendrocytes (28), while overproduction of PDGFR-α resulted in the overproduction of both OPCs and oligodendrocytes (29). Overexpression of PDGF in the brain leads to excessive production of OPCs and has been shown in some models to result in oligodendroglioma-like tumors (30). In 2004, Chojnaki and Weiss used the mouse neurosphere culture system to identify two distinct populations of cells responsive to EGF and PDGF in the embryonic mouse brain (31). These distinct populations were characterized by mutually exclusive EGFR and PDGFR-α expression, with the PDGF-responsive progenitor cells capable of differentiation into oligodendrocytes and neurons, but not astrocytes (31). However, in the presence of PDGF, differentiated mature

astrocytes have been shown to acquire a stem-like phenotype, specifically the ability to self-renew (32). This identifies yet another potential reservoir of cancer-prone cells.

Similar to the work by Uhrbom *et al.* (1998) Assanah *et al.* tested the tumorigenic potential of adult glial progenitors by injection of PDGF-B retrovirus in rat corpus callosum in which the resulting GBMs showed NG2 positive OPCs (33). Additional work showed that upon injection of retroviral PDGF-B in newborn rats, the differentiation fate of neural stem cells (NSCs) was altered. OPCs expressed PDGFR-α, NG2 and OLIG2, and did not differentiate into mature oligodendrocytes (34). These studies emphasize the heterogeneous nature of gliomagenesis, as the cellular plasticity of both progenitor and mature cells in combination with a variety of oncogenes can result in a phenotypically similar brain tumor. Thus, the answer may not lie in chasing the cell of origin, rather in studying the environment that allows cells to become cancerous.

1.3 Models of GBM

1.3.1 Types of models

The most commonly used mouse model of GBM employ **xenografts**, using cell lines such as U87 and U251 which were established as cultures from human GBMs (35). Brain tumor initiating cell lines such as these faithfully form tumors when orthotopically implanted in immune compromised mice. However as the importance of the immune system in tumor formation is now more fully appreciated (36), models which do not

require a deficient immune system are necessary to recapitulate the human disease. Also, these human derived cell lines are most often cultured in the presence of serum which can change their characteristics (37). Gliomas can be induced in rodents through exposure to **chemicals** such as the *N*-nitroso compounds, animal models have been utilized since the 1970s, and most commonly in rats (38). These models are used less frequently though as they have their limitations and have been criticized for being dissimilar histologically to human GBM (36,39). Lastly, **genetically engineered** models allow for a level of control not available in other models. Mutations can be delivered with precision to specific cells or tissues, and at a specified time. Another advantage to these models is that the immune system can remain fully intact. The drawback lies in the lack of heterogeneity, and the technical difficulty of studying the initiating events and the earliest stages of glioma (36).

1.3.2 PDGF and GBM - Modeling the human disease

Several models of PDGF-driven GBM have been created, most commonly in transgenic mice through forced expression of PDGF, and most often using PDGF-B, which promiscuously binds all forms of the PDGF receptors. In general, overexpression of PDGF in the brain leads to excessive production of OPCs and has been shown in some models to result in oligodendroglioma-like tumors (30). Most often, available PDGF models do not incorporate p53 status in their investigation. There are very few models that investigate the specific combination of PDGF-AA driven gliomagenesis in a p53 null background. [As an aside, gliomas can also be induced experimentally by driving EGFR

expression. However EGFR overexpression alone is not sufficient and must be combined with other losses such as deletion of p53 and CDK4 or Ink4/Arf (40,41).]

1.3.3 PDGF ligand and receptor physiology

The PDGF growth factor family consists of four members, PDGF-A, -B, -C, and -D(42). As monomers, the PDGFs are inactive, however they become active when they dimerize to form disulphide bond linked homo- or heterodimers (42). The five active isoforms, PDGF-AA, PDGF-AB, PDGF-BB, PDGF-CC and PDGF-DD have the ability to bind to one of two RTKs, PDGFR-α or β, which can also dimerize to form PDGFR-αα, PDGFR-ββ, and PDGFR-αβ (42,43) (**Fig. 4**). Of the PDGF ligands, PDGF-BB is the only isoform that binds and activates all three types of receptor dimers, whereas PDGF-AA has only been shown to activate the PDGFR-αα dimer (44,45). This binding specificity is important in the model that is described and characterized in this thesis.

Numerous studies have demonstrated expression of PDGF-AA, PDGF-BB, and the two PDGF RTK subunits (PDGFR-α and β) in glioblastomas. All forms of PDGF ligands and receptors have been shown to be expressed in glioblastoma (30). Specifically, PDGF ligands (A–D) show an increase in expression in approximately 30% of glioma surgical samples and cell lines (8,16,46). Differential expression of the two receptor types may change the response of the cells to exogenous PDGF since the α receptor binds both A and B chains of PDGF, while the β receptor recognizes only the B form (47–49). Evaluation of receptor distribution in tumors has shown that glial tumor cells are

primarily activated through PDGF/PDGFR-α autocrine and paracrine loops, while the tumor vasculature is stimulated through PDGFR-β (16). Several groups have formed a link between increased expression of PDGFR-β in tumor vasculature (50) and the increase in invasion potential in cultured human cell lines (51). Furthermore, an increase of secreted PDGF-B in conditioned media was shown to promote migration of PDGFR-β expressing endothelial cells (52). Even in models where tumor formation is PDGF-B driven, high levels of PDGF-A are found to be secreted in the media (33). Thus, there is increasing evidence in support of PDGF-A and -B working cooperatively, with excess PDGF-A signaling driving tumor formation and PDGF-B promoting invasion and angiogenesis.

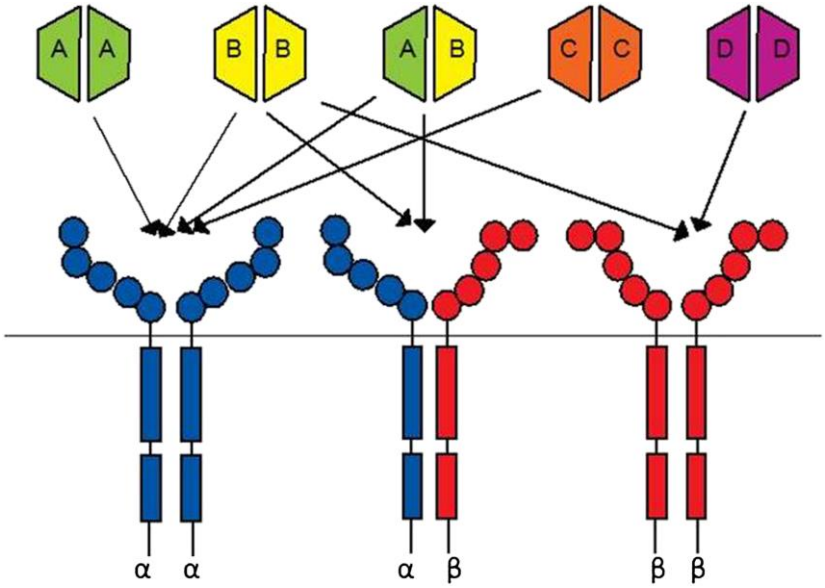

Figure 4: Schematic of known PDGF receptor and ligand interactions

PDGF ligands bind either PDGFR-α or PDGFR-β or the α/β heterodimer. Arrows indicate proven *in vitro* ligand-receptor interactions. (Adapted from Donovan et al. (45))

1.3.4 Genetic modeling of gliomas via PDGF-BB

1.3.4.1 The earliest PDGF mouse model

The first attempt to model PDGF-driven glioma was by Deinhardt in 1980 (53). The unpublished model used newborn marmosets cranially injected with SSV (simian sarcoma virus) with the *v-sis* oncogene. This model was presented in a review by Nistér and Westermark which described the resulting gliomas as indistinguishable from human tumors (54). Further work by Uhrbom, Nistér and Westermark utilized a PDGF-BB retrovirus which resulted in 40% of mice developing highly malignant brain tumors (55).

1.3.4.2 The RCAS system

Since these early retroviral models, genetically engineered mouse models have been used in a variety of ways to study the dysregulation of PDGFR signaling through overexpression of the PDGF-BB ligand. Holland *et al*. (1998) was the first group to employ the RCAS/TV-A delivery system to model human glioma in mice (40,56). The RCAS/TV-A system employs an avian retroviral vector called RCAS (Replication Competent ASLV long terminal repeat with Splice acceptor) (57). The RCAS vector is derived from the avian leukosis virus-A (ALV-A) vector. Initially, this retroviral vector was only used in avian systems until the cloning of the TV-A gene allowed access to the ALV-A receptor, and thus a suitable cell receptor for viral entry in mammalian systems (57). Mouse transgenic lines that express the TV-A cell surface receptor are therefore susceptible to RCAS virus infection and introduction of a gene of interest (57).

1.3.4.3 Targeting cells of a specific lineage

Under the control of a cell type specific promoter, PDGF-BB expression has been directed to cells expressing various lineage markers including *Nestin* (Ntv-a), *Gfap* (Gtv-a) and *CNPase* (Ctv-a) expressing cells (40,56,58). The resulting tumors in these systems were characteristic of oligodendrogliomas, however *Gfap* and *CNPase* targeted mice occasionally developed mixed oligoastrocytomas (32,58). In 2001, Dai *et al.* investigated the tumorigenic potential of differentiated cells with PDGF-BB overexpression by utilizing the RCAS/TV-A system (32). By targeting either *Nestin*-expressing neural progenitors or *Gfap*-expressing astrocytes in a p53+/+ background, they found neural progenitor targeted gene transfer resulted in 60% of mice developing oligodendroglioma-like tumors, whereas astrocytic targeted gene transfer resulted in tumor formation in only 40% of mice (32). In addition, they found loss of *Ink4a/Arf*, while not required for gliomagenesis, decreased latency and enhanced malignancy (32). Several groups have shown similar results in that tumor latency decreases in PDGF-induced glioma models with the addition of another genetic aberration such as loss of *Ink4a/Arf*, *TP53*, or *PTEN* (59–63). Through *in vitro* work, Dai *et al.* also demonstrated that forced overexpression of PDGF-BB increased proliferation of glial precursors as well as de-differentiated *Gfap* expressing astrocytes into cells characteristic of glial precursors (32). This suggests that the induced autocrine signaling of PDGF-BB could be impairing differentiation potential and promoting tumorigenesis. Impaired differentiation potential referring to cells with the ability to maintain stem-like characteristics and remain in an immature state, a known hallmark of cancer (64).

1.3.4.4 Inclusion of a p53 null background in a PDGF-BB driven model results in tumors more histologically similar to human GBM

This combined effect of p53-loss and dysregulation of PDGFR signaling was investigated by Hede *et al*. (2008) through genetically engineered mouse models. GFAP targeted transgenic mice were generated using a construct containing IRES (internal ribosome entry site) (65). In their model, mice only developed tumors when PDGF-BB was overexpressed on a p53 null background (65). Although Hede *et al*. did not find that PDGF-BB overexpression alone was sufficient for tumor formation, they did show that on a p53 null background the tumors resembled human-like GBM (65), rather than oligodendroglioma, which is the predominant finding in RCAS/TV-A generated PDGF-BB driven models. The resulting GBM-like tumors were found to express a variety of antigens, suggesting contributions from both astrocytic and oligodendroglial lineage (65). Furthermore, the PDGF-BB/p53 null tumors mainly expressed the PDGF-BB transgene in the tumor cells rather than in the vasculature (65). From the PDGF-BB transgene expression pattern, the group deduced this is reflective of both autocrine and paracrine stimulatory loops similar to those in human tumors (65), which show PDGFR-α localization on glial tumor cells, and PDGFR-β on the vasculature (16). Their results suggest that overactive PDGFR-α signaling in these tumors is not due to overproduction of the PDGF-BB ligand.

1.3.4.5 A PDGF-BB retroviral model which retains its proneural phenotype

In a model which utilized both retroviral expression of PDGF-BB and cell cultures, Sonabend *et al*. formed a murine model that resembled proneural glioma (61). PDGF-IRES-Cre retrovirus was injected into the subcortical white matter of adult *Pten* and *Tp53* floxed transgenic mice. The resulting tumors were cultured in PDGF-AA supplemented media and subsequently grafted into new adult *Pten* and *Tp53* floxed transgenic mice (61). They were able to show the retention of the proneural phenotype *in vitro* in up to 6 passages (61). Using the same model, Sonabend *et al.* examined the temporal progression of tumorigenesis by sequencing tumor samples from three time points. They found that the proneural phenotype preceded the accumulation of gene deletions, deletions that were highly consistent by the time the tumors reached end-stage (66). While highly insightful as to the non-random acquisition of mutations in proneural glioma, the shortened time span of tumor formation is likely not capturing early and initiating alterations.

1.3.5 Glioma modeling via PDGF-AA

1.3.5.1 Investigation of A, C and D ligands is less common

Only a few models have used the PDGF-AA ligand compared to PDGF-BB in their models, and even fewer have explored the role of the more recently identified PDGF-C and -D ligands. Lokker *et al.* demonstrated that these PDGFs are also routinely expressed in glioma cell lines and in primary glioblastoma tissues along with their cognate PDGF receptors, indicating their potential role in the development of brain tumors (67).

1.3.5.2 PDGF-AA in a non-retroviral system

Two groups have used the PDGF-AA ligand in a non-retroviral system in order to assess the expression of astrocyte lineage marker GFAP in adult human PDGFR-α-expressing neural precursors. While the groups had conflicting findings with respect to the co-expression of GFAP and PDGFR-α in the adult mouse brain, the infusion of PDGF-AA into the lateral ventricle over 6-7 days resulted in glioma-like masses (68,69).

1.3.5.3 Expressing PDGF-AA in astrocytic cells

In another transgenic mouse model Nazarenko *et al.* (2011) overexpressed long form PDGF-AA (PDGF-A_L) in the astrocytic cells of mice by a human *GFAP* promoter. The PDGF A-chain gene contains seven exons, of which, two PDGF-A isoforms exist as a result of alternative splicing; the long form contains exon 6, the short form does not (70). Both the short and long PDGF isoforms are found in normal tissue, however the short-form is more prevalent (71,72). In contrast, PDGF-A_L has been characterized in human glioma cells (71,72), implicating this form of the protein in tumorigenesis (70). In their study, PDGF-A_L-overexpressing mice developed glioma-like lesions (73). The tumors that formed were a mixed population of GFAP+ astrocytic and OPC-like cells which expressed PDGFR-α, NG2 and OLIG2 (73).

1.3.6 PDGF-driven models which include loss of p53

1.3.6.1 An early investigation of p53 and PDGFR-α

As p53 mutation is a known early event in most GBM, and thus an integral step in the progressive pathway to GBM (74,75), it is important to address this mutation in a workable mouse model. Successful modeling of GBM might require a provision for inactivation of p53 which is not tumorigenic in the brain in isolation but permissive. A study by Hermanson *et al.* (1996) showed a high correlation between loss of heterozygosity of chromosome 17p13, the genomic location of *TP53*, and PDGFR-α amplification in *secondary* GBM progression. At the time and as a result of their studies, their hypothesis was that p53 loss of function may have an oncogenic effect only in the presence of PDGFR-α amplification (76).

1.3.6.2 Mathematical modeling leads to a PDGF-AA/p53 null mouse model

Recently, Ozawa *et al*. delved further into the biology of non-GCIMP subgroup of GBM (20). Their findings suggest that most non-GCIMP mesenchymal GBMs arise as, and evolve from, a proneural-like precursor. By first using mathematical approaches and data from TCGA, they identified gains of chromosome 7 and losses of chromosome 10 as candidate 'first events' in the genesis of human GBM. In their conceptualization of GBM pathogenesis, these early alterations of chromosomes 7 and 10 are followed by loss of function of CDKN2A and p53. Further analysis suggested that "elevation in the expression of PDGFA" on chromosome 7, might be an important initiating event. They

then showed *in vivo* in the mouse brain that loss of p53 function when combined with overexpression of PDGF-AA through their RCAS/TV-A system results in lethal GBM-like tumors of the proneural subtype.

In summary, since the first mouse model of GBM in 1980 (53), there have been many well-designed models which have investigated the PDGF ligands as specific drivers (32,40,54–56,73), and those which have incorporated loss of a tumor suppressor such as p53 or PTEN (59–63,65). These models can mimic the phenotype of human GBM through genetic manipulations that incorporate one or two aberrations found in the human disease, however this method of generating models does not allow for easy investigation of the natural progression of GBM.

1.4 Synopsis of our PDGF-AA initiated model of GBM

We have developed a mouse model of GBM based on two key molecular alterations commonly found in *primary*, *IDH1* WT **proneural** GBM: mutated **p53** and activation of **PDGFR-α**. In this model, neurosphere cultures established from the subventricular zone (SVZ) of p53 null mice transform *in vitro* after approximately 100 days in PDGF-AA. These transformed cells yield GBM-like tumors in the brains of p53 WT immunocompetent mice. In contrast, p53 null cells cultured in EGF and FGF, rather than PDGF-AA, do not transform (77) (**Fig. 5**). Our *in vitro* system allows for investigation of

the early events that contribute to the transformation of PDGF-AA responsive cells, a feature that is lacking in currently available models of GBM.

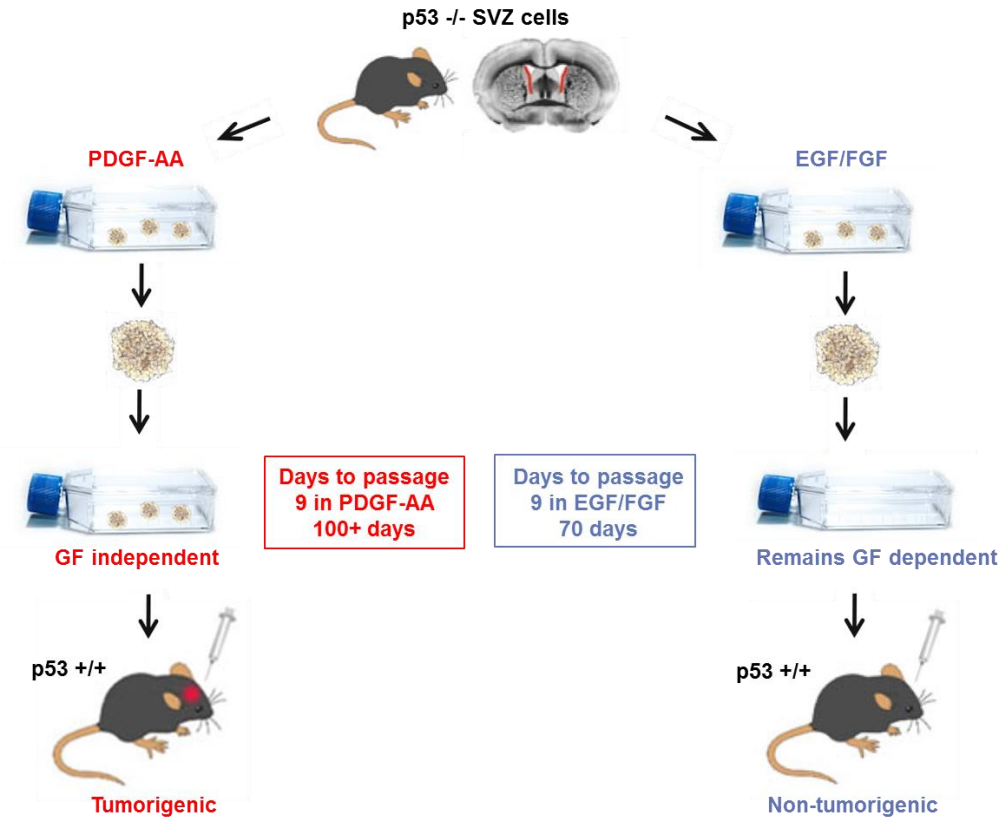

Figure 5: p53 null, PDGF-AA initiated model of glioblastoma multiforme

Chapter Two: Aims and Objectives

My project aims to characterize the p53 null cells that have become exogenous PDGF-AA independent after approximately 100 days in culture and compare them to: i) pre-transformed PDGF-AA grown cells and ii) p53 null cells cultured in EGF and FGF. My project also aims to characterize the tumors that form in the brains of p53 WT immune competent mice. My underlying hypothesis was that EGF/FGF and PDGF-AA selected for different populations of SVZ cells with different receptor and marker profiles.

Objectives:

1.) Investigate which growth factor receptors are expressed in p53 null PDGF-AA grown cells pre- and post-transformation and as compared to the growth factors, which are expressed in p53 null EGF/FGF grown cells that do not transform.

2.) Investigate the evolution of the neural stem cell/lineage marker expression of the p53 null PDGF-AA grown cells over time and compared to p53 null EGF/FGF grown cells.

3.) Investigate whether EGF/FGF cultured cells retain the capacity to transform in PDGF-AA.

4.) Analyze the *in vivo* GF receptor, lineage marker, and gene expression profiles of the tumors that form in p53 WT immune competent mice that have been grafted with PDGF-AA transformed cells.

Chapter Three: Materials and Methods

3.1 Mice

Eight to twelve-week-old male (p53-/-(null) B6.129S2-Trp53tm1Tyj/J and female p53+/+ (WT) C57BL/6J) mice were purchased from The Jackson Laboratory for neurosphere culture and syngeneic intracranial implantation of neurospheres, respectively. *TP53* null mice are generated by replacing exons 2-6 of p53 with a neomycin cassette. All experiments involving mice were conducted in accordance with animal care procedures at the University of Calgary.

3.2 Neurosphere Culture

Mice were sacrificed by cervical dislocation and brains removed under sterile conditions. Neurosphere cultures were established as described by Chojnacki and Weiss (78). To ensure sufficient cell numbers in the early passage PDGF-AA cultures, where rates of cell death were extraordinarily high (see below), SVZ tissue from three mice was combined; tissue from only one mouse was required to establish the EGF/FGF cultures. SVZ tissue was micro-dissected and cut into small pieces. Tissue was transferred to serum-free culture medium (SFM; NeuroCult™ NSC Basal Medium, Stem Cell Technologies, 05700) and digested enzymatically for 15 minutes (1.33 mg/mL Trypsin, Sigma, T1005; 0.2 mg/mL Kynurenic Acid, Sigma, K3375; and 0.67 mg/mL hyaluronidase, Sigma, H3884). Tissue pieces were triturated by plastic pipette tip (P1000) until the solution was cloudy and pieces no longer visible. After centrifugation at 600 rcf for 6 minutes,

enzyme-containing media was replaced with SFM supplemented with Trypsin-inhibitor (Sigma, T6552, 0.5 mg/mL), followed by re-suspension in enzyme-free SFM. Next, 10,000-20,000 cells/mL were plated and incubated for 3 weeks at 37°C in SFM containing human PDGF-AA (20 ng/mL; Peprotech 100-13A) or EGF (20 ng/mL; Peprotech AF-100-15) plus FGF-2 (FGF; 20 ng/mL; Peprotech AF-100-18B) and heparin sulfate (2 μg/mL; Stem Cell Technologies 07980). Spheres were passaged at a density of 10,000-20,000 cells/mL, or when diameter reached 2 μm, or every 2-3 weeks. After cultures became PDGF-AA independent, cells were plated at 20,000 cells/mL in fresh SFM with no exogenous growth factors and were passaged once a week.

3.3 Cell Proliferation Assay

Cell proliferation was analyzed for cultures in both PDGF-AA and EGF and FGF-2 plus heparin sulfate at every third passage (ie. P0, P3, P6, P9 or P[9], P12 or P[12], and P15 or P[15]). Cells were incubated for 2.5 hours with 5-ethynyl-2'-deoxyuridine (EdU), a DNA analog that is incorporated into DNA during active DNA replication and synthesis. Following labeling, spheres were dissociated into single-cell suspension and fixed with 4% paraformaldehyde (PFA) for 30 minutes. After fixation, cells were blocked and permeabilized in 1X PBS with 10% horse serum and 0.1% TritonX100 for 30 minutes. Cells were visualized by incubation for 30 minutes with Pacific-Blue labeling, which binds to the EdU DNA analog, and sorted with fluorescence-activated cell sorting (FACS). Experiment was repeated in triplicate. (Method performed by C. Binding and presented here with permission).

3.4 Cell Death Assay

The extent and nature of cell death was examined using cultures in both PDGF-AA and EGF/FGF at every third passage (ie. P0, P3, P6, P9 or P[9], and P12 or P[12]). Spheres were dissociated into single-cell suspension and resuspended in binding buffer (Invitrogen). Cells were then incubated with AnnexinV, an indicator of apoptosis, and/or propidium iodide (PI) (Invitrogen), an indicator of dead cells, for 15 minutes in the dark. Utilizing the fluorescein isothiocyanate (FITC) signal detector for AnnexinV and the phycoerythrin emission signal detector for PI, cells were visualized and sorted with FACS. Experiment was repeated in triplicate. (Method performed by C. Binding and presented here with permission).

3.5 Western blot

Cell pellets were collected from sphere cultures growing in PDGF-AA or EGF/FGF. Protein was extracted from cell pellets using RIPA buffer (50 mM Tris, 150 mM NaCl, 0.1% SDS, 0.5% NA Deoxycholate, 1% NP-40) supplemented with protease and phosphatase inhibitor cocktails (Thermo Scientific 78415 and 78420) at a ratio of 10 μl per 1 mL of RIPA lysis buffer. Samples were triturated in the RIPA master mix, incubated at 4°C for 1 hour and centrifuged at 16,000xg for 20 minutes; supernatants were removed and stored at -80°C. Protein concentrations were quantified with the Bio-Rad protein assay (Bio-Rad 500-0006) with the UltraSpec 3100 Pro UV/Visible spectrophotometer. Reduced protein samples (25 μg) were prepared via incubation with NuPage LDS buffer (NP0008) and 1M DTT at 70°C for 10 minutes. Proteins were loaded

beside Novex Pre-Stained Protein Standard (Life Technologies LC5800). Proteins were resolved on a 4-12% gradient Bis-Tris gel (Life Technologies BG04120) using SDS-polyacrylamide gel electrophoresis (SDS-PAGE) in 1X MOPS SDS running buffer (Life Technologies, NP0001) at 200V for 50 minutes. After resolution, proteins were transferred to nitrocellulose using NuPage Transfer Buffer (Life Technologies NP0006-1) at 30V for 60 minutes. After transfer, membranes were incubated in a blocking buffer solution (1X TBS, 5% BSA, 0.1% Tween or 5% skim milk, 1X TBS, 0.1% Tween) for 1 hour at room temperature, then overnight with primary antibody at 4°C. Following incubation, membranes were washed 3 times for 10 minutes in blocking buffer and re-incubated with secondary antibody at room temperature for 1 hour. Immunoblots were washed 3 times for 10 minutes in blocking buffer and rinsed briefly with 1X PBS prior to a brief incubation in enhanced chemoluminescence (ECL) reagent (PerkinElmer NEL10400) and film exposure (GE Healthcare 28906835). The following antibodies were used: ***Primary*** - anti-PDGFR-α (1:1000; Cell Signaling 3174); anti-EGFR (1:2000; Cell Signaling 4267); anti-OLIG2 (1:2000; Millipore MABN50); anti-NESTIN (1:2000; Millipore MAB353); anti-NG2 (1:1000; Cell Signaling 4235); anti-GFAP (1:1000; Millipore MAB360); anti-β3-Tubulin (1:1000; Cell Signaling 4466); anti-β-Actin (1:5000; Cell Signaling 3700); Anti-FGFR2 (1:1000; Abcam 10648 and 109372); and Met (1:1000; Santa Cruz sc-162-R) ***Secondary*** - goat anti-mouse IgG-HRP and goat anti-rabbit IgG-HRP (1:2000; Santa Cruz sc-2005 and sc-2004, respectively).

3.6 Real-time PCR

Cell pellets were collected from sphere cultures growing in PDGF-AA or EGF/FGF. RNA was isolated from samples using a DNA/RNA extraction kit (Qiagen 80204), as per manufacturer instructions. RNA (50 ng) was reverse transcribed with Sensiscript RT Kit (Qiagen 205211) and random primers (Invitrogen 48190-011) to synthesize cDNA. Using probes for PDGFR-α and EGFR (Life Technologies Mm00440701_m1 and Mm00433023_m1), 2 μL of cDNA was used to detect and quantify gene expression relative to GAPDH (Life Technologies 4352339E). Real-time PCR was performed on the 7900HT Fast Real-Time PCR system (Applied Biosystems).

3.7 Fluorescence immunocytochemistry

3.7.1 Cell adherence via laminin

Spheres from PDGF-AA or EGF/FGF cultures were dissociated into single cells and plated at a density of $1x10^5$ cells/coverslip on poly-L-ornithine and laminin-coated coverslips (1:10 and 1:100; Sigma P4957 and Sigma L2020) and allowed to adhere for 1 to 2 hours at 37°C in the appropriate media with growth factors. Adherent cells were subsequently fixed for 20 minutes in 4% PFA.

3.7.2 Cell adherence via cytospin

In order to assess cells without using a receptor mediated adhesion substrate, cells were adhered to slides with centrifugation. Spheres from PDGF-AA or EGF/FGF cultures were dissociated into single cells and suspended at a density of $1x10^5$ cells/mL and washed

twice in cold 1X PBS before centrifuging for 3 minutes at 800 rcf in the cytospin (Shandon). Cells were allowed to dry before being fixed for 20 minutes in 4% PFA.

3.7.3 Fluorescent staining

Cells were permeabilized for 20 minutes in 1X TBS with 0.1% TritonX-100 (1X TBST) and blocked for 1 hour in 1X TBS with 5% goat serum. After blocking, coverslips were incubated for 1 hour at 37°C with anti-PDGFR-α (1:500-1:1000; Cell Signaling 3174) or anti-EGFR (1:500-1:1000; Millipore 05-1047) in 1X TBS/5% goat serum. After 3 washes in 1X TBST, coverslips were incubated for 1 hour at room temperature in the dark with goat anti-rabbit IgG-R or goat anti-mouse IgG-FITC antibody (1:200; Santa Cruz sc-2091 and sc-2010) in 1X TBS/5% goat serum. After washing in 1X TBST, coverslips were mounted on slides with Vectashield with DAPI (Vector Labs H-1200). For anti-EGFR, Mouse on Mouse Basic Kit was used as instructed by the manufacturer (Vector labs BMK-2202). Blocking peptides were used to verify staining specificity: PDGFR-α blocking peptide (1:250; Cell Signaling 14945S) and EGFR blocking peptide (1:250; Millipore 14-531). Cells incubated only with the secondary antibody showed no signal. Cells were visualized on a Virtual Slide System Macro Slide Scanner and analyzed using CellSens software (Olympus).

3.8 Fluorescence activated cell sorting (FACS) analysis

Spheres from PDGF-AA cultures were dissociated into single cells, washed three times in ice-cold 1X PBS and re-suspended in a blocking solution of 1X PBS with 1% bovine serum albumin (BSA) to a density of 2-3x10^5 cells/mL. Cells were incubated with anti-PDGFR-α conjugated to Phycoerythrin (1:200; Abcam ab93531) and anti-EGFR conjugated to FITC (1:10; Abcam ab11400) for 45 minutes in 1X PBS with 1% BSA on ice in the dark. After three washes in 1X PBS with 1% BSA, cells were analyzed using a fluorescence activated cell sorter (BD Biosciences LSRII, FACSDiva and FlowJo software). The controls used were mouse IgG2a conjugated to FITC (1:10; Abcam ab81197) and unlabeled cells. Events were gated by SSC and FSC plots by cell size to exclude debris. Cells that clearly labeled as PE or FITC positive by single labeling were correlated with dual labeled populations.

3.9 Switching EGF/FGF cultures to PDGF-AA

Late passage EGF/FGF cells that had been in continuous sphere culture for 9 months or longer were counted and viable cells re-plated in media supplemented with PDGF-AA (20 ng/mL) only. Subsequently, cultures were harvested, dissociated, counted and re-plated (i.e., passaged) into PDGF-AA on alternate weeks. At each passage, total cell count, live cell count, and percentage viability were assessed using Trypan Blue exclusion. When viability suddenly increased (i.e., passage 7-9 or near 100 days in

PDGF-AA), cultures were maintained in either PDGF-AA supplemented media, or media alone, and monitored.

3.10 Syngeneic intracranial implantation of neurosphere cultures

Sphere cultures in PDGF-AA or EGF/FGF were implanted, as previously described (79). Spheres were dissociated into single cells with a plastic pipette tip (P200) and counted with Trypan blue exclusion using an automated cell counter (Bio-Rad TC10). Single cell suspensions were re-suspended at a density of 33,333 cells/μL in 1X PBS. Wild type (p53) syngeneic mice were anaesthetized with Ketamine/Xylazine (~10 μL/g body weight) and placed in a stereotactic frame for microsurgery. The skull was exposed by a 1/4" midline cranial incision and a hole made in the right frontal bone with a Micro-drill. The coordinates for implantation were AP 1.0 / ML 2.0 to bregma. With a microsyringe (Hamilton), 3 μL of suspension ($1x10^5$ cells) was injected into the right striatum of each mouse at a depth of 3 mm (DV 3.0). The incision was closed with surgical staples and mice were monitored after surgery until fully conscious. Thereafter, mice were evaluated daily until signs of illness or distress were seen (i.e. hunching, weight loss), and then they were sacrificed. Brains of sick mice were removed and examined grossly for evidence of tumor. Brains were then fixed via cardiac cannulation and perfusion with 4% PFA, or through submersion in 4% PFA overnight.

3.11 Fluorescence Immunohistochemistry

After cervical dislocation, brains were fixed by cardiac perfusion with 4% PFA, or by submersion in 4% PFA overnight. Fixed brains were cryo-protected in 30% sucrose for 24 hours and embedded in optical cutting temperature (OCT) compound. Each brain was cut in the coronal plane in 8-10 μm sections. Sections were mounted and stored at -80°C or dried for 2 hours before staining. Sections were processed for immunohistochemistry as described for cells on coverslips.

3.12 Staining and immunohistochemistry

Formalin-fixed, paraffin-embedded tissue sections were de-paraffinized and rehydrated in a graduated xylene/ethanol series and stained with hematoxylin and eosin (H&E) following standard procedures. For immunohistochemistry (IHC), paraffin sections were pre-treated by microwaving in 10mM citrate buffer (pH 6.0) for 2 minutes at high power and 20 minutes at 20% power. Endogenous peroxidase was quenched in 3% H_2O_2 in methanol for 10 minutes and rinsed in 1X TBS before blocking for 1 hour in 1X TBS/5% goat serum. After rinsing with 1X TBS, the following primary antibodies were incubated overnight at 4°C: Anti-NESTIN (1:200; Millipore MAB353), Anti-GFAP (1:500; Millipore MAB360) and Anti-OLIG2 (1:400; Millipore MABN50). After rinsing in 1X TBS/5% goat serum, sections were incubated for 1 hour at room temperature with goat anti-mouse IgG-HRP secondary antibody (1:2000; Santa Cruz sc-2005). Peroxidase signal was detected using the ABC Elite kit (Vector Laboratories) and DAB substrate kit

(Sigma D4168) as instructed by the manufacturer. After color development, slides were rinsed in water, counterstained with hematoxylin, dehydrated in a graded ethanol series and rinsed in xylene before mounting (Shandon Mount Thermo Scientific 9990001).

3.13 NanoString gene expression

Gene expression was performed using an in-house mouse neural development code set (NanoString Technologies) that measured the absolute number of 117 specific mRNA sequences (**Supp. Fig. S1**). For *in vitro* expression, PDGF-AA and EGF/FGF cultured cells were pelleted. For xenografts, tumor tissue was dissected from 1 to 2 16 μm thick sections of OCT frozen tissue guided by paired H&E slides. RNA was isolated from frozen cell pellets and frozen tumor tissue using a DNA/RNA extraction kit (Qiagen 80204). RNA (50-100 ng) was hybridized with the 117 gene code set for 18 hours at 65 °C and processed as per manufacturer instructions on the nCounter system.

3.14 NanoString gene expression data analysis

Gene expression profiles of 2 normal mouse cortex and tumors resulting from implantation of growth factor independent p53 null cell lines were analyzed by NanoString using a custom codeset of mouse genes corresponding to the TCGA defined proneural, classical and mesenchymal subtypes (**Supp. Fig. S1**) (10). A set of 37 human GBM samples and 3 non-neoplastic human brain samples (2 biobank sourced samples and 1 cerebral cortex RNA from Clontech 636561) were similarly analyzed with an equivalent human codeset. Raw counts were subject to background subtraction using

nSolver Analysis Software version 2.0 and mouse and human data were independently normalized by positive control and housekeeping gene controls. For each gene, fold changes between tumors and mean values of their respective species-specific control tissues were calculated and log2 transformed. The resulting data were collectively subjected to Nearest Template Prediction (NTP module v (80–82), Gene Pattern, Broad Institute (83)). Human tumor and non-neoplastic brain samples were obtained with consent as per protocol from the Clark Smith Tumor Bank, with approval from the Conjoint Health Research Ethics Board at the University of Calgary. These data were assembled and analyzed with the assistance of Dr. S. Lawn.

3.15 Statistical Analysis

Data are reported as mean ± SE of at least three experiments except where noted. For comparisons of proliferation and cell death assays, One-way ANOVA was performed using Prism 6.0 software. Kaplan-Meyer curves for mouse tumor latency were made using Prism 6.0 software and analyzed with standard log rank test (GraphPad Software). To classify mouse tumors and lines, a panel of human GBM samples (N=37) and non-neoplastic human brain samples (N=3) were analyzed using nSolver 2.0 Analysis Software. Fold changes between tumors and mean values of their respective species-specific control tissues were calculated and log2 transformed using Microsoft Excel. Nearest Template Prediction (NTP module v (80–82), Gene Pattern, Broad Institute (83)) was used for generating heatmaps. The False Discovery Rate was calculated using the method of Benjamini and Hochberg (BH-FDR).

Chapter Four: Results

4.1 Cells from the SVZ of p53 null adult mice cultured in PDGF-AA become exogenous growth factor independent after approximately 100 days *in vitro*

There is a growing body of evidence to suggest that the majority of human glial cell cancers, including GBM, arise from precursor cells in the brain (24,25,27), a high proportion of which are located in the SVZ which lines the lateral ventricles of the mammalian brain (84). To simulate an oncogenic environment, SVZ cells were isolated from young adult mice and primary cultures were supplemented with PDGF-AA or EGF/FGF, growth factors that drive proliferative pathways in neural stem cells and are frequently deregulated in human GBM (68,85). To target PDGFR-α and not PDGFR-β, PDGF-AA was used instead of PDGF-BB (see 1.3.3). We used the neurosphere culture system developed by Reynolds and Weiss (86) and used cells from p53 null mice because most GBMs have an inactivating p53 pathway alteration or mutation (11).

4.1.1 Neurospheres cultured in EGF/FGF require continual addition of exogenous mitogens for survival

Previous work in our laboratory has described and measured the proliferative nature of these PDGF-AA and EGF/FGF supplemented cultures (77), and these findings were confirmed and extended in this thesis. SVZ cells from p53 null adult mice cultured in EGF/FGF quickly formed large healthy spheres that proliferated rapidly and survived indefinitely (**Fig. 6**). EdU incorporation and AnnexinV and PI labeled FACS analysis

were used to quantify cell proliferation and cell death. The proportion of proliferating cells exceeded 20% at P-0 and increased to 40% by P-6 while the proportion of dead or dying cells remained constant at 50% (**Fig. 7**). This pattern of growth of p53 null SVZ cells in EGF/FGF was observed in more than ten independent experiments by multiple investigators (Drs. Kelly and Blough, Ms. Carmen Binding and myself). Furthermore, at all time points, including after 18 months in continuous culture in EGF/FGF, p53 null cells dissected from the SVZ immediately stopped proliferating when these exogenous growth factors were removed from the media (**Fig. 6 & 7**). Neural cells isolated from the SVZ of p53 wild type adult mice behaved similarly in EGF/FGF; they grew well and required the continual addition of EGF/FGF for survival (**Supp. Fig. S2**).

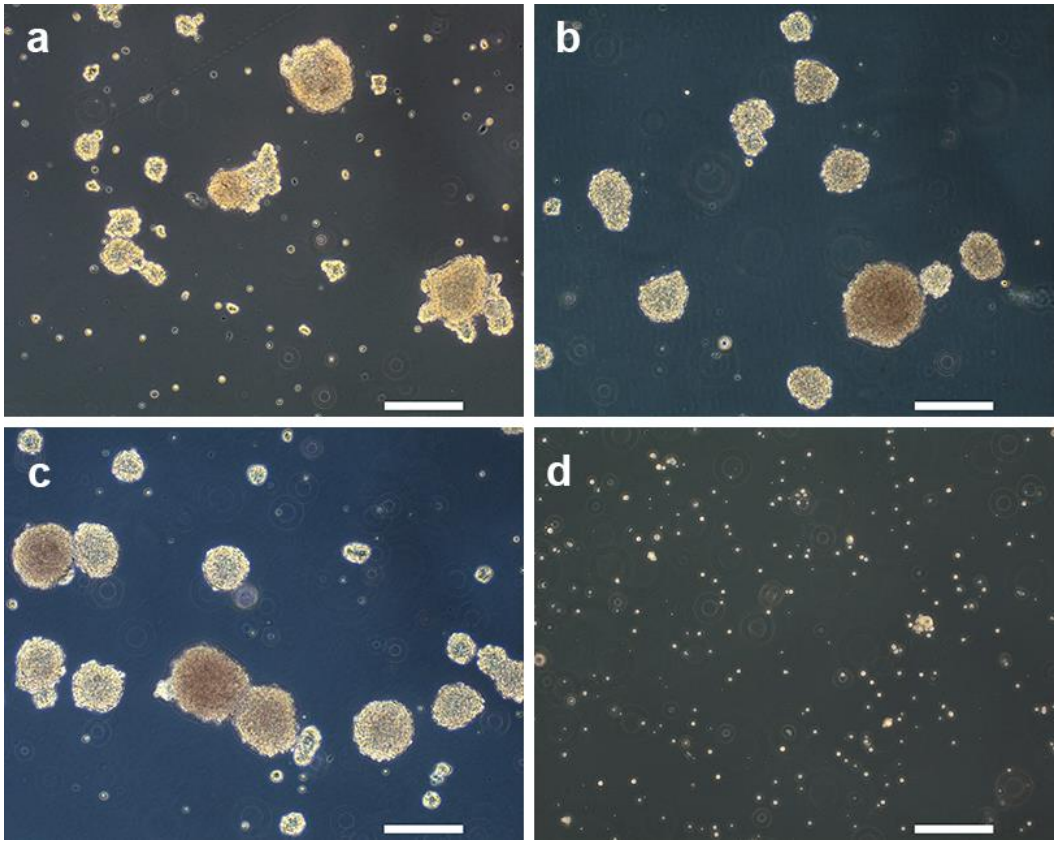

Figure 6: p53 null spheres with and without exogenous EGF/FGF

p53 null SVZ cells cultured in EGF/FGF self-renew to form neurospheres in passage 0 (**a**), passage 6 (**b**), and passage 12 (**c**), but following an absence of exogenous EGF/FGF sphere formation is arrested, shown in passage 12 (**d**). Shown are representative photomicrographs (10x) of neurosphere cultures grown in EGF/FGF. Scale bar = 200 μm.

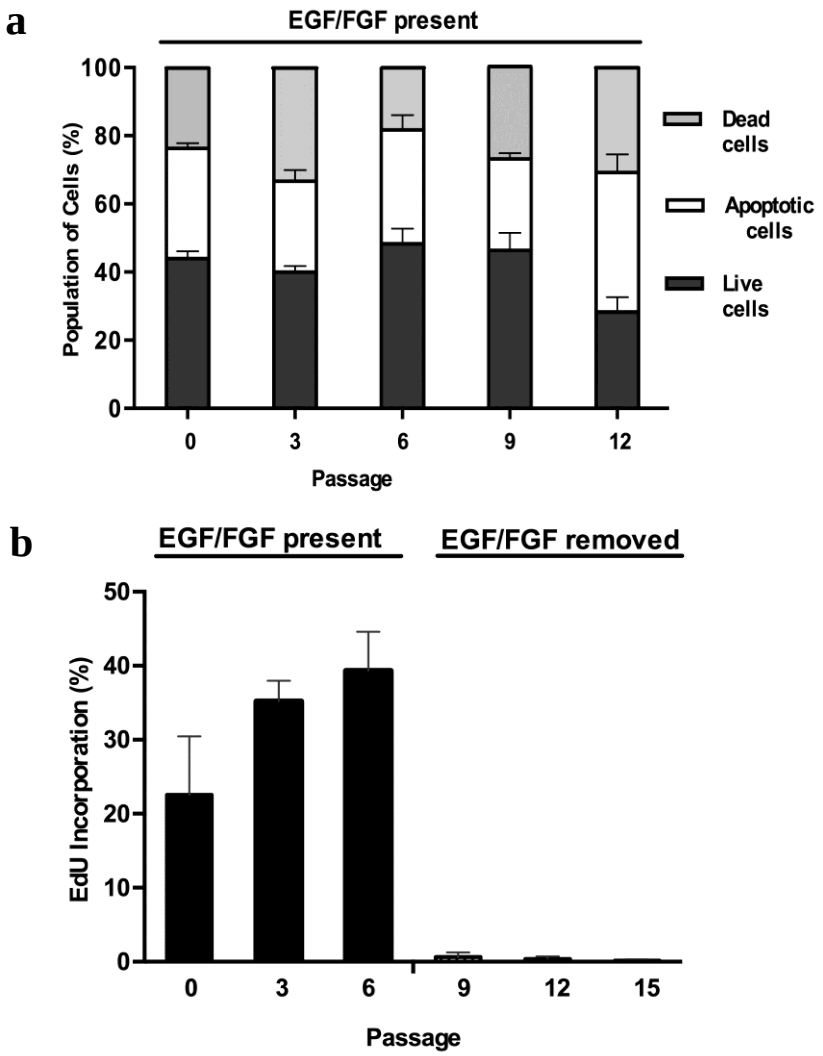

Figure 7: Proliferation and cell death in EGF/FGF grown p53 null spheres

(**a**) Neurosphere cultures maintained in EGF/FGF show approximately 50% of cells are viable and that the composition of viable, apoptotic and dead cells remains uniform over time. The relative proportions of viable, apoptotic and dead cells are not significantly different between passages (One-way ANOVA). (**b**) The proportion of proliferating cells in p53 null EGF/FGF neurosphere cultures increases over time, however these cultures fail to proliferate following removal of exogenous EGF/FGF as measured by EdU incorporation. Means ±SE with EGF/FGF present and removed are significantly different (One-way ANOVA, $p<0.0001$, N=3) (Adapted with permission from C. Binding (77)).

4.1.2 Neurospheres cultured in PDGF-AA become exogenous mitogen independent

In PDGF-AA, cultured SVZ cells behaved differently than those cultured in EGF/FGF. Cells from the SVZ of WT mice did not survive when grown in PDGF-AA supplemented media (**Supp. Fig. S2**), and this outcome has been observed by others as well (87). In contrast, SVZ cells from p53 null mice survived in PDGF-AA but displayed attenuated proliferation. P53 null SVZ cells grew as tiny ragged spheres or as individual cells for the first 10 weeks in PDGF-AA and these cultures appeared to contain a high proportion of dead or dying cells (**Fig. 8 & 9**). These visual observations of cell behavior in PDGF-AA were confirmed and quantified by EdU incorporation and AnnexinV and PI labeled fluorescence activated cell sorting (FACS) analysis (77). PDGF-AA cultures had low rates of proliferation that increased slowly over several months. The proportion of proliferating cells in early passage PDGF-AA cultures was 5% at P-0, 10% at P-3; and 20% at P-6 (**Fig. 9**). In keeping with these findings, the proportion of dead or dying cells slowly decreased in PDGF-AA cultures from 90% at P-0 to 40% at P-12 (**Fig. 9**).

Prior to passage 7, p53 null cells isolated from the SVZ did not survive when PDGF-AA was removed from the media. At or near passage 9, however, after approximately 100 days in culture, p53 null cells in PDGF-AA began to proliferate rapidly forming large, irregular spheres (**Fig. 8**). Strikingly, p53 null SVZ cells that had been continuously cultured in PDGF-AA acquired the capacity to grow rapidly in the absence of exogenous PDGF-AA: upon removal of exogenous growth factors the cells continued to proliferate. This shift to independence of exogenous PDGF-AA was accompanied by a dramatic

decrease in the proportion of dead or dying cells (<40% at P-12; **Fig. 9**). This pattern of gradual adaptation of p53 null cells from the SVZ to PDGF-AA, accompanied by high rates of cell death, followed approximately 100 days later by rapid exogenous PDGF-AA-independent proliferation, was highly reproducible. Our laboratory has observed this sequence of events unfailingly in over 20 independent experiments including reproduction of the system in my own hands during my time in the laboratory.

Two of the hallmarks of cancer are the ability of cells to proliferate independently of growth factors, and anchorage-independent growth (64,88). While we have demonstrated the ability of PDGF-AA grown cells to survive and proliferate without exogenous growth factors, another method often employed to test for malignant transformation is the soft agar colony-forming assay. Within our model, we define transformation of p53 null SVZ cells through their acquired independence of exogenous growth factors and the tumorigenicity of cells after approximately 100 days of culturing in PDGF-AA. Assessing anchorage-independent growth in the PDGF-AA cultures would complete the transformed profile of these cells.

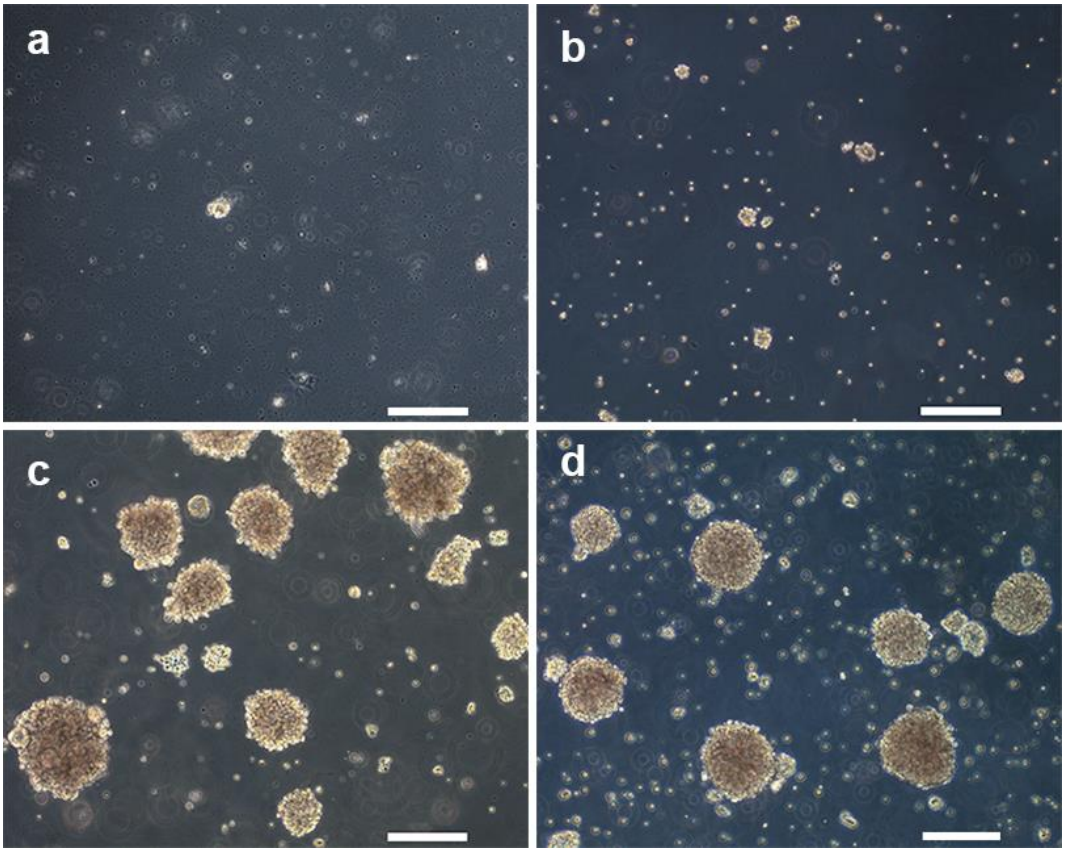

Figure 8: p53 null spheres with and without exogenous PDGF-AA

p53 null SVZ cells cultured in PDGF-AA initially struggle in culture as shown at passage 0 (**a**), but begin to self-renew as passages increase shown at passage 4 (**b**). Near 100 days in culture and thereafter, spheres proliferate rapidly as shown at passage 12 (**c**). In absence of exogenous PDGF-AA as represented at passage [12] (**d**), spheres continue to self-renew. Shown are representative photomicrographs (10x) of neurosphere cultures. Scale bar = 200 μm. **[] = exogenous PDGF-AA-independence**.

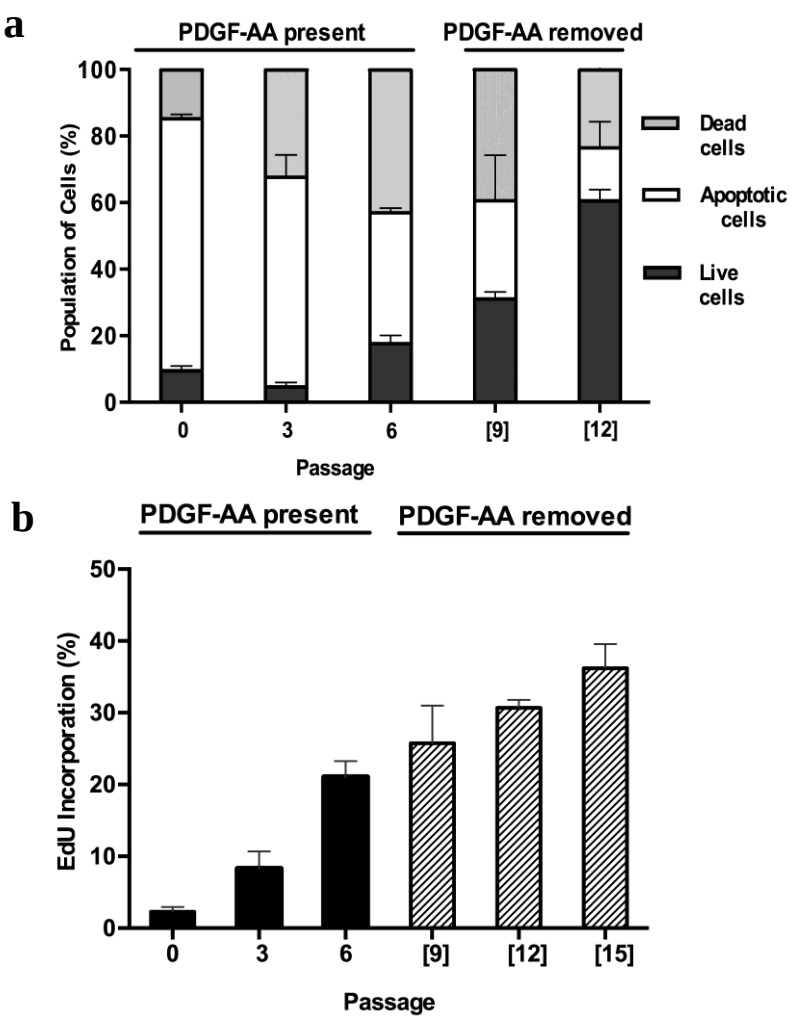

Figure 9: Proliferation and cell death in PDGF-AA grown p53 null spheres

(**a**) With increasing passage and after reaching growth factor independence, p53-/- neurosphere cultures initiated in PDGF-AA showed a steady increase in the proportion of living cells compared to apoptotic and dead. The relative proportions of viable and apoptotic cells are significantly different between passages (One-way ANOVA, $p<0.0001$ and 0.0016, respectively). (**b**) p53-/- neurospheres maintained in PDGF-AA show low levels of proliferation in early passages (0 and 3) and a continual increase in proliferation upon removal of exogenous PDGF-AA at passage 9 and beyond ([9], [12] and [15]) Means ±SE from passage 0 to [15] with PDGF-AA present and removed are significantly different (One-way ANOVA, $p<0.0001$, N=3). **[] = exogenous PDGF-AA-independence**. (Adapted with permission from C. Binding (77)).

4.2 p53 null SVZ cells cultured in PDGF-AA co-express PDGFR-α and EGFR

To investigate the presence of the receptors to which EGF and PDGF-AA bind and that might play a role in transformation, the expression of PDGFR-α and EGFR was assessed in PDGF-AA and EGF/FGF cultures from multiple time points (passages) by western blotting. PDGFR-α was expressed in both culture conditions and at all passages examined, whereas the expression of EGFR protein decreased slightly over time in PDGF-AA cultures, while increasing in EGF/FGF cultures (**Fig. 10 & Supp. Fig. S3**). Growth factor receptor expression levels displayed variability between passages, most significantly in the EGF/FGF cultures. This variability was investigated further by harvesting cells at different time points post passaging. Through investigation of protein expression of the EGF receptor with western blot, it was seen that protein expression changed in a time-dependent manner related to when cultures were passaged and received fresh media and growth factors (**Supp. Fig. S4**) indicating a possible depletion of EGF or degradation of EGF in culture.

Using qRT-PCR, expression of PDGFRA and EGFR was found to be present at all time points (passages) examined in both culture conditions, and increased over time relative to the expression of GAPDH. Gene expression levels were variable between independent cultures (cell lines) examined, and PDGFRA gene expression was elevated in PDGF-AA cultures compared to EGF/FGF cultures (**Fig. 11**). Although gene and protein expression are not closely aligned, the review by Vogel and Marcotte (2012) highlights the issues associated with correlating gene and protein expression and why the variable nature of

cellular processes such as transcription and translation make this a difficult task in many cases (89).

We also sought to assess the protein expression of two additional growth factor receptors: i) FGFR2 since our EGF/FGF cultures contain FGF2, ii) and c-Met, as the c-Met receptor has recently been implicated in GBM (90) and has been shown to interact with other RTKs (91,92). The expression of these two receptors was similar in PDGF-AA pre-and post-transformation cultures as well as EGF/FGF supplemented cultures (**Supp Fig. S5**).

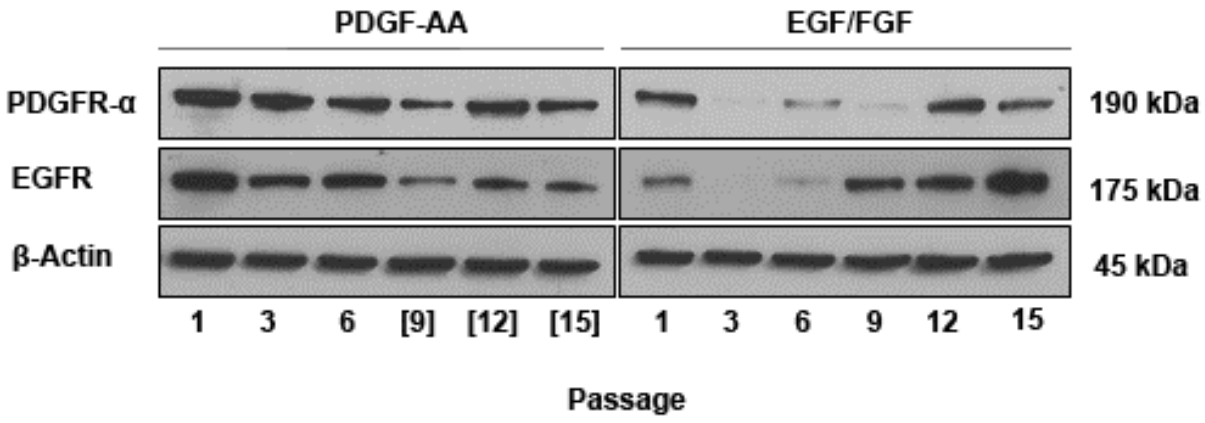

Figure 10: PDGF-AA and EGF/FGF supplemented neurospheres express PDGFR-α and EGFR protein

In PDGF-AA cultures, PDGFR-α and EGFR proteins were expressed at all passages examined. In EGF/FGF supplemented cultures, PDGFR-α and EGFR were expressed, but protein levels varied (**Supp. Fig. S3**). This western blot is representative of at least three blots from independent cultures. **[] = exogenous PDGF-AA-independence**.

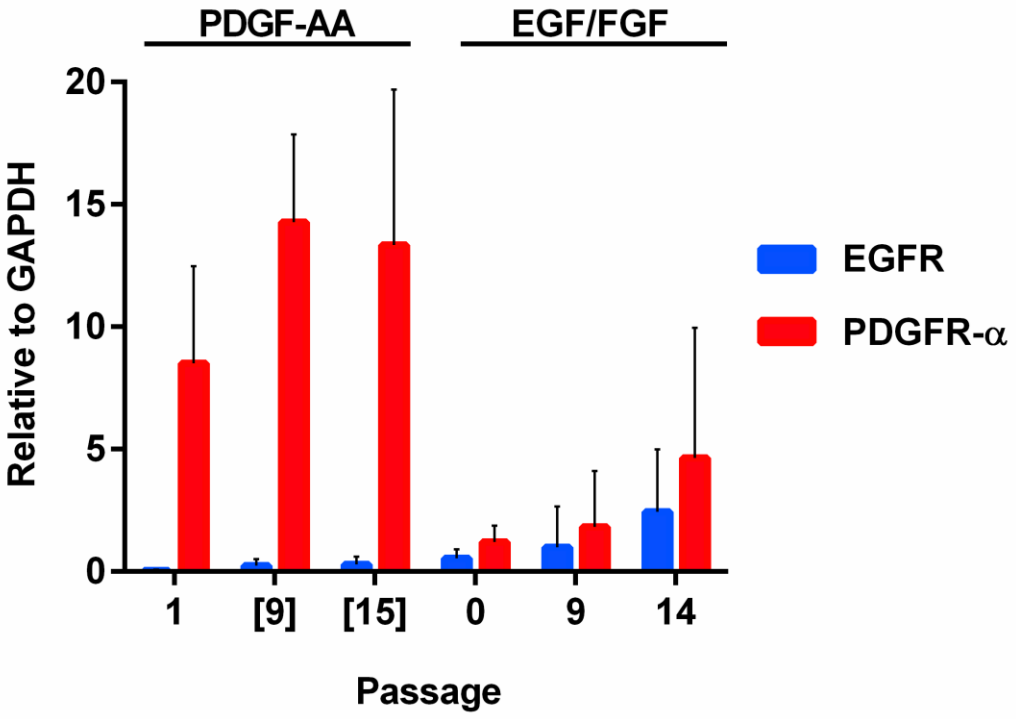

Figure 11: *PDGFRA* and *EGFR* gene expression in PDGF-AA and EGF/FGF supplemented neurospheres

qRT-PCR gene expression shows expression of *PDGFRA* and *EGFR* in PDGF-AA p53 null neurosphere cultures. Expression of *PDGFRA* is greater than that of *EGFR* in PDGF-AA cultures pre- and post-transformation. Both *PDGFRA* and *EGFR* are expressed in p53 null neurosphere cultures maintained in EGF/FGF and increase over time. Means ± SE of triplicate gene expression analysis are shown relative to the expression of *GAPDH*. Means from *PDGFRA* in PDGF-AA [9] and [15] are significantly different than *PDGFRA* in EGF/FGF cultures (Two-way ANOVA, $p<0.0001$). **[] = exogenous PDGF-AA-independence**.

After assessing whole populations of cells, we inquired whether PDGFR-α and EGFR were expressed on the same cell (i.e., co-expressed) or different cells in PDGF-AA and EGF/FGF cultures. To assess growth factor receptor expression in p53 null SVZ cells, early and late passage spheres grown in both PDGF-AA and EGF/FGF were dissociated into single cells and the expression of PDGFR-α and EGFR was visualized by double-label immunofluorescence. Most SVZ cells were observed to co-express PDGFR-α and EGFR, irrespective of the passage number (early *vs* late passage) and the growth factors added (PDGF-AA or EGF/FGF; **Fig. 12 & 13**). The co-expression of GF receptors was verified through several techniques, including cytospin (**Supp. Fig. S6**) and FACS (**Supp. Fig. S7**). In all immunocytochemical techniques, the dominant population of cells was co-labeled with PDGFR-α and EGFR, with proportion of co-stained cells varying from 70-80% by visual assessment by immunofluorescence to 44% in exogenous PDGF-AA independent cells by FACS. In EGF/FGF cultured cells, there was not a visible population of cells that labeled for EGFR alone, however this population emerged when these cells were analyzed with FACS. The variability in the abundance of receptor staining between these techniques might be due to the permeabilization step in the immunofluorescence protocol, where internalized receptors would also become visible.

Due to the interesting observation that cells plated on laminin coated coverslips showed a focal receptor staining pattern, cell adherence via cytospin was employed to assess the possibility of receptor expression pattern alteration through adherence with laminin, and blocking peptides specific to the antibodies used verified receptor staining specificity

(**Supp. Fig. S6**). Within the cytospin prepared samples, receptor staining did not appear to be focal, suggesting this feature is associated with using laminin to cause cells that grow in suspension to adhere. Using blocking peptides, virtually all fluorescence staining was eliminated except for that which appeared to be associated with nuclei showing abnormal, condensed morphology, the appearance in these cases resembled autofluorescence.

4.3 SVZ cells from p53 null mice grown in PDGF-AA and EGF/FGF have similar lineage marker profiles and resemble OPCs

We next sought to determine lineage marker profiles of p53 null neurospheres cultured in PDGF-AA or EGF/FGF. We wondered whether culturing p53 null SVZ cells in PDGF-AA versus EGF/FGF would cause differentiation over time in culture or selection of a specific neural cell lineage which may point to a cell of origin in the PDGF-AA cells that transform in culture. The expression of NESTIN, OLIG2, NG2, GFAP and β3-Tubulin was examined in both neurosphere culture conditions and at multiple time points (passages) by western blotting (**Fig. 15**) and NanoString (**Fig. 16)**. With the exception of stem cell marker NESTIN, whose expression increased with serial passaging in the presence of exogenous PDGF-AA, marker profiles were similar in PDGF-AA and EGF/FGF cultures. Weak expression of GFAP and β3-tubulin, accompanied by strong expression of NG2 and OLIG2, suggested that p53 null SVZ cells grown in PDGF-AA and EGF/FGF have a lineage marker profile most similar to that of OPCs.

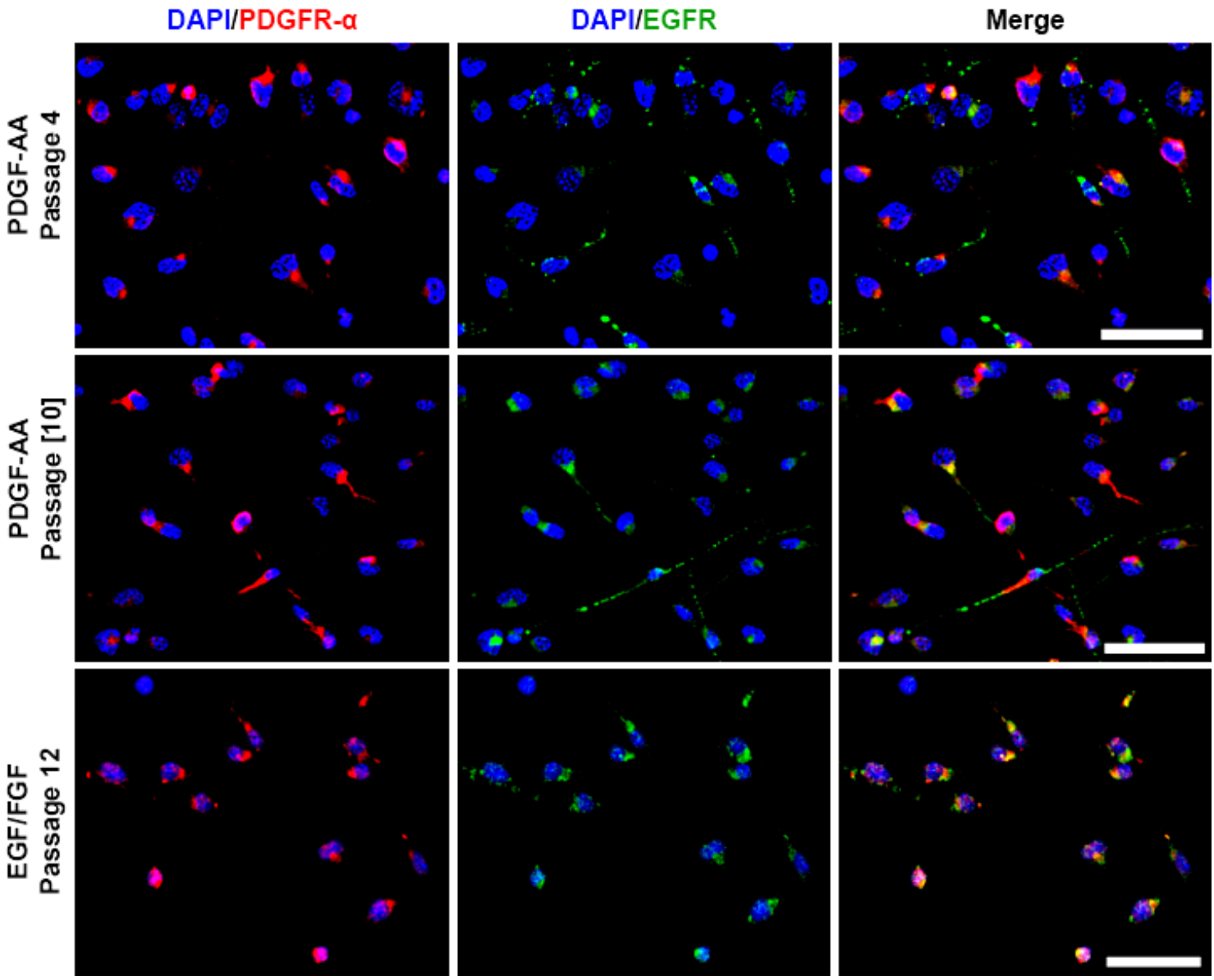

Figure 12: PDGFR-α and EGFR positive cells in p53 null neurosphere cultures

In this representative fluorescence immunocytochemistry image (20x), dissociated, poly-L-ornithine and laminin plated neurosphere cells are co-labeled with PDGFR-α and EGFR in pre- and post- transformation PDGF-AA cells as well as EGF/FGF maintained cells. Scale bar = 20 μm. **[] = exogenous PDGF-AA-independence.**

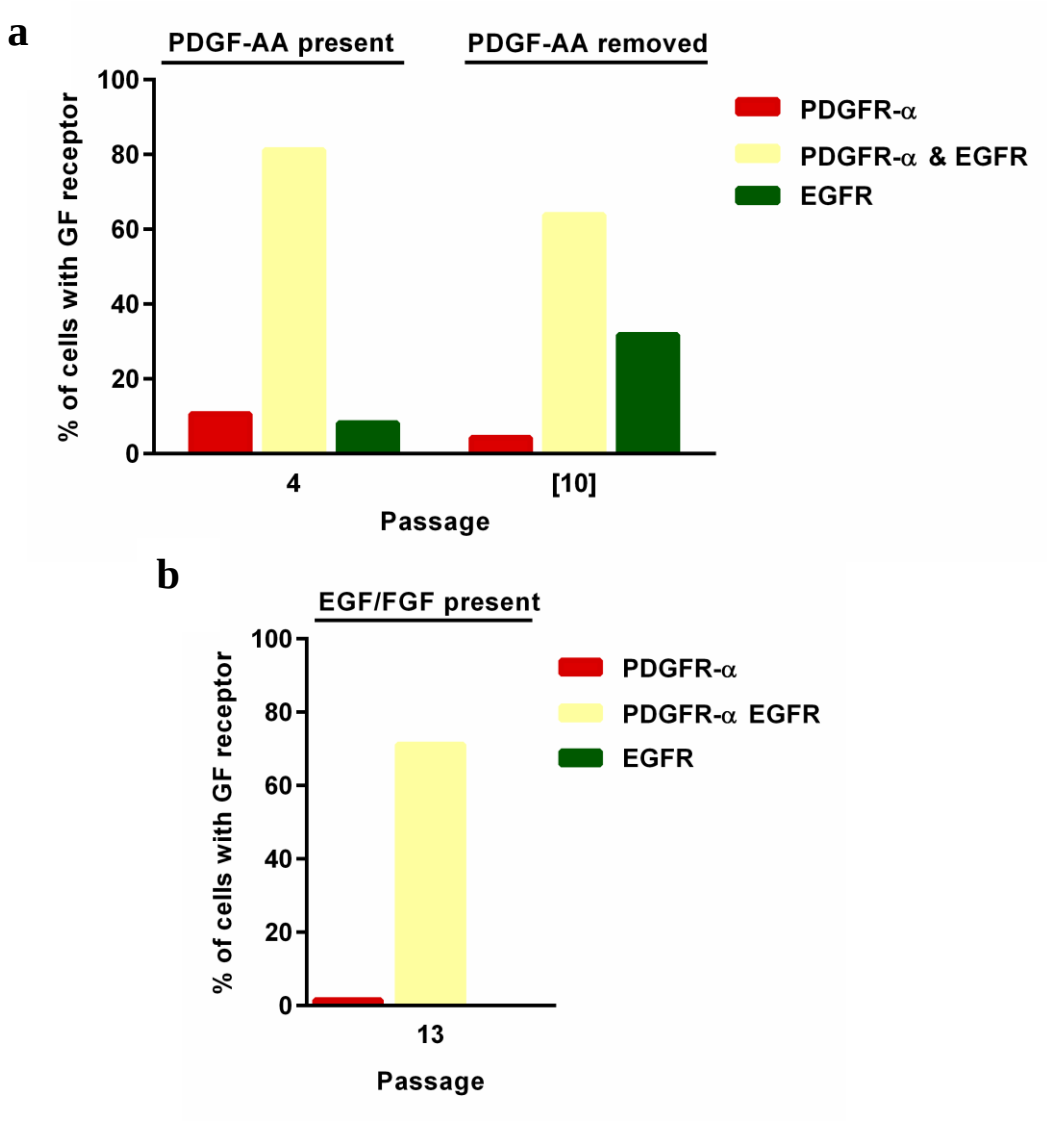

Figure 13: Quantification for cells dual and single labeled for PDGFR-α and EGFR

Manual counting of cells displaying dual or single labeling for growth factor receptors shows most cells express both PDGFR-α and EGFR by immunofluorescence. In p53 null PDGF-AA cultures, (**a**) the number of EGFR only labeled cells increases after cells are exogenous PDGF-AA independent. In p53 null EGF/FGF supplemented cultures, visually the majority of cells are dual labeled and there is an absence of EGFR only labeled cells (**b**). Graphs are from one representative culture from each condition, at least 500 cells were counted for each culture, similar trends were observed in at least 2 additional cultures from each condition. **[] = exogenous PDGF-AA-independence.**

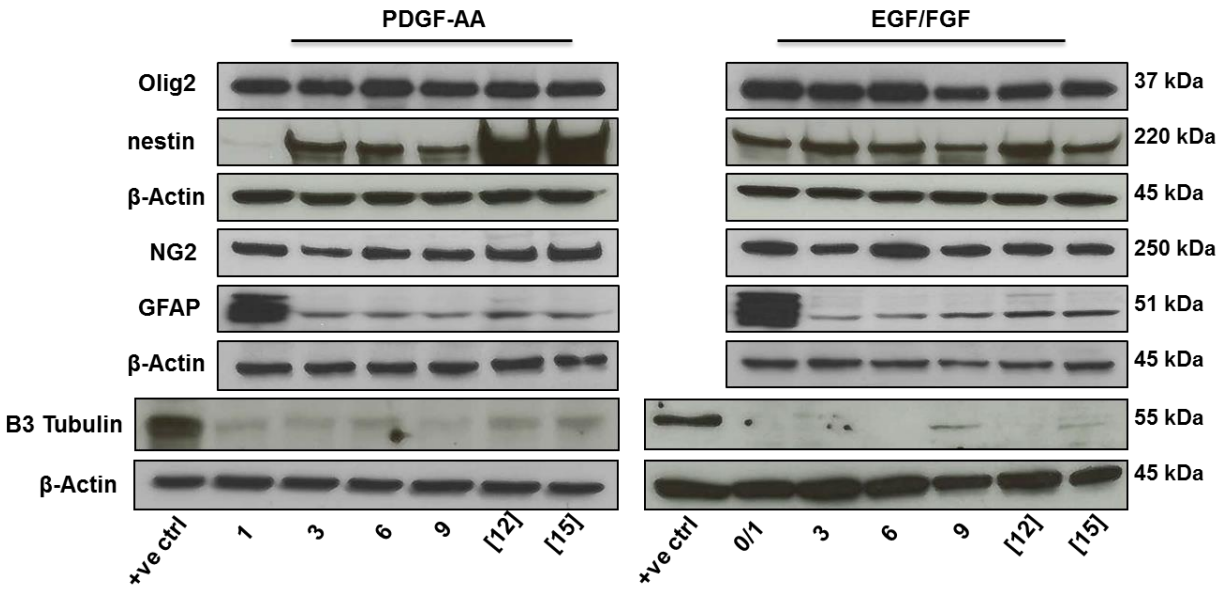

Figure 15: Neural lineage markers protein expression

Protein expression of lineage markers reveals similar profiles in both PDGF-AA and EGF/FGF supplemented cultures, and a decrease in expression of astrocytic marker GFAP and neuronal marker β3 Tubulin. NESTIN expression increases in late passage PDGF-AA cultures only (passage [12] and [15]) which may indicate a shift to a more stem-like, undifferentiated state in exogenous PDGF-AA independent cultures. **[] = exogenous PDGF-AA-independence.**

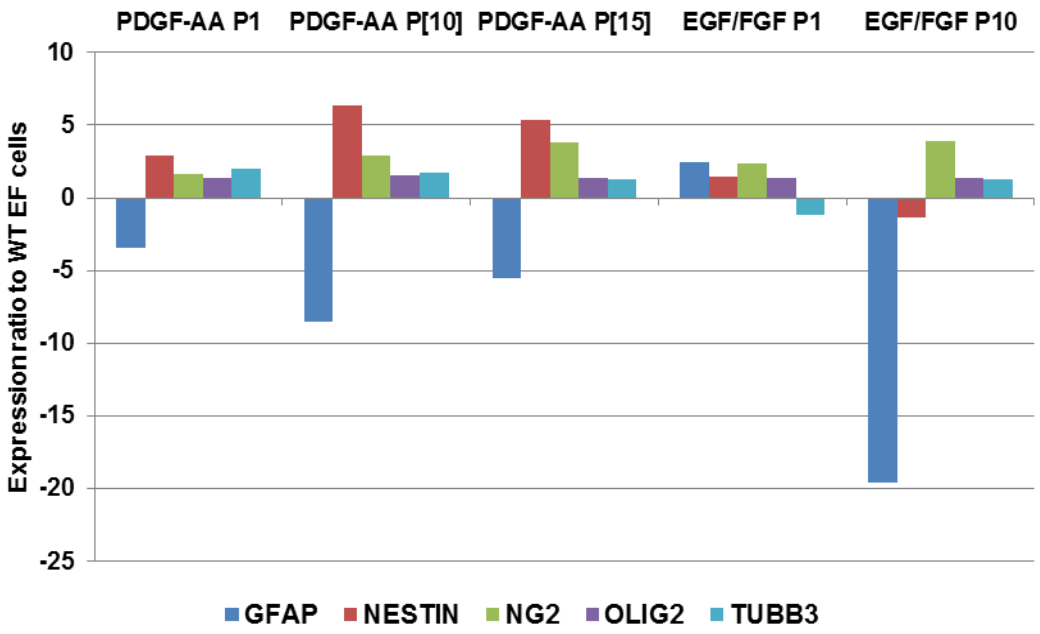

Figure 16: Gene expression as compared to wild type SVZ cells cultured in EGF/FGF

Gene expression (NanoString) shows similar patterns in gene expression to that of lineage marker protein expression with elevated NESTIN expression in PDGF-AA grown cells and relatively consistent levels of OPC genes NG2 and OLIG2 and neuronal gene TUBB3 and low expression of astrocytic gene GFAP. These patterns may indicate that over time, PDGF-AA cultures maintain an OPC-like state with increased self-renewal capacity as the expression of NESTIN increases. In this subset of representative pre- and post-transformation PDGF-AA grown cells and EGF/FGF grown cells, gene expression is normalized to WT SVZ neurospheres cultured in EGF/FGF. **[] = exogenous PDGF-AA independence.**

4.4 SVZ cells from p53 null mice cultured long-term in EGF/FGF become exogenous growth factor independent within 100 days of being switched to PDGF-AA

Similar lineage marker profiles in PDGF-AA and EGF/FGF cultures of p53 null SVZ cells and co-expression of PDGFR-α and EGFR in both PDGF-AA and EGF/FGF SVZ cultures suggested the possibility that these two populations of p53 null SVZ cells might be more similar than different. It raised the further possibility that SVZ cells might retain the capacity for transformation even after many months of continuous growth in EGF/FGF. To test this hypothesis, long-term EGF/FGF cultures were switched to PDGF-AA and a familiar sequence of events was observed. EGF/FGF cells switched to PDGF-AA abruptly entered a period of crisis with attenuated growth that lasted several months: rates of proliferation rapidly declined and cellular viability decreased to 5% (**Fig. 17**). Then, after approximately 100 days in PDGF-AA, their proliferation rate and viability increased dramatically and they became exogenous PDGF-AA independent. Control cultures that were not switched to PDFG-AA ceased to proliferate when EFG/FGF was removed from the media. [Merely adding PDGF-AA to EGF/FGF did not lead to growth factor independence.] (**Fig. 17**). Similar to PDGF-AA independent cells grown directly in PDGF-AA, those derived from long-term EGF/FGF cultures co-expressed PDGFR-α and EGFR (**Fig. 18 & 19**); likewise, they were positive for OPC markers NG2 and OLIG2 and neural stem cell marker NESTIN (**Fig. 18**).

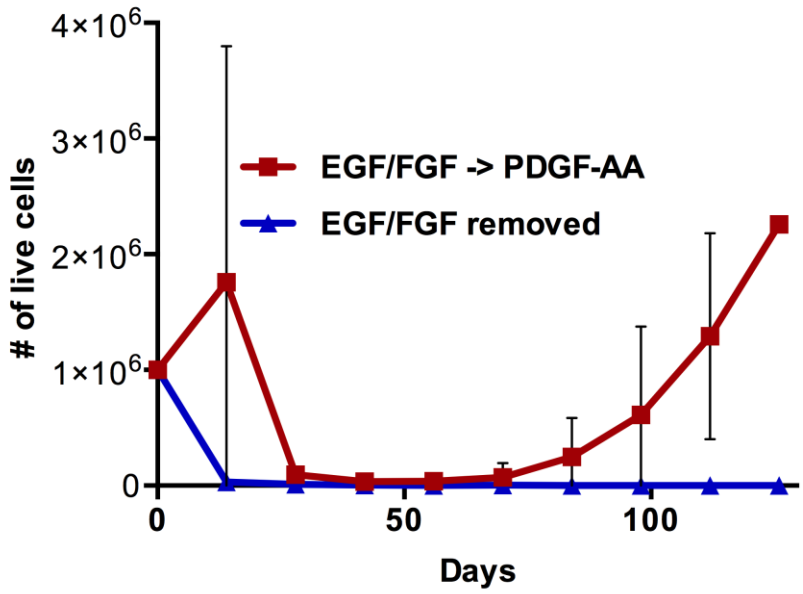

Figure 17: Long term EGF/FGF maintained cultures transform after switching to PDGF-AA

Tp53 null cells cultured in EGF/FGF maintain the ability to transform (i.e. become exogenous PDGF-AA independent) once they are switched to culturing in PDGF-AA. After an extended period of decreased cell viability, proliferation and viability increases dramatically near 100 days after being switched to PDGF-AA at which point exogenous PDGF-AA is no longer required. This graph shows the transformation of four EGF/FGF cultures, each with multiple replicates that were switched to PDGF-AA and became independent of exogenous growth factors. Viability in the initial two weeks after switching to culturing in PDGF-AA varied depending on how long the EGF/FGF cultures had been maintained in EGF/FGF before switching.

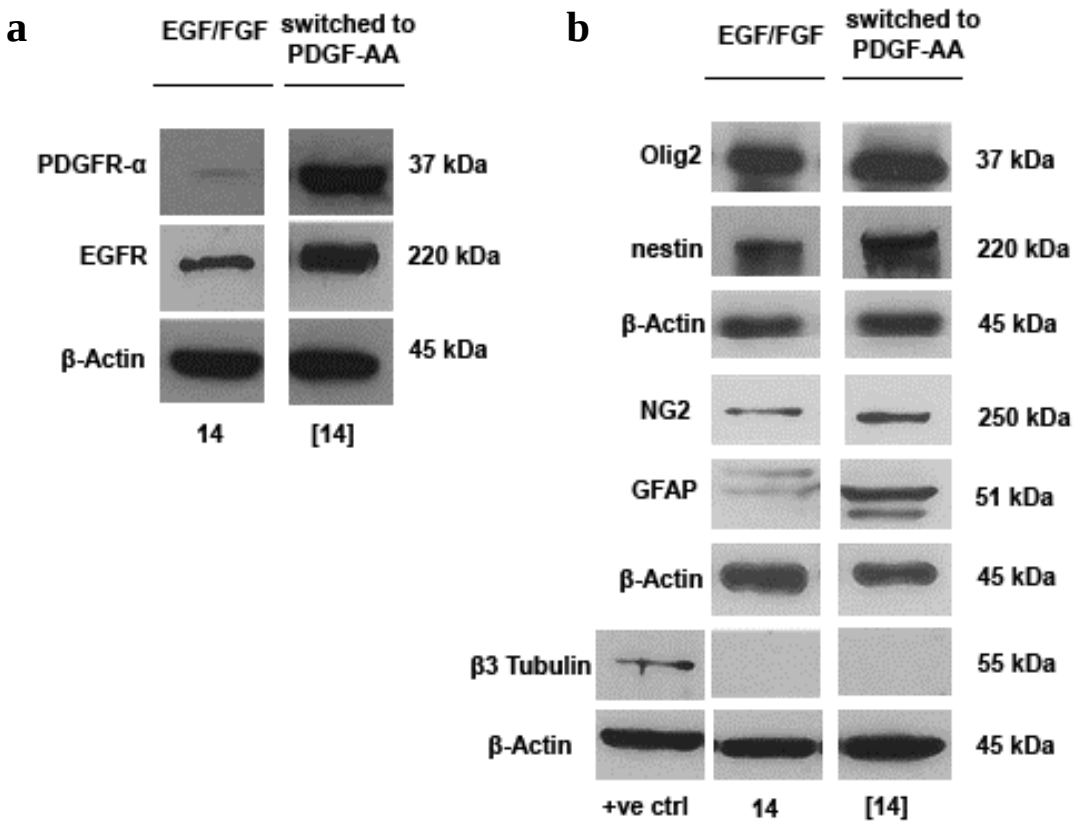

Figure 18: Long term EGF/FGF maintained cultures switched to PDGF-AA express similar markers to p53 null SVZ cells directly cultured in PDGF-AA

p53 null cells initially cultured in EGF/FGF but switched to PDGF-AA express (**a**) PDGFR-α, EGFR, and (**b**) markers of OPCs. In western blots, EGF/FGF cells were harvested at passage 14. EGF/FGF cells were switched to PDGF-AA for approximately 100 days before an increase in viability was observed and PDGF-AA was removed. These switched cells underwent 14 passages post switching before being harvested for protein. **[] = exogenous PDGF-AA independence.**

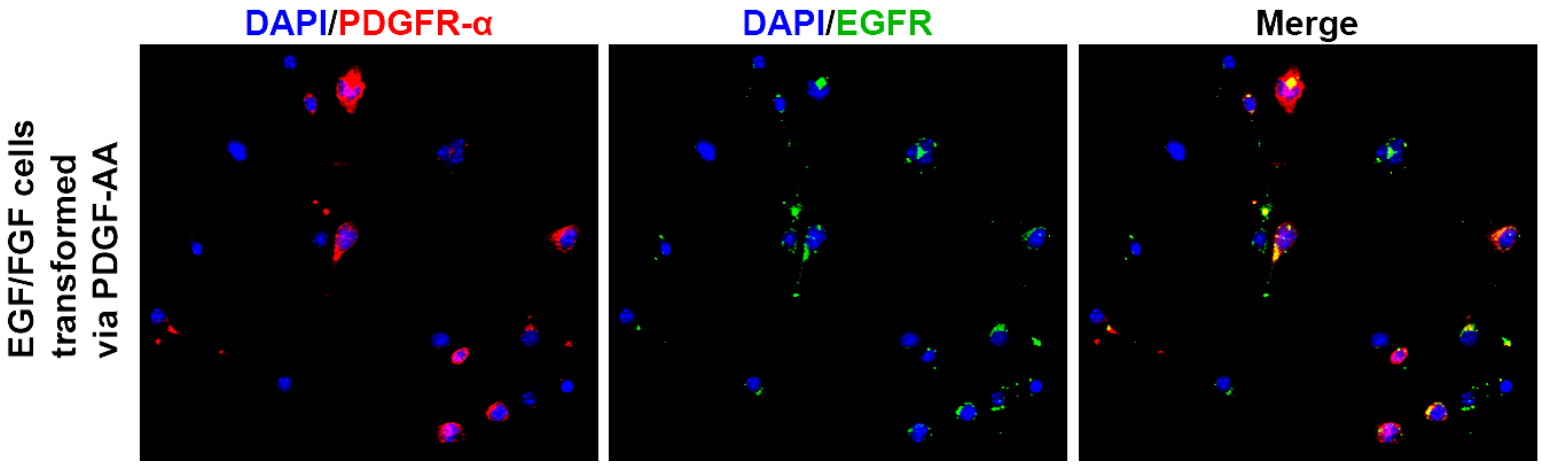

Figure 19: Most p53 null EGF/FGF initiated cells co-express PDGFR-α and EGFR once they have reached exogenous GF independence.

Once p53 null EGF/FGF cultured neurospheres have become exogenous GF independent after a period of culturing in PDGF-AA, these transformed cultures also display cells which co-express PDGFR-α and EGFR. This immunofluorescence staining panel is representative of four independent p53 null EGF/FGF cultures that were switched to culturing in PDGF-AA and became exogenous GF independent.

4.5 p53 null neurospheres cultured in PDGF-AA exhibit a proneural subtype gene expression pattern

In order to compare the similarity of the *in vitro* portion of the model to the human disease, gene expression analysis was used to assess the gene expression profile of independent cell lines as compared to those observed in the molecular subtypes of human GBM. Twenty genes were selected as classifiers based on TCGA subtyping and genes which were available in both human and mouse NanoString codesets. Both p53 null SVZ cultured directly and PDGF-AA and long-term EGF/FGF cultures switched to PGDF-AA classified as proneural in subtype using gene expression profiling (**Fig. 20**). In comparison, p53 null SVZ cells cultured only in EGF/FGF show a classical gene expression profile. Analysis consisted of a combined analysis of fold changes between normal human brain and human GBM samples compared to normal mouse brain and mouse cell lines. Human GBM samples used classified as predicted and in agreement with previous classification undertaken using RNA sequencing (completed by Dr. Yaoqing Shen at BC Genome Sciences Centre, Vancouver, BC). PDGF-AA, p53 null cell lines included four independent cell lines at early, middle and late passages (passages 0 to [15]). Two independent p53 null, EGF/FGF grown cell lines at early and late passages (passage 0 and 1, and passage 10 and 14) were also analyzed.

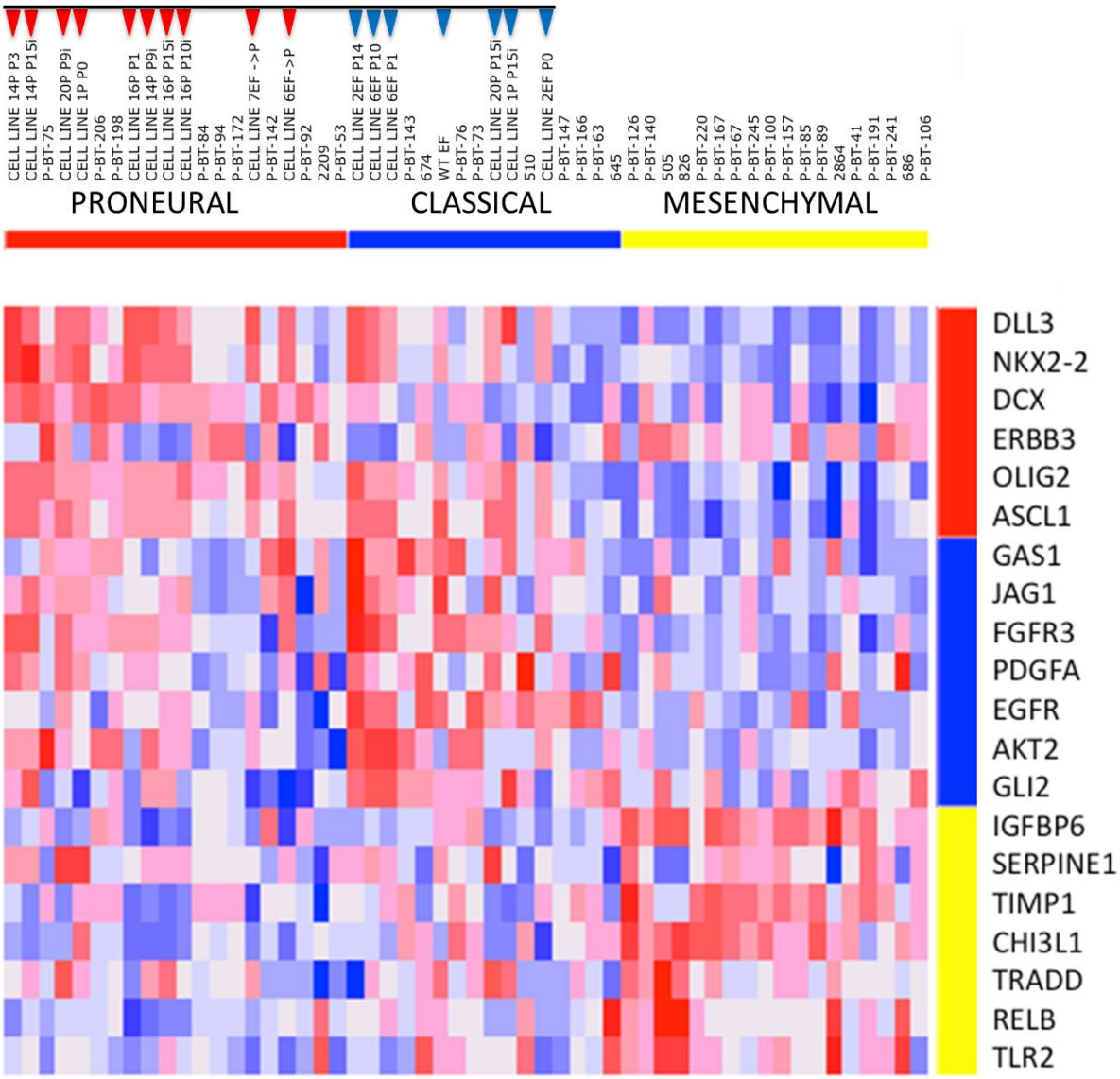

Figure 20: p53 null neurospheres cultured in PDGF-AA classify as proneural

Out of ten p53 null SVZ cell lines cultured initiated in PDGF-AA, eight classify as proneural in gene expression patterns. Two PDGF-AA p53 null lines, both at passage 15 and exogenous GF independent appear as classical in gene expression subtype. All four p53 null EGF/FGF grown cell lines and one WT p53 cell line also cultured in EGF/FGF classify as the classical subtype as compared to human GBM and normal human brain tissue samples (data analysis completed with assistance from Dr. S. Lawn).

4.6 Exogenous PDGF-AA-independent p53 null SVZ cells form high-grade astrocytic GBM-like tumors in immune competent, p53 wild type mice

The ability of PDGF-AA cells to proliferate *in vitro* in the absence of exogenous PDGF-AA suggested they might also be tumorigenic. To test this possibility, 10^5 cells from early (≤3), mid (4-7), and late passage (≥8) PDGF-AA and EGF/FGF derived cultures were implanted into the right striatum of 8-12 week-old, p53 wild type, immune competent mice. After 40 days, the mice implanted with late passage cells derived from exogenous PDGF-AA-independent cultures became ill and had to be sacrificed. The right cerebral hemispheres of affected animals were enlarged. Histopathological analysis by a neuropathologist (Dr J. Chan) revealed infiltrating, necrotic, high-grade gliomas that resembled human GBMs (**Fig. 21**). All tumors displayed astrocytic morphology and were strongly GFAP positive; most tumor cells were also strongly OLIG2 positive and occasional cells were NESTIN postitive (**Fig. 21**). Mice implanted with p53 null cells that had been continuously cultured in EGF/FGF do not form tumors (**Fig. 21**). Fluorescence immunohistochemistry revealed co-expression of PDGFR-α and EGFR on most tumor cells with more prominent EGFR staining toward the periphery of the tumor (**Fig. 22**).

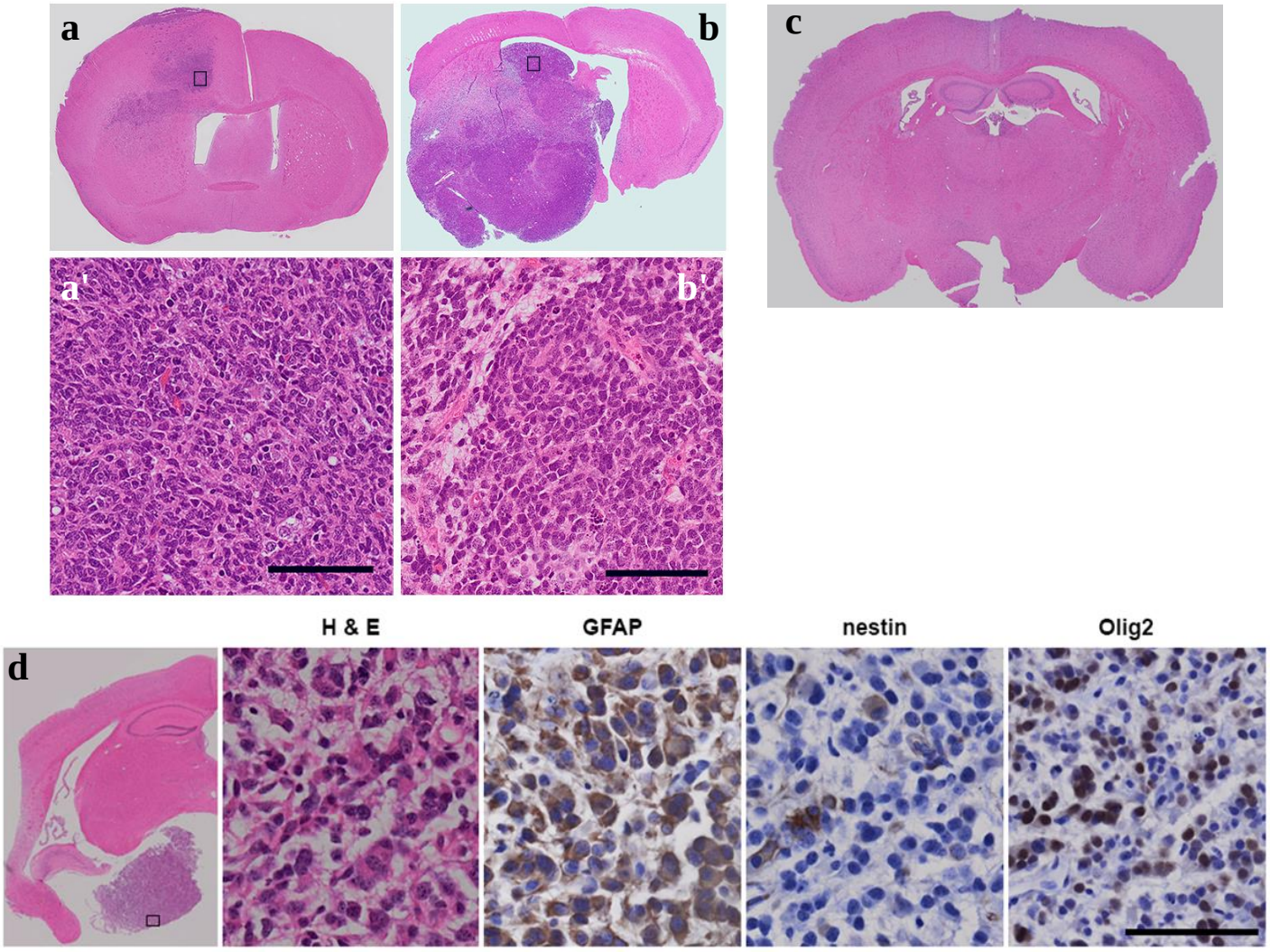

Figure 21: H&E and IHC of PDGF-AA formed tumors

Representative H&E (**a**) shows a high-grade astrocytoma with diffuse parenchymal infiltration and areas of perivascular growth, subpial accumulation, and subarachnoid spread. PDGF-AA formed tumors showing tumor formed from same cell line, sacrificed at first potential signs of illness (**a & a'**) versus later when illness was more obvious (**b & b'**). Presence of well-developed vascular proliferation and necrosis varies depending on when the animal is sacrificed. Scale bar = 100 μm. Brain from mouse implanted with p53 -/- EGF/FGF grown cells (control) (**c**). Representative H&E and corresponding IHC displaying GFAP and OLIG2 positive cells and occasional NESTIN positive cells (**d**). Scale bar = 50 μm.

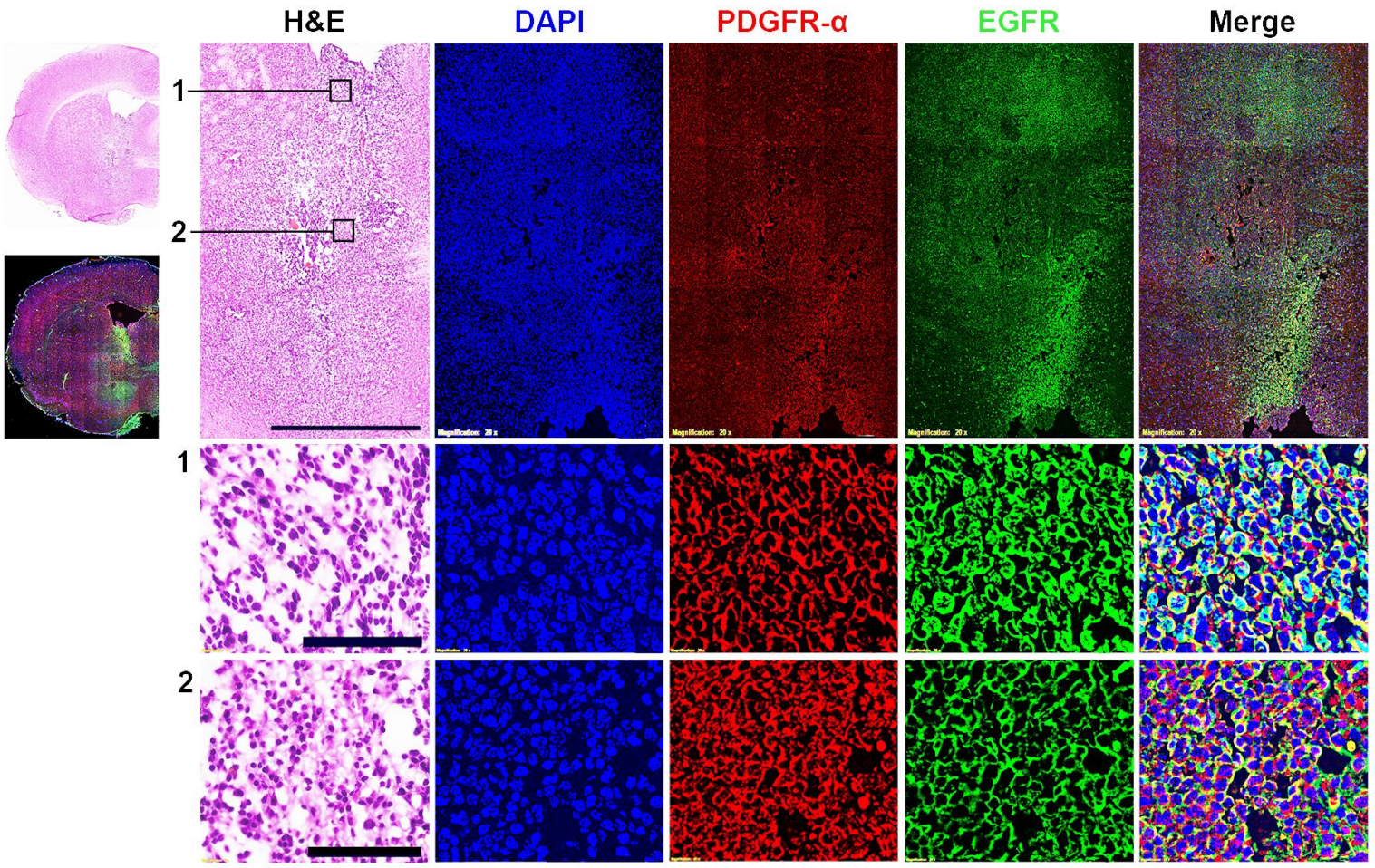

Figure 22: H&E and corresponding immunofluorescence displaying co-expression of PDGFR-α and EGFR in PDGF-AA formed tumor

Cells are co-labeled throughout the tumor, however the periphery of the tumor (**1**) displays more pronounced EGFR staining as compared to the center (**2**) indicating EGFR may play a role in the continual growth and invasion or expansion of the tumor. Scale bars = 1 mm (top), 100 μm (bottom).

4.6.1 Tumors from exogenous PDGF-AA-independent p53 null SVZ cells resemble the proneural human GBM subtype

In order to investigate the similarity of tumors formed by exogenous PDGF-AA independent cultures to that of human GBM, gene expression analysis was used to assess the gene expression profile of mouse tumor samples as compared to those observed in the molecular subtypes of human GBM. Twenty genes were selected as classifiers based on TCGA subtyping and genes which were available on both human and mouse NanoString codesets. Both p53 null SVZ cultured directly in PDGF-AA and long-term EGF/FGF cultures switched to PGDF-AA form GBM-like tumors in immune competent, p53 wild type mice which display a predominantly proneural expression profile (**Fig. 23**). In comparison, p53 null SVZ cells cultured only in EGF/FGF show a classical gene expression profile (**Fig. 20**). Interestingly, this expression profile switched to proneural after these cultures were switched to PDGF-AA, and this expression pattern is mirrored in the tumors formed by these proneural cell lines. Assessment consisted of a combined analysis of fold changes between normal human brain and human GBM samples compared to normal mouse brain and mouse tumors. Human GBM samples used classified as predicted and in agreement with previous classification undertaken using RNA sequencing (completed by Dr. Yaoqing Shen at BC Genome Sciences Centre, Vancouver, BC).

4.6.2 Survival and tumor latency is associated with passage number of exogenous PDGF-AA implanted cells

Previous work in our laboratory (77) has established that tumor latency is associated with the passage number of the implanted cells: PDGF-AA independent high passage cultures (P15) formed tumors within 50 days or less, cells at critical *in vitro* passage 9, which have just become PDGF-AA independent, typically formed tumors within 6 months, mid passage cultures (P7) that were still dependent on exogenous PDGF-AA for survival required up to 250 days to form brain tumors, whereas early passage cells (P3) that were PDGF-AA dependent did not form tumors (**Fig. 24**). Mice implanted with early, mid and late passage EGF/FGF cultures did not form tumors, even after long periods of observation of up to 18 months (data not shown). The ability of passage 7 cells to illicit tumor formation is supportive of the interpretation that the proportion of transformed cells in PDGF-AA cultures reaches a critical threshold for *in vivo* tumorigenesis by passage 7.

4.6.3 Long-term EGF/FGF cultures become tumorigenic within 100 days of being switched to PDGF-AA

To determine whether EGF/FGF cultures that became GF independent after approximately 100 days in culture were also tumorigenic, 10^5 cells from these cultures were implanted into the right striatum of p53 wild type, immune-competent mice. After approximately 120 days, mice began to display signs of illness and had to be sacrificed.

These exogenous growth factor independent cells derived from long-term EGF/FGF cultures that were switched to culturing in PDGF-AA formed GFAP positive, OLIG2 positive, high-grade astrocytic tumors that resembled GBMs (**Fig. 25**). Fluorescence immunohistochemistry again showed co-expression of PDGFR-α and EGFR on most tumor cells with prominent EGFR staining toward the periphery of the tumor (**Fig. 25**). Similar to PDGF-AA formed tumors, these GBM-like tumors displayed a predominantly proneural expression profile (**Fig. 23**).

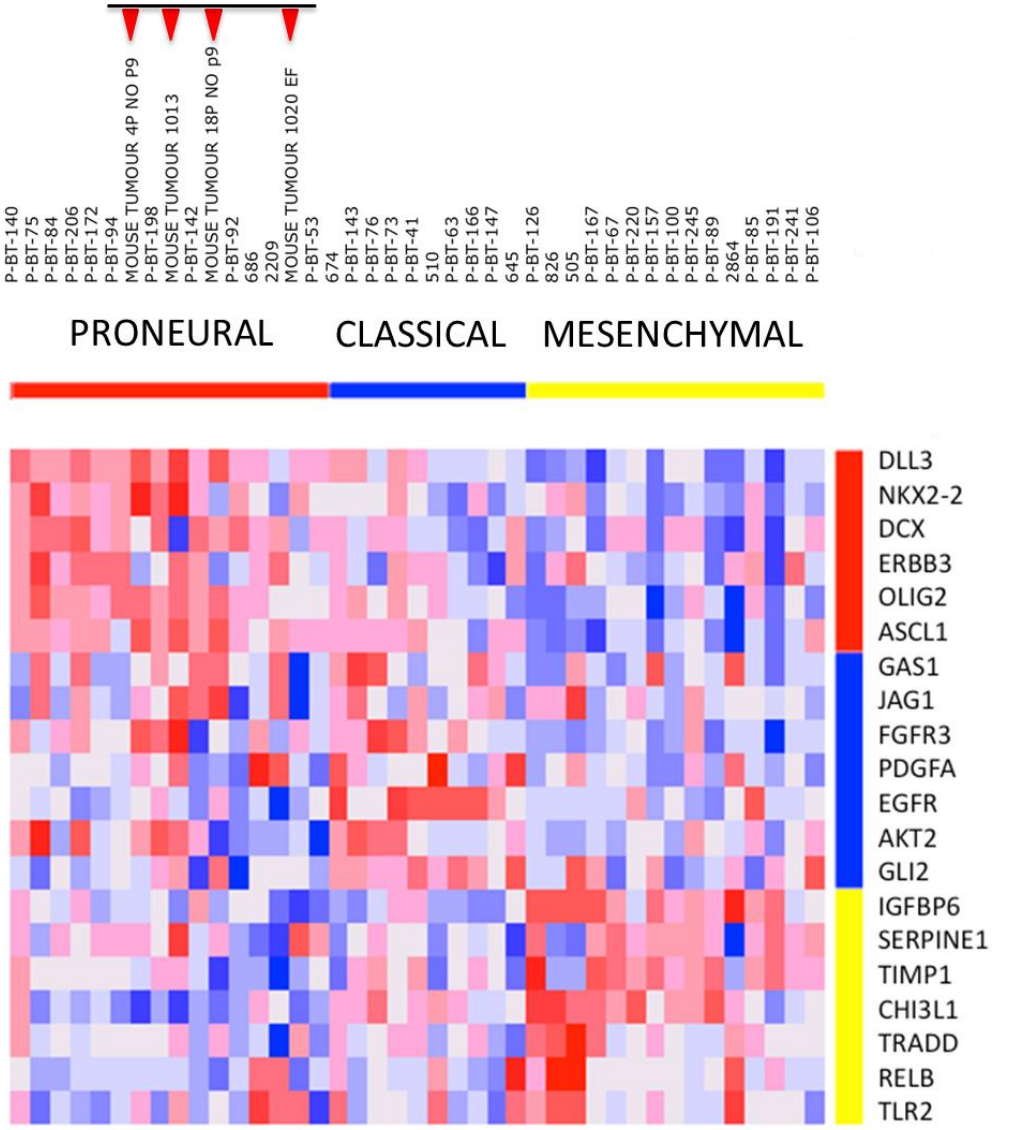

Figure 23: Exogenous PDGF-AA formed tumors classify as proneural by gene expression

Four representative mouse tumors classify as proneural in gene expression when compared against the gene expression patterns in normal human brain and human GBM. Of the four samples analyzed, three tumors were formed from p53 null SVZ samples cultured directly in PDGF-AA and the other from a p53 null EGF/FGF initiated cell line that had become GF independent after culturing in PDGF-AA (data analysis completed with assistance from Dr. S. Lawn).

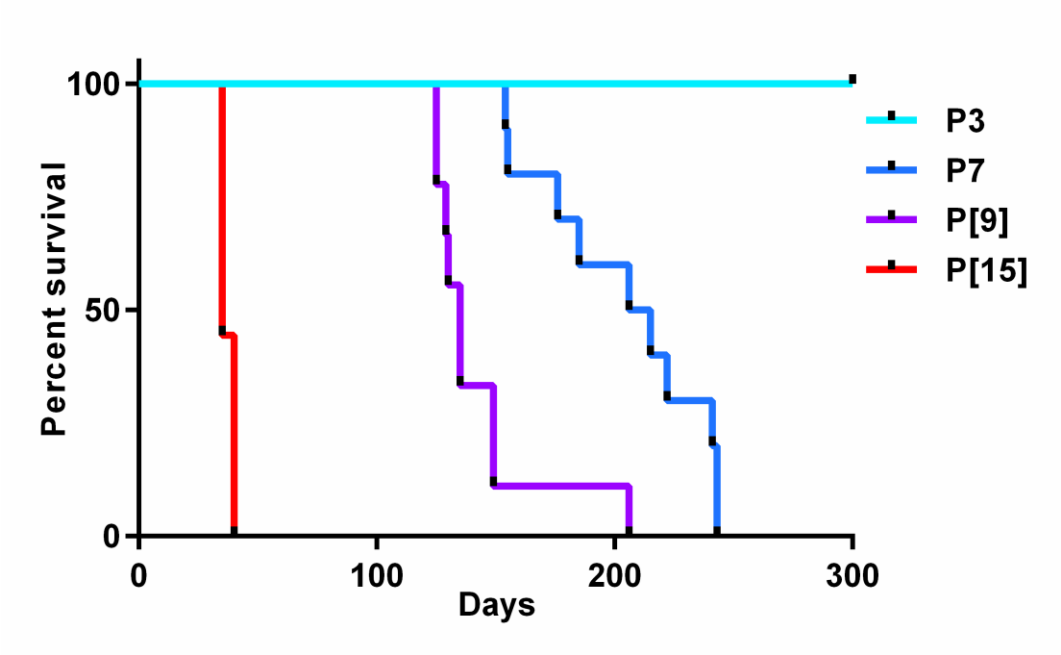

Figure 24: Survival curve mice implanted with p53-/- exogenous PDGF-AA independent cells

Temporal profile of p53-/- PDGF-AA responsive cells implanted at various passages illustrating that tumor latency is associated with the passage number of the implanted cells. Passage 7 cells which are not yet independent of exogenous PDGF-AA form tumors after approximately 250 days. Time to tumor formation decreases with passage 9 (P[9]) and P[15], both of which are exogenous PDGF-AA independent. Cells implanted from early passage 3 (P3) do not display tumor formation in up to 300 days. Survival curves are significantly different ($P<0.0001$ standard log rank test; P3=8 mice, P7= 10 mice, P[9]=9 mice, P[15]=9 mice). **[] = exogenous PDGF-AA independence.** (Adapted with permission from C. Binding(77)).

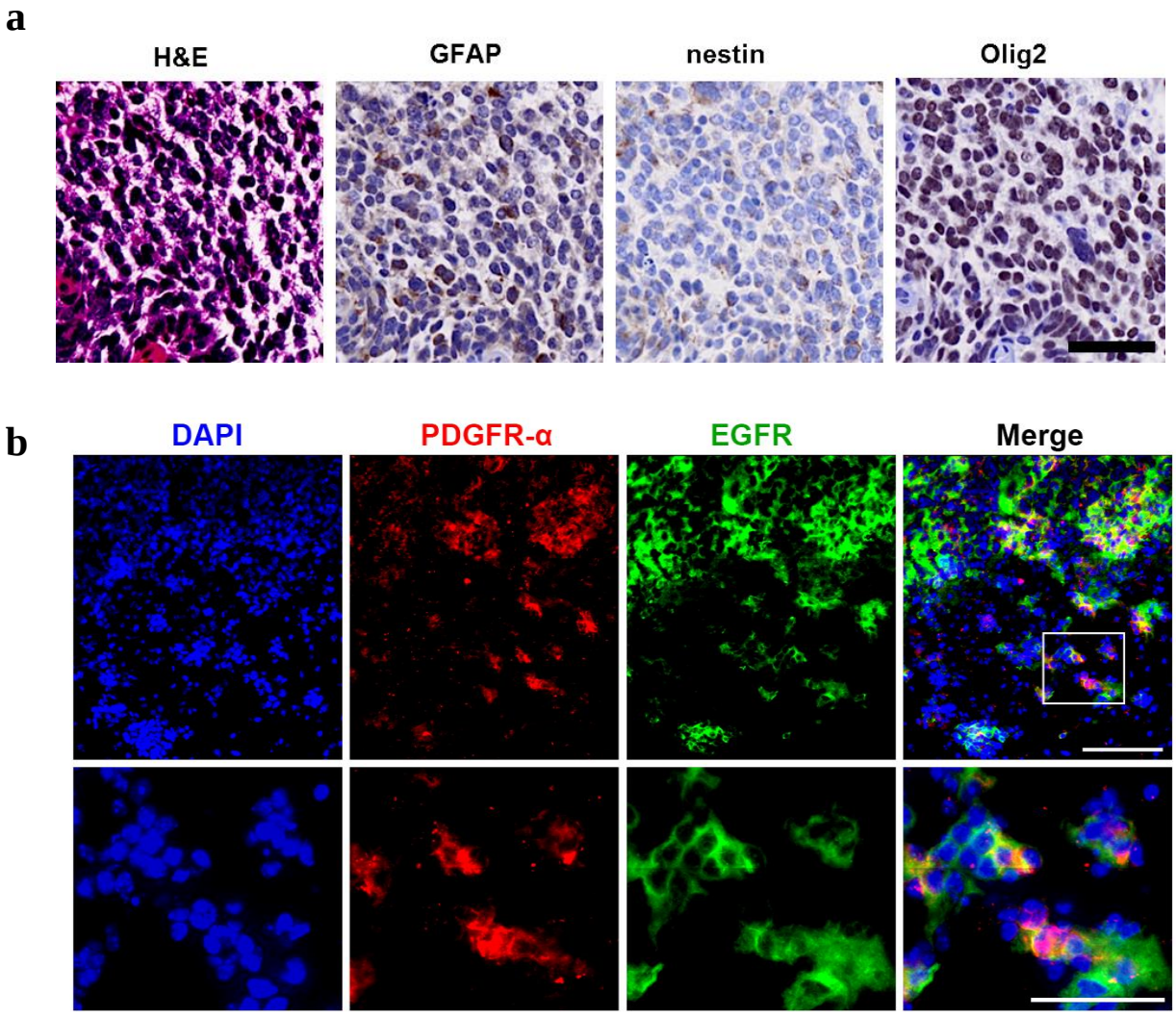

Figure 25: IHC and immunofluorescence from tumors formed by EGF/FGF cells which have been switched to PDGF-AA

Similar to tumors formed from p53 -/- cells cultured in PDGF-AA directly from the mouse SVZ, EGF/FGF cultures that have become exogenous GF independent after a period of culturing in PDGF-AA form highly cellular tumors that are GFAP and OLIG2 positive (**a**). Scale bar = 100 μm. PDGFR-α is expressed throughout the tumor with strong expression of EGFR near the tumor margin (**b**). Scale bar = 50 μm.

Chapter Five: Discussion

Significant progress has been made in our understanding of the molecular underpinnings and cellular biology of GBM, but this knowledge has not yet been successfully translated into targeted therapies that will replace, complement, or synergize with existing treatments. Today, we can generate long lists of the genetic and epigenetic changes that occur in human GBM, but from the all-important clinical perspectives of disease prevention and therapeutics, we are unable to distinguish the important 'driver' from the less important 'passenger' alterations in this disease. Still missing from our 'translational research armamentarium' is a laboratory model of GBM that is simple, accessible, reproducible, authentic, affordable and versatile - a model in which the earliest events in the genesis of GBM can be identified, investigated and understood, where the critical therapeutic targets can be differentiated from the trivial alterations, and where all types of therapies can be tested, including agents that prevent or negate initiating events, inhibit alterations that drive or sustain the cancer phenotype or activate the immune system to neutralize the disease. Our model of human GBM encompasses many of these desirable features, and as such, may be a useful addition to the 'tool kit' for understanding GBM and for finding new therapies.

5.1 The unique combination of p53 null and PDGF-AA in transformation

Within the developing and normal adult brain, GF signaling is a vital process. The PDGFs are widely expressed throughout the body including the brain. PDGFR-α is

important for normal skeletal development and vital for cell migration and wound healing. In the embryonic developing brain, PDGFR-α is required for cephalic closure. PDGFR-β is involved in vascular proliferation and angiogenesis (93–95). EGFR is essential in the normal brain for proliferation of neural precursor cells and is hence regionally expressed in the SVZ. EGFR is also involved in survival, migration and differentiation of immature cells. (96) However under certain pathological circumstances PDGF and EGF receptors can mediate tumorigenesis and metastasis. Loss of a tumor suppressor such as p53 may provide this permissive, tumorigenic setting. This setting can be viewed and further explored in our model where the effect of p53 status on the viability of SVZ cells in EGF/FGF versus PDGF-AA is strikingly different. In EGF/FGF, wild type cells and null cells proliferate continuously and rapidly and remain growth factor dependent, whereas in PDGF-AA, their viability and proliferative capacity are severely restricted. Wild type cells do not survive in PDGF-AA and p53 null cells survive by transforming, and only after a protracted period of 'crisis', which is characterized by low rates of viability and high rates of cell death. These events, which are visible *in vitro*, would be difficult to appreciate in the *in vivo* models of GBM.

These findings identify a connection between PDGF-AA and p53, and suggest that under wild type conditions, activation of PDGFR-α suppresses cellular proliferation in the SVZ through the p53 pathway. The idea of interplay between the PDGFs and p53 is not new, however the details of this connection have yet to be fully elucidated. In several models the expression of p53 has been seen to be reduced when PDGFR-α is directly activated

by way of PDGF ligands (82,83), and through indirect and continuous activation via reactive oxygen species (ROS) and Src family kinases (SFKs) (99,100). While initially it seems puzzling, that activation of PDGFR-α would in fact reduce the expression of p53, in the context of wound healing (101), it seems quite logical that initially p53 activation would be down-regulated until such time it is needed to stop PDGF-related proliferation. It may be that it is not solely p53 that is responsible for allowing transformation, rather that proteins downstream of p53 play a crucial role.

In 2003, Yu *et al*. showed that p21, a cyclin-dependent kinase inhibitor responsible for cell-cycle progression downstream of p53 was upregulated in cells treated with either PDGF-AA or BB even in the absence of p53 (102). Our model would suggest that PDGF-AA activates the p53 pathway. It could be inferred that presence of p53 is necessary to contend with the crisis period inflicted by PDGF-AA, and as a tumor suppressor, p53 prevents cells from continuing proliferation under detrimental conditions. Absence of p53 clearly permits the cells to remain viable in culture, and endure the crisis period. This was shown by Hesselager *et al.* when they cultured cells from the brains of p53 null or WT mice with PDGF-BB, which binds to both PDGFR-α and β, and found that only the p53 null cells survived in culture (59). In contrast, the ability of p53 null cells to grow well in EGF/FGF might imply these culture conditions do not activate the p53 pathway, and are substantially less stressful on cell viability, possibly because EGFR in the normal brain is responsible for proliferation of neural precursors within the SVZ. We have begun investigating the nature of the cellular crisis induced by PDGF-AA and preliminary

observations show expression of Fas, an apoptosis protein downstream of p53(103), only in p53 WT cells, not in early passage p53 null cells. This interesting observation is currently being studied, in order to determine the survival advantage of the p53 null cells. The potential relationship between p53, p21 and Fas as a result of culturing in PDGF-AA *vs* EGF/FGF is depicted below (**Fig. 26**).

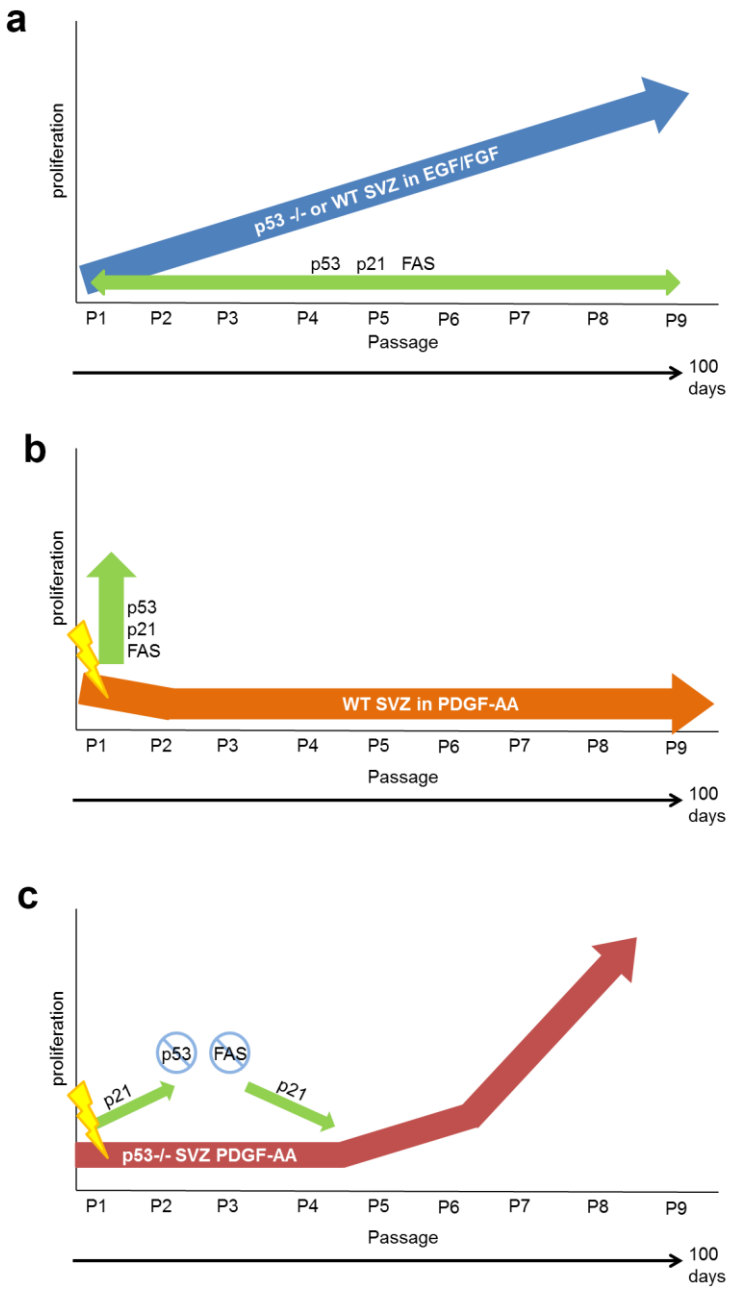

Figure 26: Depiction of hypothetical response of tumor suppressor expression in cells cultured in PDGF-AA vs EGF/FGF in p53 WT vs null conditions

EGF/FGF is not sufficiently stressful on cells, as such, p53 and downstream proteins p21 and Fas remain stable (**a**). PDGF-AA has been shown to be induce cell death in WT SVZ cells and thus the p53 pathway is activated in response (**b**). In p53 null SVZ cells which potentially also lack functional Fas, p21 alone is not sufficient to arrest proliferation in the presence of PDGF-AA oncogenic signaling (**c**).

5.2 The predictable transformation

There are two other intriguing features of our model that call for further study: first, is the predictable interval (~100 days) between exposure to PDGF-AA and the emergence of tumorigenic SVZ cells; and second, is the speed with which this change occurs in vitro. The transition from small ragged spheres that proliferate slowly in a 'pool' of apparently dead and dying cells to a 'sea' of large, rapidly proliferating spheres occurs at or near passage 9 and appears abrupt under the microscope. These observations suggest that a specific constellation of genetic events may be needed in null SVZ cells before the cancer phenotype emerges. These observations raise the further possibility that their accumulation is predictable, perhaps or clock-like. Speculating further, the behavior of SVZ cells in PDGF-AA, where a small number of p53 null cells survive a period of 'crisis' and then expand explosively, is reminiscent of *primary* human GBM, which is often called *de novo* GBM because of its abrupt onset without a visible antecedent phase. Since *primary* GBM harbors many molecular changes at diagnosis it is conceivable that a period of intense genomic instability exists prior to overt tumor growth. As such, the theory of accumulated mutations that leads to a cancer phenotype refers to the accumulation of 'passenger' mutations that do not contribute to the overall survival advantage of a tumor, versus specific 'driver' mutations that do (104). Using this model of glioma progression, we may be able to investigate the accumulation of genetic events and separate the 'passengers' from the 'drivers.'

In addition to the work presented here, I isolated DNA from p53 null PDGF-AA and EGF/FGF samples at early and late time points. These samples have been sequenced (exome sequencing) to analyze the coding regions of the genome. Analysis of these results will allow us to compare early passage, non-transformed PDGF-AA cultures and late passage, transformed PDGF-AA cultures to those maintained in EGF/FGF at sequential passages to investigate the step-wise transformation in these genomes. Molecular alterations found will be compared to those found in human GBM. It is possible that the key to transformation lies in further genomic analysis, especially that which is focused on the earliest stages of p53 null SVZ cells subjected to PDGF-AA.

The intriguing and reproducible timing of the PDGF-AA induced transformation brings to mind the clock-like nature of the Hayflick limit, first described in 1961 (104). This important observation described the phases of cell growth in culture: the primary culture or Phase I, which begins with culture initiation and ends with culture confluence; Phase II wherein cells proliferate rapidly and require frequent passaging; and Phase III in which cells in culture ultimately cease to grow. However a culture can escape Phase III with the acquisition of an alteration, such as loss of a tumor suppressor.

In our model, the escape from Phase III in which the PDGF-AA cells transform may be related to p53 and/or p21. An interesting study of the variability of the Hayflick limit demonstrated that the escape from Phase III coincided with a switch in p21 expression from upregulation in passages 1-3 to down regulation beginning around passage 5, paired

with reduced proliferation in early passages and increased proliferation which peaked near passage ten (105). This is similar to what we observe in our PDGF-AA grown cultures, where growth and proliferation is severely restricted during the first 3 passages, and the culture is primarily composed of dead or dying cells. The viable proportion of cells was observed to be at its lowest in passages 0 and 3, with the first significant upturn seen near passage 6 (**Fig. 9**). The remarkable similarity in the timing of their observations and our system is even more striking when considering the previously mentioned study by Yu *et al*. where p21 was upregulated in cells treated with either PDGF-AA or BB (102).

Excessive proliferative signaling can induce cell senescence (64,105), and it has been shown that PDGFR signaling may induce genomic instability in cells (106). This is consistent with our model in which p53-null neurospheres cultured in EGF/FGF are immortalized in culture, yet they do not transform and are not tumorigenic. In our system, the absence of p53 may provide the foundation of genomic instability for the tumorigenic effects of PDGF-AA to build upon. In a system such as this, proteins downstream of p53 related to cellular senescence and apoptosis such as p21 could be easily examined over time (passages) in p53 null and wild type cultures which are supplemented with PDGF-AA or EGF/FGF, in a similar fashion to the study by Yu *et al.* (102). Finding the protein or proteins, which allow the bypass of senescence in this system, would reveal some of the early events in this model system.

In addition, it has been shown that PDGFR signaling may induce genomic instability in cells (106). This is shown in our model in which p53 null neurospheres cultured in EGF/FGF are immortalized in culture, yet they do not transform and are not tumorigenic. While we have quantified the live, dead and apoptotic populations of the cultures, we have not yet examined the type of damage which triggers cell death. A study by Westermark and colleagues showed that PDGF-B induced gliomas displayed increased levels of DNA damage repair (DDR) markers, γH2AX and RAD51. An interesting additional observation was that immortalized $p19^{Arf}$-null cells remained diploid, whereas PDGF-B overexpression in combination with loss of $p19^{Arf}$ led to tetraploidy (106). Examining markers of DNA damage would also prove useful in the pre-transformation stage of this model.

5.3 Our model supports OPCs as a cell of origin for GBM

Lineage marker and growth factor receptor characterization of p53 null SVZ cultures were initiated with the expectation that different subtypes of cells grew in EGF/FGF versus PDGF-AA: one type proliferated in EGF/FGF but was resistant to transformation, while the other struggled to survive in PDGF-AA and ultimately transformed. Interestingly, EGF/FGF and PDGF-AA cultures were more similar than different by these measures. In both sets of growth factor conditions, cultures expressed OPC markers NG2 and OLIG2, and both GF receptors, EGFR and PDFGR-α. One difference is noteworthy however, PDGF-AA transformed cells express high levels of NESTIN, which may be indicative of a less differentiated neural stem cell population which is capable of self-

renewal (107). The most dramatic testament to their similarity was the fascinating observation that p53 null cells grown in EFG/FGF for 12 months or longer became exogenous growth factor independent and tumorigenic when switched to PDGF-AA. Transformation occurred approximately 100 days after EGF/FGF was removed and PDGF-AA introduced, exactly as we had seen when p53 null SVZ cells were cultured immediately in PDGF-AA. In further support of their inherent plasticity, p53 null EGF/FGF cultures, which are initially non-tumorigenic, display a classical gene signature, which switches to proneural after transformation via PDGF-AA (**Figs. 20 & 23**). Lineage tracing experiments (108) could help shed light on the nature of transformation in this system where a subpopulation of cells is amenable to transformation via PDGF-AA.

5.4 PDGF-AA driven, EGFR maintained

The observation that p53 null cells grown in EGF/FGF do not transform, while retaining the potential to do so when switched to PDGF-AA, is also noteworthy. Despite prolonged exposure to EGF/FGF, p53 null SVZ cells remain exogenous growth factor dependent and non-tumorigenic. This is an intriguing result because EGFR amplification and mutation are often considered to be defining molecular features of human GBM. In this regard, recent observations by Ozawa *et al*. may be relevant: they have suggested that activation of EGFR may not be an initiating event in GBM, but rather, a contributor to maintenance of the cancer phenotype. Our model may prove helpful in studying the link between SVZ cells, PDGF-AA, EGF/FGF, receptor biology, and the p53 pathway.

As the downstream signaling of EGFR and PDGFR-α is very similar, additional factors may contribute to the initially very different behavior observed in p53 null neurospheres cultured in EGF/FGF versus PDGF-AA. At culture initiation, a subpopulation of the cells from the SVZ of p53 null mice are not responsive to PDGF-AA, as exhibited by high levels of apoptosis and viability of only 5% in early passages. It could be that this small population of NSCs remains and repopulates the culture over time. Considering this possibility, it is generally assumed that pro-oncogenic changes accumulate within a hypothetical tumor cell of origin, ultimately leading to the evolution of the most viable clone (109). There are however studies that show this may not be the case, and in fact heterogeneity can be attributed to a single precursor clone which has developed into subclones that continue to survive in stable coexistence (110).

Remarkably, the tumors in our model, both those derived from PDGF-AA cultures and those from cells which have become tumorigenic after switching to PDGF-AA supplemented media, show increased levels of EGFR on the periphery of the tumors (**Figs. 22 & 25**). Okada *et al.* also observed this pattern, when fluorescence *in situ* hybridization (FISH) was used to study tumor heterogeneity with respect to EGFR amplification in the glioblastoma microenvironment. EGFR amplified cells were often found at the invading edge of the tumors rather than the tumor center (111). Interestingly, It has been reported by several groups that EGFR amplification is rapidly lost when tumors such as these are cultured (112,113). This indicates that *in vivo* and lysate based

studies of formed tumors may not be as informative as amplification events can be diluted out or lost in cases of mosaicism (109).

Considering the high level of EGFR protein on the periphery of our PDGF-AA initiated tumors, in agreement with what has been observed by others (109,112), two arguments could be made: i) EGFR positive/amplified cells on the periphery of the tumor are infiltrative, ii) the hypoxic environment in the center of the tumor is driving EGFR positive/amplified cells outward towards a more favorable environment. The escape from a hypoxic environment was examined by Schulte *et al*. in their study which sought to understand and resolve the challenge of EGFR amplified GBM tumor samples which quickly lose their EGFR amplification status upon culturing (112). EGFR amplification was lost under both normoxic and hypoxic conditions, excluding oxygen levels as the reason. However they showed that by removing or greatly reducing the concentration of EGF in the media EGFR amplification returned. Interestingly, and similar to what we have observed, they saw that EGF supplemented cultures proliferated at a higher rate than those without EGF, however they were not tumorigenic. Schulte *et al*. hypothesized that the absence of EGF in cultures might lead to selection of EGFR amplified cells in what is initially a heterogeneous cell population. Considering these findings together with the mathematical modeling of Ozawa *et al*., our model is promising as it may be able to accurately mirror both the initiating and invading stages of GBM.

5.5 Dynamic expression of PDGFR-α and EGFR

Since the growth factor in which p53 null SVZ cells are cultured clearly plays a role in the transformation process, the expression of PDGFR-α and EGFR was investigated thoroughly using multiple techniques. While both GF receptors were found to be present in both culture conditions, the levels of expression appeared to vary, sometimes with no discernable pattern. By western blotting PDGFR-α protein expression was relatively consistent in PDGF-AA derived cultures, and although present at some level, the amount seemed to vary in EGF/FGF cultures. Similarly, using qRT-PCR, PDGFR-α and EGFR were present in both culture conditions and generally appeared to increase with passage number, however expression levels varied between cultures (cell lines) and PDGFR-α was expressed at a higher level than EGFR. Assessing the cellular population by FISH could help clarify gene expression in what appears to be a mosaic population. Through both immunofluorescence and FACS, most cells co-expressed PDGFR-α and EGFR, regardless of the passage number and the growth factors added, however the proportions varied between techniques. As cellular adhesion methods such as laminin has been shown to alter receptor distribution (114–116) this may explain the increased amount of labeled cells observed using this technique. The population of EGF/FGF grown cells that did not stain positive for either EGFR or PDGFR-α could represent uncommitted quiescent cells, or the rapid internalization of receptors. Staining the same population after various windows of exposure to GF or staining for other RTKs or markers could clarify this disparity. In addition, the variability in receptor staining abundance between techniques could be attributed to the permeabilization step used in the immunofluorescence protocol

where internalized receptors could also be visualized. Using a biotin labeling assay could help determine the proportion of receptors on the cell surface versus those that are internalized.

In our EGF supplemented cultures, receptor turnover may play a role in the varied levels of expression. Upon ligand binding, EGFR is rapidly internalized within a matter of minutes, after internalization, EGFR and EGF are degraded (117). The process of internalization and degradation of EGFR initially leads to a reduction in cell surface receptors, and eventually to a decrease in activated receptors inside the cell (118). This negative feedback and quick degradation when ligands are present is a negative control of receptor signaling. RTKs can also undergo spontaneous degradation without ligand binding: both PDGFR-α and EGFR have a short half-life of only several hours which shortens with ligand binding (119,120). Harvesting cells at precise time points post GF addition could be informative in exploring this possibility. In terms of the initially PDGF-AA grown cells which no longer require the addition of PDGF-AA, the autocrine or paracrine production of growth factors could influence the expression of RTKs. Using mass spectrometry to evaluate the components of cultured, or 'conditioned' media would help define what the transformed cells are secreting. This assay could be helpful in determining what is driving transformation, as well as what is influencing the RTKs. It is possible that the variability of expression observed *in vitro* is related to culturing conditions such as when cultures are fed or passaged with fresh media, or cell density in cultures, all relating to the availability or depletion of nutrients. Various groups have

analyzed the effects of growth factor withdrawal in culture systems and have observed an upregulation of compensatory RTKs in a time dependent manner (121,122). As we have observed varying levels of receptor expression this is an important factor to control for experimentally.

Another factor in the variability of expression patterns may be attributed to the fact that co-activation of RTKs has been observed in human cell lines (92,121–125). In our model, the activation of RTKs as well as inhibition of PDGFR-α and EGFR are the next elements under investigation, which may help illuminate the driving force behind transformation. Also of interest are the proteins downstream of EGFR and PDGFR, considering the complexity and overlap of the signaling cascade downstream of PDGFR-α and EGFR, further investigation is needed to uncover the molecular alterations that produce the uncontrolled proliferation in our system.

5.6 Receptor morphology observation

Another interesting observation is that cells plated on laminin coated coverslips exhibit focal rather than diffuse receptor staining. Possible reasons for this might be the interaction of laminin binding to cell membranes through integrin receptors (126). Integrins and GF receptors are both located in the lipid raft and can cluster, especially when integrin receptors are bound to laminin (127,128). Other methods of assessing receptor populations were undertaken because of this potential interaction and how it

could influence staining patterns. Differences in temperature can also cause the aggregation of receptors, at 37°C receptors can cluster, cooling cells to 4°C leads to a partial reversal of this aggregation (129). As cytospin adhered cells and cells prepared for FACS are immediately placed in 4°C and cells adhered to coverslips are not suddenly cooled in the same manner, this could also explain the pattern of receptor expression observed.

5.7 Our model recapitulates the naturally occurring disease

Many elegant *in vivo* models have been developed that mimic human GBM, including xenografts, genetically engineered and chemically induced tumors (20,32,53–56,58,60,61,63,65,73). These models reproduce the phenotype of human GBM, and in the case of the genetic models, are constructed using manipulations that closely resemble, or precisely mimic, one or more of the molecular alterations that exist in the human disease. Already, these models have generated important new ideas about the possible cellular origins of GBM and have allowed the behavior of malignant cells in the brain to be explored more thoroughly. They have not, however, generated knowledge that has led to preventative strategies or new therapies for this disease. Although all models have limitations, there is a genuine concern that many of the current models of human GBM are rather ill suited to advancing knowledge toward preventative strategies, new therapeutics, or both. Current models mimic the full-blown disease but are not constructed in a way that would allow the various stages of GBM to be investigated easily, thoroughly, or step-wise. In other words, most models of human GBM are

initiated and driven by genetic alterations that occur in the human disease, but may not be the true initiators and drivers of GBM as it occurs naturally. This shortcoming will be problematic if the only way to prevent or thwart human GBM is to negate, reverse or target the earliest events in its pathogenesis. It is entirely possible that the majority of existing laboratory models of GBM do not recapitulate the naturally occurring disease, sufficiently, to be highly useful as tools for experimental therapeutics.

Models are important when they are useful; time will tell whether this one helps us understand, prevent, or treat GBM. That said, this model has desirable features. It is simple: this model does not require sophisticated equipment or genetic engineering of laboratory animals. It is accessible: pre-transformed and transformed cells can be studied step-wise and repeatedly as needed. It is reproducible: the sequence of events that occur in PDGF-AA causing p53 null SVZ cells to transform occur unfailingly. It is authentic: recent observations and hypotheses about the pathogenesis of GBM that have emerged from TCGA data and other mouse model systems point to the importance of PDGF-AA and p53 in the initiation of GBM, which are also the key determinants of this model. Finally, this model promises to be versatile: it can be used to dissect the critical early and late events in GBM pathogenesis, test strategies that interrupt initiating or sustaining molecular alterations, and assess tumor-host interactions and the potential to activate the immune system to control GBM.

References

1. Ostrom QT, Gittleman H, Farah P, Ondracek A, Chen Y, Wolinsky Y, et al. CBTRUS Statistical Report: Primary Brain and Central Nervous System Tumors Diagnosed in the United States in 2006-2010. Neuro-Oncol. 2013 Nov 1;15(suppl 2):ii1–56.

2. Stupp R, Mason WP, van den Bent MJ, Weller M, Fisher B, Taphoorn MJB, et al. Radiotherapy plus Concomitant and Adjuvant Temozolomide for Glioblastoma. N Engl J Med. 2005;352(10):987–96.

3. Ohgaki H, Kleihues P. The Definition of Primary and Secondary Glioblastoma. Clin Cancer Res. 2013 Feb 15;19(4):764–72.

4. Louis DN. Molecular Pathology of Malignant Gliomas. Annu Rev Pathol Mech Dis. 2006;1(1):97–117.

5. Louis DN, Ohgaki H, Wiestler OD, Cavenee WK, Burger PC, Jouvet A, et al. The 2007 WHO Classification of Tumours of the Central Nervous System. Acta Neuropathol (Berl). 2007 Jul 6;114(2):97–109.

6. Christaras, A. Glioblastoma (astrocytoma) WHO grade IV MRI [Internet]. 2006 [cited 2015 Feb 24]. Available from: http://commons.wikimedia.org/wiki/File:Glioblastoma_-_MR_sagittal_with_contrast.jpg

7. Parsons DW, Jones S, Zhang X, Lin JC-H, Leary RJ, Angenendt P, et al. An integrated genomic analysis of human glioblastoma multiforme. Science. 2008 Sep 26;321(5897):1807–12.

8. Smith JS, Tachibana I, Passe SM, Huntley BK, Borell TJ, Iturria N, et al. PTEN mutation, EGFR amplification, and outcome in patients with anaplastic astrocytoma and glioblastoma multiforme. J Natl Cancer Inst. 2001 Aug 15;93(16):1246–56.

9. Gan HK, Kaye AH, Luwor RB. The EGFRvIII variant in glioblastoma multiforme. J Clin Neurosci Off J Neurosurg Soc Australas. 2009 Jun;16(6):748–54.

10. Verhaak RGW, Hoadley KA, Purdom E, Wang V, Qi Y, Wilkerson MD, et al. An integrated genomic analysis identifies clinically relevant subtypes of glioblastoma characterized by abnormalities in PDGFRA, IDH1, EGFR and NF1. Cancer Cell. 2010 Jan 19;17(1):98.

11. Ohgaki H, Kleihues P. Genetic Pathways to Primary and Secondary Glioblastoma. Am J Pathol. 2007 May;170(5):1445–53.

12. Stommel JM, Kimmelman AC, Ying H, Nabioullin R, Ponugoti AH, Wiedemeyer R, et al. Coactivation of Receptor Tyrosine Kinases Affects the Response of Tumor Cells to Targeted Therapies. Science. 2007 Oct 12;318(5848):287–90.

13. Yan H, Parsons DW, Jin G, McLendon R, Rasheed BA, Yuan W, et al. IDH1 and IDH2 Mutations in Gliomas. N Engl J Med. 2009;360(8):765–73.

14. Nobusawa S, Watanabe T, Kleihues P, Ohgaki H. IDH1 Mutations as Molecular Signature and Predictive Factor of Secondary Glioblastomas. Clin Cancer Res. 2009 Oct 1;15(19):6002–7.

15. Furnari FB, Fenton T, Bachoo RM, Mukasa A, Stommel JM, Stegh A, et al. Malignant astrocytic glioma: genetics, biology, and paths to treatment. Genes Dev. 2007 Nov 1;21(21):2683–710.

16. Hermanson M, Funa K, Hartman M, Claesson-Welsh L, Heldin C-H, Westermark B, et al. Platelet-derived Growth Factor and Its Receptors in Human Glioma Tissue: Expression of Messenger RNA and Protein Suggests the Presence of Autocrine and Paracrine Loops. Cancer Res. 1992 Jun 1;52(11):3213–9.

17. Ozawa T, Brennan CW, Wang L, Squatrito M, Sasayama T, Nakada M, et al. PDGFRA gene rearrangements are frequent genetic events in PDGFRA-amplified glioblastomas. Genes Dev. 2010 Oct 1;24(19):2205–18.

18. Huse JT, Holland EC. Targeting brain cancer: advances in the molecular pathology of malignant glioma and medulloblastoma. Nat Rev Cancer. 2010 May;10(5):319–31.

19. Phillips HS, Kharbanda S, Chen R, Forrest WF, Soriano RH, Wu TD, et al. Molecular subclasses of high-grade glioma predict prognosis, delineate a pattern of disease progression, and resemble stages in neurogenesis. Cancer Cell. 2006 Jan 3;9(3):157–73.

20. Ozawa T, Riester M, Cheng Y-K, Huse JT, Squatrito M, Helmy K, et al. Most Human Non-GCIMP Glioblastoma Subtypes Evolve from a Common Proneural-like Precursor Glioma. Cancer Cell. 2014 Aug 11;26(2):288–300.

21. Noushmehr H, Weisenberger DJ, Diefes K, Phillips HS, Pujara K, Berman BP, et al. Identification of a CpG Island Methylator Phenotype that Defines a Distinct Subgroup of Glioma. Cancer Cell. 2010 May 18;17(5):510–22.

22. Nakamura M, Yonekawa Y, Kleihues P, Ohgaki H. Promoter hypermethylation of the RB1 gene in glioblastomas. Lab Investig J Tech Methods Pathol. 2001 Jan;81(1):77–82.

23. Hegi ME, Diserens A-C, Godard S, Dietrich P-Y, Regli L, Ostermann S, et al. Clinical Trial Substantiates the Predictive Value of O-6-Methylguanine-DNA Methyltransferase Promoter Methylation in Glioblastoma Patients Treated with Temozolomide. Clin Cancer Res. 2004 Mar 15;10(6):1871–4.

24. Singh SK, Clarke ID, Terasaki M, Bonn VE, Hawkins C, Squire J, et al. Identification of a Cancer Stem Cell in Human Brain Tumors. Cancer Res. 2003 Sep 15;63(18):5821–8.

25. Singh SK, Hawkins C, Clarke ID, Squire JA, Bayani J, Hide T, et al. Identification of human brain tumour initiating cells. Nature. 2004 Nov 18;432(7015):396–401.

26. Visvader JE. Cells of origin in cancer. Nature. 2011 Jan 20;469(7330):314–22.

27. Liu C, Sage JC, Miller MR, Verhaak RGW, Hippenmeyer S, Vogel H, et al. Mosaic Analysis with Double Markers Reveals Tumor Cell of Origin in Glioma. Cell. 2011 Jul 22;146(2):209–21.

28. Fruttiger M, Karlsson L, Hall AC, Abramsson A, Calver AR, Bostrom H, et al. Defective oligodendrocyte development and severe hypomyelination in PDGF-A knockout mice. Development. 1999 Feb 1;126(3):457–67.

29. Calver AR, Hall AC, Yu W-P, Walsh FS, Heath JK, Betsholtz C, et al. Oligodendrocyte Population Dynamics and the Role of PDGF In Vivo. Neuron. 1998 May;20(5):869–82.

30. Nazarenko I, Hede S-M, He X, Hedrén A, Thompson J, Lindström MS, et al. PDGF and PDGF receptors in glioma. Ups J Med Sci. 2012 May;117(2):99–112.

31. Chojnacki A, Weiss S. Isolation of a Novel Platelet-Derived Growth Factor-Responsive Precursor from the Embryonic Ventral Forebrain. J Neurosci. 2004 Dec 1;24(48):10888–99.

32. Dai C, Celestino JC, Okada Y, Louis DN, Fuller GN, Holland EC. PDGF autocrine stimulation dedifferentiates cultured astrocytes and induces oligodendrogliomas and oligoastrocytomas from neural progenitors and astrocytes in vivo. Genes Dev. 2001 Aug 1;15(15):1913–25.

33. Assanah M, Lochhead R, Ogden A, Bruce J, Goldman J, Canoll P. Glial Progenitors in Adult White Matter Are Driven to Form Malignant Gliomas by Platelet-Derived Growth Factor-Expressing Retroviruses. J Neurosci. 2006 Jun 21;26(25):6781–90.

34. Assanah MC, Bruce JN, Suzuki SO, Chen A, Goldman JE, Canoll P. PDGF stimulates the massive expansion of glial progenitors in the neonatal forebrain. Glia. 2009;57(16):1835–47.

35. Pontén J. Neoplastic Human Glia Cells in Culture. In: Fogh J, editor. Human Tumor Cells in Vitro [Internet]. Springer US; 1975 [cited 2015 Mar 5]. p. 175–206.

Available from: http://link.springer.com.ezproxy.lib.ucalgary.ca/chapter/10.1007/978-1-4757-1647-4_7

36. Jacobs VL, Valdes PA, Hickey WF, De Leo JA. Current review of in vivo GBM rodent models: emphasis on the CNS-1 tumour model. ASN NEURO [Internet]. 2011 Aug 3 [cited 2015 Mar 5];3(3). Available from: http://www.ncbi.nlm.nih.gov/pmc/articles/PMC3153964/

37. Usta SN, Scharer CD, Xu J, Frey TK, Nash RJ. Chemically defined serum-free and xeno-free media for multiple cell lineages. Ann Transl Med [Internet]. 2014 Oct [cited 2015 Mar 8];2(10). Available from: http://www.ncbi.nlm.nih.gov/pmc/articles/PMC4205861/

38. Huszthy PC, Daphu I, Niclou SP, Stieber D, Nigro JM, Sakariassen PØ, et al. In vivo models of primary brain tumors: pitfalls and perspectives. Neuro-Oncol. 2012 Jun 7;nos135.

39. Doblas S, He T, Saunders D, Pearson J, Hoyle J, Smith N, et al. Glioma morphology and tumor-induced vascular alterations revealed in seven rodent glioma models by in vivo magnetic resonance imaging and angiography. J Magn Reson Imaging JMRI. 2010 Aug;32(2):267–75.

40. Holland EC, Hively WP, Gallo V, Varmus HE. Modeling mutations in the G1 arrest pathway in human gliomas: overexpression of CDK4 but not loss of INK4a–ARF induces hyperploidy in cultured mouse astrocytes. Genes Dev. 1998 Dec 1;12(23):3644–9.

41. Zhu H, Acquaviva J, Ramachandran P, Boskovitz A, Woolfenden S, Pfannl R, et al. Oncogenic EGFR signaling cooperates with loss of tumor suppressor gene functions in gliomagenesis. Proc Natl Acad Sci. 2009 Feb 24;106(8):2712–6.

42. Fredriksson L, Li H, Eriksson U. The PDGF family: four gene products form five dimeric isoforms. Cytokine Growth Factor Rev. 2004 Aug;15(4):197–204.

43. Li X, Eriksson U. Novel PDGF family members: PDGF-C and PDGF-D. Cytokine Growth Factor Rev. 2003 Apr;14(2):91–8.

44. Cao Y. Multifarious functions of PDGFs and PDGFRs in tumor growth and metastasis. Trends Mol Med. 2013 Aug;19(8):460–73.

45. Donovan J, Shiwen X, Norman J, Abraham D. Platelet-derived growth factor alpha and beta receptors have overlapping functional activities towards fibroblasts. Fibrogenesis Tissue Repair. 2013;6(1):10.

46. Brennan CW, Verhaak RGW, McKenna A, Campos B, Noushmehr H, Salama SR, et al. The Somatic Genomic Landscape of Glioblastoma. Cell. 2013 Oct 10;155(2):462–77.

47. Matsui T, Heidaran M, Miki T, Popescu N, Rochelle WL, Kraus M, et al. Isolation of a novel receptor cDNA establishes the existence of two PDGF receptor genes. Science. 1989 Feb 10;243(4892):800–4.

48. Hart IK, Richardson WD, Heldin CH, Westermark B, Raff MC. PDGF receptors on cells of the oligodendrocyte-type-2 astrocyte (O-2A) cell lineage. Development. 1989 Mar 1;105(3):595–603.

49. Heldin CH, Backstrom G, Ostman A, Hammacher A, Ronnstrand L, Rubin K, et al. Binding of different dimeric forms of PDGF to human fibroblasts: evidence for two separate receptor types. EMBO J. 1988 May;7(5):1387–93.

50. Sato S, Sato Y, Hatakeyama K, Marutsuka K, Yamashita A, Takeshima H, et al. Quantitative analysis of vessels with smooth muscle layer in astrocytic tumors: correlation with histological grade and prognostic significance. Histol Histopathol. 2011 Apr;26(4):497–504.

51. Kim Y, Kim E, Wu Q, Guryanova O, Hitomi M, Lathia JD, et al. Platelet-derived growth factor receptors differentially inform intertumoral and intratumoral heterogeneity. Genes Dev. 2012 Jun 1;26(11):1247–62.

52. Guo P, Hu B, Gu W, Xu L, Wang D, Huang H-JS, et al. Platelet-Derived Growth Factor-B Enhances Glioma Angiogenesis by Stimulating Vascular Endothelial Growth Factor Expression in Tumor Endothelia and by Promoting Pericyte Recruitment. Am J Pathol. 2003 Apr;162(4):1083–93.

53. Deinhardt, F. The biology of primate retrovirus. In: Klein G., editor. Viral Oncology. 1980. p. 359–98.

54. Nistér M, Westermark B. Mechanisms of altered growth control; Growth factors. In: Bigner DD, McLendon RE, Bruner JM, editor. Pathology of tumors of the nervous system. 6th ed. London: Arnold, Hodder Headline Group; 1998. p. 83–116.

55. Uhrbom L, Hesselager G, Nistér M, Westermark B. Induction of Brain Tumors in Mice Using a Recombinant Platelet-derived Growth Factor B-Chain Retrovirus. Cancer Res. 1998 Dec 1;58(23):5275–9.

56. Holland EC, Hively WP, DePinho RA, Varmus HE. A constitutively active epidermal growth factor receptor cooperates with disruption of G1 cell-cycle arrest pathways to induce glioma-like lesions in mice. Genes Dev. 1998 Dec 1;12(23):3675–85.

57. Orsulic S. An RCAS-TVA-based approach to designer mouse models. Mamm Genome. 2002 Oct 1;13(10):543–7.

58. Lindberg N, Kastemar M, Olofsson T, Smits A, Uhrbom L. Oligodendrocyte progenitor cells can act as cell of origin for experimental glioma. Oncogene. 2009 Apr 27;28(23):2266–75.

59. Hesselager G, Uhrbom L, Westermark B, Nistér M. Complementary Effects of Platelet-derived Growth Factor Autocrine Stimulation and p53 or Ink4a-Arf Deletion in a Mouse Glioma Model. Cancer Res. 2003 Aug 1;63(15):4305–9.

60. Hambardzumyan D, Amankulor NM, Helmy KY, Becher OJ, Holland EC. Modeling Adult Gliomas Using RCAS/t-va Technology. Transl Oncol. 2009 May;2(2):89–95.

61. Sonabend AM, Yun J, Lei L, Leung R, Soderquist C, Crisman C, et al. Murine cell line model of proneural glioma for evaluation of anti-tumor therapies. J Neurooncol. 2013 May;112(3):375–82.

62. Uhrbom L, Hesselager G, Östman A, Nistér M, Westermark B. Dependence of autocrine growth factor stimulation in platelet-derived growth factor-B-induced mouse brain tumor cells. Int J Cancer. 2000;85(3):398–406.

63. Tchougounova E, Kastemar M, Bråsäter D, Holland EC, Westermark B, Uhrbom L. Loss of Arf causes tumor progression of PDGFB-induced oligodendroglioma. Oncogene. 2007 Apr 16;26(43):6289–96.

64. Hanahan D, Weinberg RA. Hallmarks of Cancer: The Next Generation. Cell. 2011 Mar 4;144(5):646–74.

65. Hede S-M, Hansson I, Afink GB, Eriksson A, Nazarenko I, Andrae J, et al. GFAP promoter driven transgenic expression of PDGFB in the mouse brain leads to glioblastoma in a Trp53 null background. Glia. 2009;57(11):1143–53.

66. Sonabend AM, Bansal M, Guarnieri P, Lei L, Amendolara B, Soderquist C, et al. The Transcriptional Regulatory Network of Proneural Glioma Determines the Genetic Alterations Selected during Tumor Progression. Cancer Res. 2014 Mar 1;74(5):1440–51.

67. Lokker NA, Sullivan CM, Hollenbach SJ, Israel MA, Giese NA. Platelet-derived Growth Factor (PDGF) Autocrine Signaling Regulates Survival and Mitogenic Pathways in Glioblastoma Cells Evidence That the Novel PDGF-C and PDGF-D Ligands May Play a Role in the Development of Brain Tumors. Cancer Res. 2002 Jul 1;62(13):3729–35.

68. Jackson EL, Garcia-Verdugo JM, Gil-Perotin S, Roy M, Quinones-Hinojosa A, VandenBerg S, et al. PDGFRα-Positive B Cells Are Neural Stem Cells in the Adult SVZ that Form Glioma-like Growths in Response to Increased PDGF Signaling. Neuron. 2006 Jul 20;51(2):187–99.

69. Chojnacki A, Mak G, Weiss S. PDGFRα expression distinguishes GFAP-expressing neural stem cells from PDGF-responsive neural precursors in the adult periventricular area. J Neurosci Off J Soc Neurosci. 2011 Jun 29;31(26):9503–12.

70. Fukuda N, Kishioka H, Satoh C, Nakayama T, Watanabe Y, Soma M, et al. Role of long-form PDGF A-chain in the growth of vascular smooth muscle cells from spontaneously hypertensive rats. Am J Hypertens. 1997 Oct;10(10 Pt 1):1117–24.

71. Tong BD, Auer DE, Jaye M, Kaplow JM, Ricca G, McConathy E, et al. cDNA clones reveal differences between human glial and endothelial cell platelet-derived growth factor A-chains. Publ Online 13 August 1987 Doi101038328619a0. 1987 Aug 13;328(6131):619–21.

72. Betsholtz C, Johnsson A, Heldin C-H, Westermark B, Lind P, Urdea MS, et al. cDNA sequence and chromosomal localization of human platelet-derived growth factor A-chain and its expression in tumour cell lines. Nature. 1986 Apr 24;320(6064):695–9.

73. Nazarenko I, Hedrén A, Sjödin H, Orrego A, Andrae J, Afink GB, et al. Brain Abnormalities and Glioma-Like Lesions in Mice Overexpressing the Long Isoform of PDGF-A in Astrocytic Cells. PLoS ONE. 2011 Apr 7;6(4):e18303.

74. Bögler O, Huang HJ, Kleihues P, Cavenee WK. The p53 gene and its role in human brain tumors. Glia. 1995 Nov;15(3):308–27.

75. Wang Y, Yang J, Zheng H, Tomasek GJ, Zhang P, McKeever PE, et al. Expression of mutant p53 proteins implicates a lineage relationship between neural stem cells and malignant astrocytic glioma in a murine model. Cancer Cell. 2009 Jun 2;15(6):514–26.

76. Hermanson M, Funa K, Koopmann J, Maintz D, Waha A, Westermark B, et al. Association of Loss of Heterozygosity on Chromosome 17p with High Platelet-derived

Growth Factor α Receptor Expression in Human Malignant Gliomas. Cancer Res. 1996 Jan 1;56(1):164–71.

77. Binding C. Characterization of a novel PDGF-A driven in vitro model of high-grade glioma [Master's Thesis]. [Calgary, Canada]: Master's Thesis, University of Calgary; 2012.

78. Chojnacki A, Weiss S. Production of neurons, astrocytes and oligodendrocytes from mammalian CNS stem cells. Nat Protoc. 2008 May;3(6):935–40.

79. Kelly JJP, Stechishin O, Chojnacki A, Lun X, Sun B, Senger DL, et al. Proliferation of Human Glioblastoma Stem Cells Occurs Independently of Exogenous Mitogens. STEM CELLS. 2009;27(8):1722–33.

80. Hoshida Y, Villanueva A, Kobayashi M, Peix J, Chiang DY, Camargo A, et al. Gene expression in fixed tissues and outcome in hepatocellular carcinoma. N Engl J Med. 2008 Nov 6;359(19):1995–2004.

81. Xu L, Shen SS, Hoshida Y, Subramanian A, Ross K, Brunet J-P, et al. Gene expression changes in an animal melanoma model correlate with aggressiveness of human melanoma metastases. Mol Cancer Res MCR. 2008 May;6(5):760–9.

82. Reiner A, Yekutieli D, Benjamini Y. Identifying differentially expressed genes using false discovery rate controlling procedures. Bioinforma Oxf Engl. 2003 Feb 12;19(3):368–75.

83. Reich M, Liefeld T, Gould J, Lerner J, Tamayo P, Mesirov JP. GenePattern 2.0. Nat Genet. 2006 May;38(5):500–1.

84. Doetsch F, Caillé I, Lim DA, García-Verdugo JM, Alvarez-Buylla A. Subventricular zone astrocytes are neural stem cells in the adult mammalian brain. Cell. 1999 Jun 11;97(6):703–16.

85. Dunn IF, Heese O, Black PM. Growth Factors in Glioma Angiogenesis: FGFs, PDGF, EGF, and TGFs. J Neurooncol. 2000 Oct 1;50(1-2):121–37.

86. Reynolds BA, Weiss S. Generation of neurons and astrocytes from isolated cells of the adult mammalian central nervous system. Science. 1992 Mar 27;255(5052):1707–10.

87. Whittemore SR, Morassutti DJ, Walters WM, Liu R-H, Magnuson DSK. Mitogen and Substrate Differentially Affect the Lineage Restriction of Adult Rat Subventricular Zone Neural Precursor Cell Populations. Exp Cell Res. 1999 Oct 10;252(1):75–95.

88. Hanahan D, Weinberg RA. The Hallmarks of Cancer. Cell. 2000 Jan 7;100(1):57–70.

89. Vogel C, Marcotte EM. Insights into the regulation of protein abundance from proteomic and transcriptomic analyses. Nat Rev Genet. 2012 Apr 1;13(4):227–32.

90. Boccaccio C, Comoglio PM. The MET Oncogene in Glioblastoma Stem Cells: Implications as a Diagnostic Marker and a Therapeutic Target. Cancer Res. 2013 Jun 1;73(11):3193–9.

91. Engelman JA, Zejnullahu K, Mitsudomi T, Song Y, Hyland C, Park JO, et al. MET Amplification Leads to Gefitinib Resistance in Lung Cancer by Activating ERBB3 Signaling. Science. 2007 May 18;316(5827):1039–43.

92. Jo M, Stolz DB, Esplen JE, Dorko K, Michalopoulos GK, Strom SC. Cross-talk between Epidermal Growth Factor Receptor and c-Met Signal Pathways in Transformed Cells. J Biol Chem. 2000 Mar 24;275(12):8806–11.

93. Westermark B, Wasteson Å. A platelet factor stimulating human normal glial cells. Exp Cell Res. 1976 Mar 1;98(1):170–4.

94. Cimpean AM, Ceauşu R, Encică S, Gaje PN, Ribatti D, Raica M. Platelet-derived growth factor and platelet-derived growth factor receptor-α expression in the normal human thymus and thymoma. Int J Exp Pathol. 2011 Oct;92(5):340–4.

95. Soriano P. The PDGF alpha receptor is required for neural crest cell development and for normal patterning of the somites. Dev Camb Engl. 1997 Jul;124(14):2691–700.

96. Estrada C, Villalobo A. Epidermal Growth Factor Receptor in the Adult Brain. In: Janigro D, editor. The Cell Cycle in the Central Nervous System [Internet]. Humana Press; 2006 [cited 2015 Mar 11]. p. 265–77. Available from: http://link.springer.com.ezproxy.lib.ucalgary.ca/chapter/10.1007/978-1-59745-021-8_20

97. Fantauzzo KA, Soriano P. PI3K-mediated PDGFR signaling regulates survival and proliferation in skeletal development through p53-dependent intracellular pathways. Genes Dev. 2014 May 1;28(9):1005–17.

98. Liu Z, Liu H, Jiang J, Tan S, Yang Y, Zhan Y, et al. PDGF-BB and bFGF ameliorate radiation-induced intestinal progenitor/stem cell apoptosis via Akt/p53 signaling in mice. Am J Physiol - Gastrointest Liver Physiol. 2014 Dec 1;307(11):G1033–43.

99. Lei H, Velez G, Kazlauskas A. Pathological Signaling via Platelet-Derived Growth Factor Receptor Involves Chronic Activation of Akt and Suppression of p53. Mol Cell Biol. 2011 May 1;31(9):1788–99.

100. Lei H, Kazlauskas A. A reactive oxygen species-mediated, self-perpetuating loop persistently activates platelet-derived growth factor receptor α. Mol Cell Biol. 2014 Jan;34(1):110–22.

101. Antoniades HN, Galanopoulos T, Neville-Golden J, Kiritsy CP, Lynch SE. p53 expression during normal tissue regeneration in response to acute cutaneous injury in swine. J Clin Invest. 1994 May;93(5):2206–14.

102. Yu J, Liu X-W, Kim H-RC. Platelet-derived Growth Factor (PDGF) Receptor-α-activated c-Jun NH2-terminal Kinase-1 Is Critical for PDGF-induced p21WAF1/CIP1 Promoter Activity Independent of p53. J Biol Chem. 2003 Dec 5;278(49):49582–8.

103. Wajant H. The Fas Signaling Pathway: More Than a Paradigm. Science. 2002 May 31;296(5573):1635–6.

104. Hayflick L, Moorhead PS. The serial cultivation of human diploid cell strains. Exp Cell Res. 1961 Dec;25(3):585–621.

105. Rizzo M, Evangelista M, Simili M, Mariani L, Pitto L, Rainaldi G. Immortalization of MEF is characterized by the deregulation of specific miRNAs with potential tumor suppressor activity. Aging. 2011 Jul;3(7):665–71.

106. Westermark UK, Lindberg N, Roswall P, Bråsäter D, Helgadottir HR, Hede S-M, et al. RAD51 can inhibit PDGF-B–induced gliomagenesis and genomic instability. Neuro-Oncol. 2011 Dec;13(12):1277–87.

107. Calabrese C, Poppleton H, Kocak M, Hogg TL, Fuller C, Hamner B, et al. A Perivascular Niche for Brain Tumor Stem Cells. Cancer Cell. 2007 Jan;11(1):69–82.

108. Spradling. Lineage analysis of stem cells. StemBook [Internet]. 2009 [cited 2015 Mar 11]; Available from: http://www.stembook.org/node/542

109. Snuderl M, Fazlollahi L, Le LP, Nitta M, Zhelyazkova BH, Davidson CJ, et al. Mosaic Amplification of Multiple Receptor Tyrosine Kinase Genes in Glioblastoma. Cancer Cell. 2011 Dec 13;20(6):810–7.

110. Bach LA, Bentzen SM, Alsner J, Christiansen FB. An evolutionary-game model of tumour–cell interactions: possible relevance to gene therapy. Eur J Cancer. 2001 Nov;37(16):2116–20.

111. Okada Y, Hurwitz EE, Esposito JM, Brower MA, Nutt CL, Louis DN. Selection Pressures of TP53 Mutation and Microenvironmental Location Influence Epidermal Growth Factor Receptor Gene Amplification in Human Glioblastomas. Cancer Res. 2003 Jan 15;63(2):413–6.

112. Schulte A, Günther HS, Martens T, Zapf S, Riethdorf S, Wülfing C, et al. Glioblastoma stem-like cell lines with either maintenance or loss of high-level EGFR amplification, generated via modulation of ligand concentration. Clin Cancer Res Off J Am Assoc Cancer Res. 2012 Apr 1;18(7):1901–13.

113. Humphrey PA, Wong AJ, Vogelstein B, Friedman HS, Werner MH, Bigner DD, et al. Amplification and Expression of the Epidermal Growth Factor Receptor Gene in Human Glioma Xenografts. Cancer Res. 1988 Apr 15;48(8):2231–8.

114. Yamada KM, Even-Ram S. Integrin regulation of growth factor receptors. Nat Cell Biol. 2002 Apr;4(4):E75–6.

115. Sundberg C, Rubin K. Stimulation of beta1 integrins on fibroblasts induces PDGF independent tyrosine phosphorylation of PDGF beta-receptors. J Cell Biol. 1996 Feb 15;132(4):741–52.

116. Moro L, Venturino M, Bozzo C, Silengo L, Altruda F, Beguinot L, et al. Integrins induce activation of EGF receptor: role in MAP kinase induction and adhesion-dependent cell survival. EMBO J. 1998 Nov 16;17(22):6622–32.

117. Stoscheck CM, Carpenter G. Down regulation of epidermal growth factor receptors: direct demonstration of receptor degradation in human fibroblasts. J Cell Biol. 1984 Mar;98(3):1048–53.

118. Sorkin A, Goh LK. Endocytosis and intracellular trafficking of ErbBs. Exp Cell Res. 2008 Oct 15;314(17):3093–106.

119. Sebastian S, Settleman J, Reshkin SJ, Azzariti A, Bellizzi A, Paradiso A. The complexity of targeting EGFR signalling in cancer: From expression to turnover. Biochim Biophys Acta BBA - Rev Cancer. 2006 Aug;1766(1):120–39.

120. Coats S, Olashaw N, Pledger W. Characterization of platelet-derived growth factor alpha receptor synthesis and metabolic turnover. Cell Growth Differ. 1994 Sep 1;5(9):937–42.

121. Schwindt TT, Motta FL, Filoso Barnabé G, Gonçalves Massant C, de Oliveira Guimarães A, Calcagnotto ME, et al. Short-Term Withdrawal of Mitogens Prior to

Plating Increases Neuronal Differentiation of Human Neural Precursor Cells. Chan-Ling T, editor. PLoS ONE. 2009 Feb 27;4(2):e4642.

122. Nieto-Estévez V, Pignatelli J, Araúzo-Bravo MJ, Hurtado-Chong A, Vicario-Abejón C. A Global Transcriptome Analysis Reveals Molecular Hallmarks of Neural Stem Cell Death, Survival, and Differentiation in Response to Partial FGF-2 and EGF Deprivation. PLoS ONE. 2013 Jan 7;8(1):e53594.

123. Saito Y, Haendeler J, Hojo Y, Yamamoto K, Berk BC. Receptor Heterodimerization: Essential Mechanism for Platelet-Derived Growth Factor-Induced Epidermal Growth Factor Receptor Transactivation. Mol Cell Biol. 2001 Oct 1;21(19):6387–94.

124. Bowen-Pope DF, Dicorleto PE, Ross R. Interactions between the receptors for platelet-derived growth factor and epidermal growth factor. J Cell Biol. 1983 Mar 1;96(3):679–83.

125. Biscardi JS, Maa M-C, Tice DA, Cox ME, Leu T-H, Parsons SJ. c-Src-mediated Phosphorylation of the Epidermal Growth Factor Receptor on Tyr845 and Tyr1101 Is Associated with Modulation of Receptor Function. J Biol Chem. 1999 Mar 19;274(12):8335–43.

126. Ross RS. Molecular and mechanical synergy: cross-talk between integrins and growth factor receptors. Cardiovasc Res. 2004 Aug 15;63(3):381–90.

127. Miyamoto S, Teramoto H, Gutkind JS, Yamada KM. Integrins can collaborate with growth factors for phosphorylation of receptor tyrosine kinases and MAP kinase

activation: roles of integrin aggregation and occupancy of receptors. J Cell Biol. 1996 Dec;135(6 Pt 1):1633–42.

128. Baron W, Decker L, Colognato H, ffrench-Constant C. Regulation of integrin growth factor interactions in oligodendrocytes by lipid raft microdomains. Curr Biol CB. 2003 Jan 21;13(2):151–5.

129. Zidovetzki R, Yarden Y, Schlessinger J, Jovin TM. Microaggregation of hormone-occupied epidermal growth factor receptors on plasma membrane preparations. EMBO J. 1986 Feb;5(2):247–50.

Supplementary Figures and Data

Genes in NanoString custom codeset:

ACTB	CDKN2C	DNM3	GALNT13	IGFBP6	MSI1	NOTCH3	NEUN	SOX2
AKT2	CHI3L1	DNMT1	GAPDH	JAG1	MYCN	OLIG1	RELB	SOX9
AKT3	CIC	EGFR	GAS1	KIT	NANOG	OLIG2	S100A11	SPP1
ASCL1	CLEC2B	EMP3	GFAP	KLRC4	NCAM1	OMG	S100A4	TBP
BEX1	CNP	ERBB3	GLI1	LGALS3	NESTIN	PAX6	S100A9	TCF4
BMI1	COL1A2	ETV1	GLI2	LHX6	NEUROD1	PDGFA	S100B	TIMP1
CD44	COL6A3	ETV4	GLI3	LIF	NEUROD2	PDGFRA	SERPINE1	TLE4
CDH4	NG2	ETV5	GRIA2	LIN28B	NEUROG1	PDPN	SETDB2	TLR2
CDK4	IL8	FABP7	GRIK1	LIN28A	NF1	PHF11	SLC4A4	TNC
CDK6	DCX	FGFR1	HES1	MAP2	NFIA	OCT3	SNAI1	TNFRSF1A
CDKN1A	DENND2A	FGFR3	HGF	MBP	NKX2-2	PROM1	SNAI2	TRADD
CDKN2A	DLL3	FUT9	IGF2BP3	MET	NOTCH1	PTEN	SOCS2	TUBB3
CDKN2B	DLX2	GAD1	IGFBP2	MGMT	NOTCH2	RB1	SOX10	TUBB

Genes used in subtyping:

Proneural	Classical	Mesenchymal
DLL3	GAS1	IGFBP6
NKX2-2	JAG1	SERPINE1
DCX	FGFR3	TIMP1
ERBB3	PDGFA	CHI3L1
OLIG2	EGFR	TRADD
ASCL1	AKT2	RELB
	GLI2	TLR2

Supplementary Figure S1: Genes in custom NanoString codeset

Complete list of genes in custom designed codeset, twenty of which were selected for as classifiers based on TCGA subtyping and genes which were available on both human and mouse NanoString codesets.

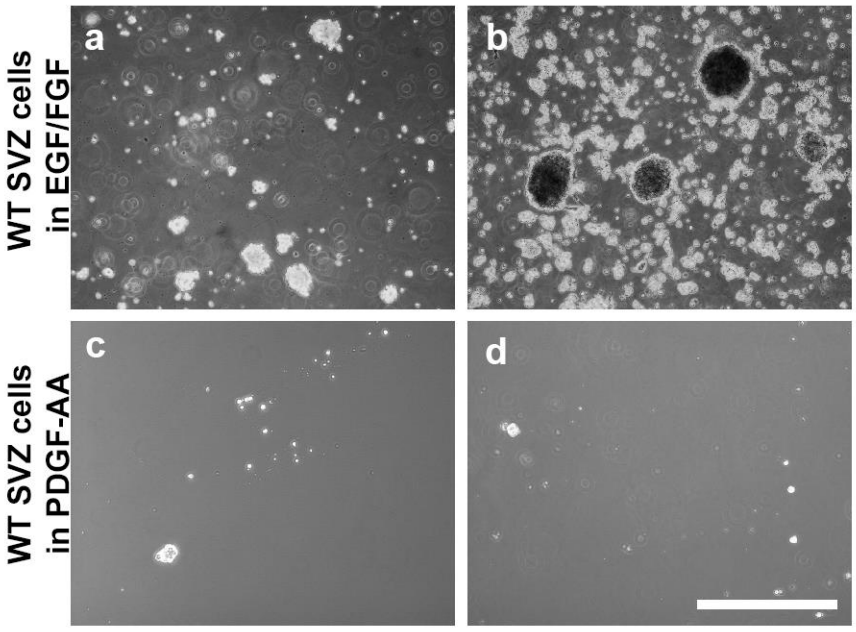

Supplementary Figure S2: Cells from the SVZ of WT mice grown in EGF/FGF vs PDGF-AA

WT SVZ cultures proliferate readily in EGF/FGF (**a,b**). In contrast, WT SZV cells do not proliferate or survive in PDGF-AA (**c,d**). Scale bar = 200 μm. Images by C. Binding.

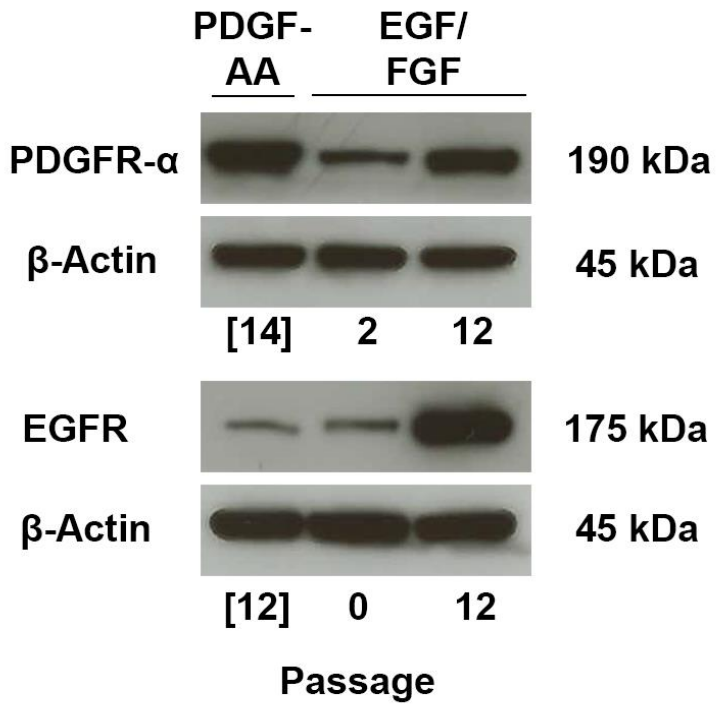

Supplementary Figure S3: Additional western blot of PDGFR-α and EGFR

Additional time points for PDGF-AA exogenous cells and EGF/FGF grown cells assessed for the protein expression of PDGFR-α and EGFR show a slight increase over time of PDGFR-α in EGF/FGF grown cells. EGFR expression appears low in exogenous PDGF-AA independent cells passage [12] and early passage EGF/FGF cells passage 0, which increases with time, shown at passage 12. **[] = exogenous PDGF-AA independence.**

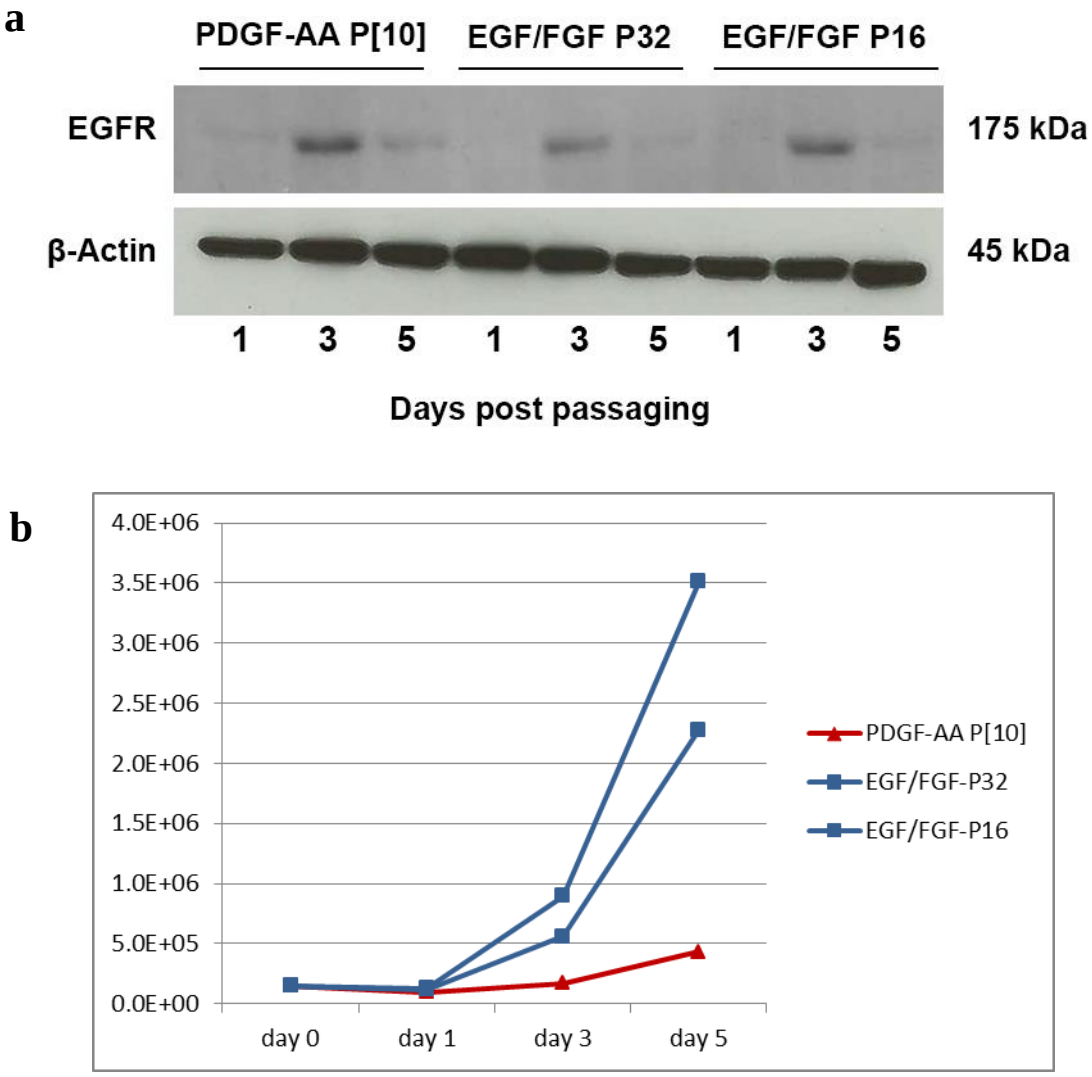

Supplementary Figure S4: Variability in EGFR receptor expression post-passaging

(**a**) Western blot of PDGF-AA and EGF/FGF supplemented cultures demonstrating varied levels of expression depending on number of days post-passaging/supplementing with fresh growth factors, notably, day 3 shows the highest expression in all three cultures. (**b**) Each culture was seeded with $1.5x10^5$ cells at day 0 and live cells were counted before cells were harvested for protein. **[]** = **exogenous PDGF-AA independence.**

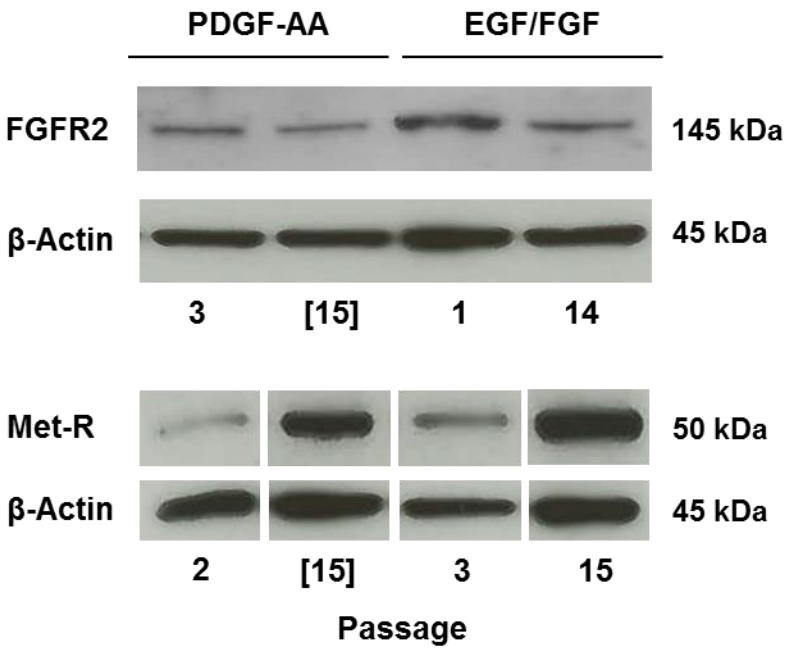

Supplementary Figure S5: FGFR2 and c-Met receptor protein expression

Western blot of PDGF-AA and EGF/FGF supplemented cultures demonstrating protein expression of FGFR2 expression remains relatively constant in PDGF-AA and decreases slightly in EGF/FGF cultures over time, indicating FGFR2 is likely not playing a role in the transformative process of PDGF-AA cells. Increasing levels of c-Met receptor protein over time in culture in both PDGF-AA and EGF/FGF cultured cells similarly indicate the c-Met receptor is likely not playing a unique or critical role in transformation of the PDGF-AA cultured cells. **[] = exogenous PDGF-AA-independence.**

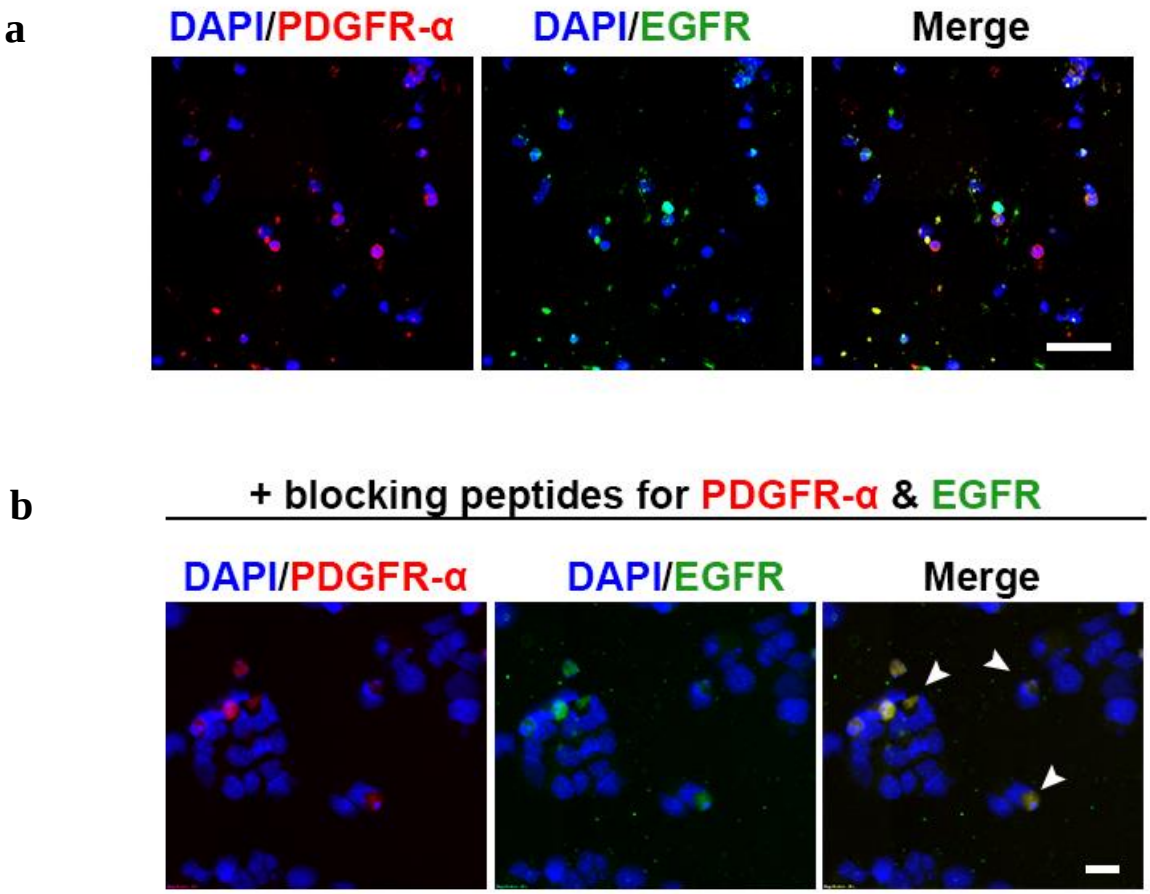

Supplementary Figure S6: Controls for immunofluorescence

Cells adhered via cytospin do not appear to show focal receptor staining (**a**). Scale bar = 100 μm. Immunofluorescence on laminin adhered cells using blocking peptides specific to the PDGFR-α and EGFR antibodies used (**b**). Dead cells with abnormal, condensed nuclear morphology exhibit autofluorescence and are indicated with arrows in Merge panel. Scale bar = 20 μm.

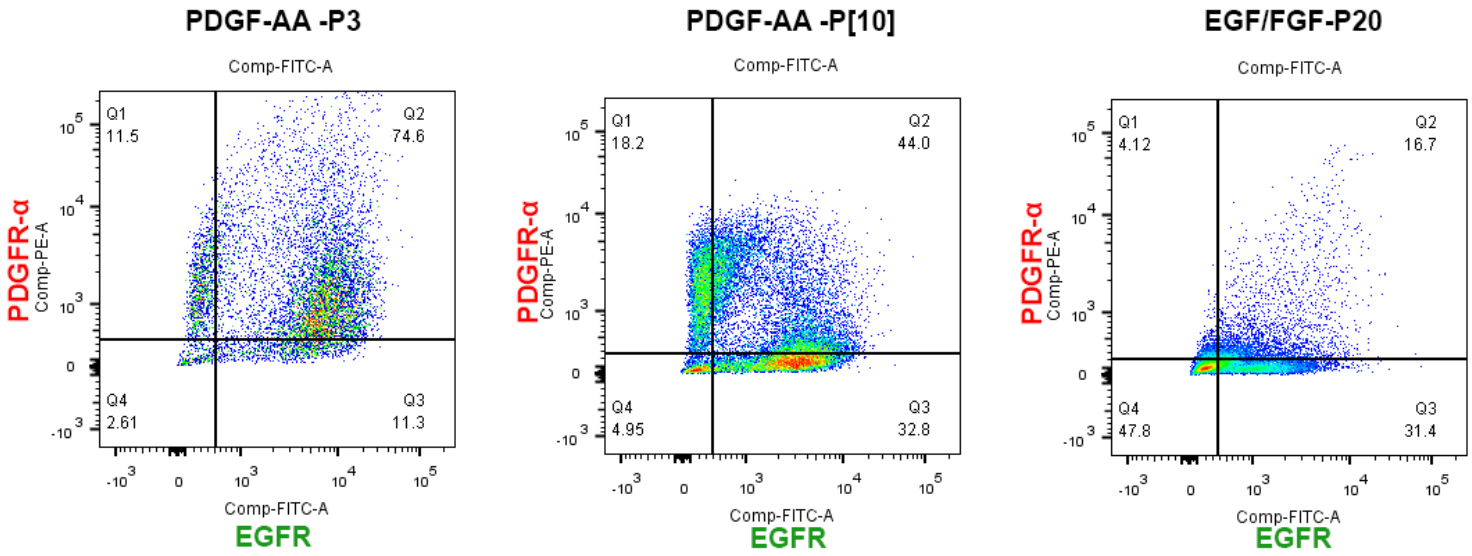

Supplementary Figure S7: Dual and single labeled FACS analysis of PDGF-AA and EGF/FGF grown cells

Using fluorescence-activated cell sorting the majority of cells display as dual labeled for PDGFR-α and EGFR in PDGF-AA cultures. In EGF/FGF grown cultures, 16.7% show as dual labeled and 31.4% display as EGFR labeled only. Receptor internalization or sensitivity in techniques could explain the differences in single versus dual labeled cells observed in immunofluorescence versus FACS. **[] = exogenous PDGF-AA independence.**

Copyright Permission:

On Apr 30, 2015, at 9:48 AM, "Jessica Ann DePetro" <jadepetr@ucalgary.ca> wrote:

Hi Carmen,

Because your project with Dr. Cairncross was the foundation of my project as well, I would like to ask your permission to use several of your graphs in my thesis. Specifically, the ones pertaining to proliferation and cell death, and the tumor latency graphs. I have cited your thesis and your work in my thesis, however the University requires I also obtain permission from you in order to use these. An email reply indicating this is ok with you is sufficient.

Thank you for your consideration,

Jessica DePetro

Re: copyright permission
Carmen Elizabeth Binding
Thu 4/30/2015 10:07 AM
Inbox
To: Jessica Ann DePetro <jadepetr@ucalgary.ca>;
Yes, of course you have my permission to use these.

I, Carmen Binding, provide permission for Jessica Ann DePetro to use graphs from my thesis for use in her thesis.

Let me know if you need anything further!

Sincerely,
Carmen Binding